JGERI
Journal of Green Energy Research and Innovation
ISSN: 3041-9018

Journal of Green Energy Research and Innovation

Volume 1, Issue 3, Summer 2024

PUBLISHER
Arak University

Journal of Green Energy Research and Innovation (JGERI)

Publisher: **Arak University**

Director-in-Charge: **Dr. Ali Asghar Ghadimi**

Editor-in-Chief: **Prof. Gevork B. Gharehpetian**

Deputy Editor: **Dr. Abolghasem Daeichian**

Executive Editor**: Dr. Mahyar Abasi**

Coverage area: **International**

Journal Type: **Scientific and technical**

Language: **English**

Frequency: **Quarterly**

Review Time: **4-8 Weeks**

Publication Type: **Electronic, Print**

Open Access: **Yes**

Policy: **Peer-Reviewed**

DOI**: 10.61186/jgeri**

E-mails: **jgeri@araku.ac.ir**

Website: **https://jgeri.araku.ac.ir/**

Address: **Department of Electrical Engineering, Faculty of Engineering, Arak University, Arak, Iran.**

P.O. Box: **38156-8-8349**

Tel: **086-32625099**

Editorial Board

About Journal

JGERI is interested in the results of research in the field of green and renewable energies. The scope of publications of this journal in the field of green energy is extensive and it welcomes novel and innovative studies. Due to the increasing influence of renewable energy in power systems, studies, research, and reports resulting from scientific achievements in this specific area have risen compared to previous decades. This journal is ready to publish specialized articles in all fields related to green energy and interdisciplinary topics related to this scientific branch in the form of open access, which is published annually in four issues as free and open access by Arak University, Iran. **JGERI** is ready to receive the latest research results ranging from analytical methods, numerical simulation, experimental research, and development studies concerning the knowledge and application of green energy.

The following articles are acceptable:

- **Research articles** are expected to present innovative solutions, new concepts, or creative ideas that can help solve existing or emerging technical challenges in the field of green and renewable energy.
- **Review articles** are expected to provide enlightening and specialized reviews, trainings, or case studies on an important topic, timely and widely in the field of green and renewable energies.
- **Applied articles** are expected to share the results of the industry's valuable experiences in dealing with challenging technical issues, developing/adopting new standards, applying new technologies or solving complex problems in the field of green and renewable energies. These articles can have a significant impact on the strategic plans of the industry in the coming years.

Aims and Scope

JGERI is interested on the qualified international multidisciplinary research results related to all aspects of green energy. The scope of **JGERI** is very broad, and welcomes original, novel fundamental and engineering research. We also publish reviews and industrial reports of green energy and its impact on the eco-environment.

We welcome research papers that focus on, but are not limited to, the following areas:

- Policies and Strategies for Green Energy Systems
- Fundamental And Industrial Applications for Green Energy Systems
- Energy Conversion, Control Techniques, and Grid Interactive Systems for Green Energy Systems
- Environmental Impacts of Energy Technologies and Pollution Control
- Materials And Catalysis for Green Energy Systems
- Green Energy Consumption
- Artificial Intelligence, Machine Learning, and Computational Methods in Green Energy Systems
- Public Awareness and Education for Green Energy Systems
- Solar Energy and Photovoltaic
- Wind Energy
- Hydrogen Energy and Energy Storage
- Biofuel and Bioenergy

Each manuscript will go through a rigors peer-review process. you can visit our Instructions for Authors page for information on preparing your manuscript.

Guide for Authors

1. Important points and rules for manuscript submission and publication

-Submitting a manuscript to a journal means that the manuscript is not under review or has not been published anywhere in any other language before.
-The submission of the manuscript for publication by the author, implicitly or explicitly, implies the approval of the organization or body where the author works and has used its affiliation.
-By submitting the manuscript, all authors officially declare their agreement to grant the copyright of the manuscript in case of acceptance to Arak University and **JGERI**. However, the authors are responsible for all the contents published in the manuscript, and the journal is only a reviewer and publisher.
- All authors are required to declare any actual or potential conflicts of interest, including financial, personal, or relationships with individuals or organizations that could affect their work.
- Each of the authors must declare their contribution and role in the manuscript on the Title Page to the journal. The statement of approval of all authors and their role in the manuscript is the responsibility of the corresponding author.
- Authors should note that all manuscripts sent to **JGERI** are checked with Authenticate's CrossCheck software to analyze the authenticity of the content. In this analysis, the overlap and similar texts presented in the submitted manuscripts will be determined.
- **JGERI** makes its manuscripts open to access after publication and there is no charge (APC) for reviewing and publication of manuscripts, and readers can download and use the articles for free.
- All authors, if they had financial support in conducting research related to this manuscript, should briefly state their role. If financial source(s) have no role in the results of the research published by the article, this should also be mentioned by the authors.
- Acknowledgments to individuals and institutions can be mentioned in a separate section at the end of the manuscript before References, and they must not be included as footnotes or in any other form. In this section, it is recommended to mention the names of those who have collaborated during the research (such as those helping in the language correctness aspect of the manuscript, assisting in writing the manuscript or proofreading it, and other cases).
- Non-commercial use of the manuscript will be governed by the Creative Commons Attribution-NonCommercial 4.0 International License, which is currently available at the link (https://creativecommons.org/licenses/by-nc/4.0/). This certificate allows others to use the authors' work in a non-commercial way and utilize it in their research work, although in the new work, they need to acknowledge the authors and mention its non-commercial nature.

2. Initial submission of the manuscript

Submission to this journal is online and you will be accompanied in all the steps of creating a user account and uploading files. All correspondence, including notification of the editor's decision and request for revision, will be made via email. To submit your manuscript, just click on the **Submit Manuscript** option on the journal page. Then, click on **Register** to create an author account. A message will be sent to your email containing your username and password. Then, log in to the manuscript submission system on the Users login page, where you need to enter the username and password and submit your new manuscript. Once you are logged in, you can change your password by clicking on My Home in the top menu. For the next time, just log in to your account. Please include the names, addresses, and email addresses of at least three potential academic reviewers with the paper. Please include reviewers' names and their academic rank, affiliation, and contact information (mail address is mandatory). However, only the editor has the right to decide on the use of suggested reviewers. All the submitted manuscripts undergo the process of plagiarism check with IThenticate software and the review process begins. According to the journal policy, there is a difference between the requirements for initial and revised submission files. Required files for initial submission include three files: **JGERI_Main_Manuscript**, **JGERI_Form_for_Copyright_Transfer_Statement and Conflict_ of_ Interest_ Disclosure** and **JGERI_Cover_Letter**, all three of which must be sent to the journal in PDF format. You can use the links below to download the requirements and suggestions files of these three files.

- JGERI_Guideline_for_Main_Manuscript
- JGERI_Guideline_for_Cover_Letter
- JGERI_Form_for_Copyright_Transfer_Statement and Conflict_ of_ Interest_ Disclosure

3. Submission of the revised manuscript

If the submitted manuscript, after going through the initial review process, is evaluated by the officials and reviewers of the journal and a decision is made to make corrections and revisions in the form of minor or major, the authors are obliged to make the corrections and prepare the response letter to the reviewers within the time specified by the journal. Three files must be sent to the journal at this stage: WORD and PDF files of the revised manuscript (changes should be highlighted), PDF file of the response to the reviewers (including the comments and responses of each of the reviewers separately), Title Page and Authorship file in WORD format (containing two main forms: Title Page and Authorship). The link to download the necessary files along with their requirements and instructions is given below. Points raised in the file **JGERI_Revised_Manuscript** must be followed for compiling the revised manuscript. The authors are obliged to submit the revised file in PDF and WORD format to the journal. Also, different parts of the file **JGERI_Form_for_Title_Page_ and_ Authorship** needs to be completed and signed by the corresponding author, but **JGERI_Response_to_the_Reviewers_Comments** is suggested by the journal and it is not necessary to follow all the points of that file. It should be noted that all the stages of page layout and editing in the form of final publication are the responsibility of the journal. In the completion stages of this process, the cooperation of the authors is needed, and we will inform you at each stage. Thus, the minimum requirements for file compilation are provided in the template file.

- JGERI_Guideline_for_Revised_Manuscript
- JGERI_Form_for_Title_Page_ and_ Authorship
- JGERI_Guideline_for_Response_to_the_Reviewers_Comments

4. **After the final acceptance of the manuscript**

After announcing the final acceptance of the manuscript (reviews may happen several times), the files **JGERI_Revised_Manuscript** and **JGERI_Form_for_Title_Page_ and_ Authorship** will be sent to the paging unit for page layout and final editing. After the final acceptance announcement, the authors will be asked to send a graphic abstract included in a single file. Then, the process of compilation of the manuscript will be completed by the journal and finally, the proof version of the manuscript will be sent to the authors. The authors are obliged to check the proof file completely and report to the journal if they find any ambiguity or error in the final file. In some cases, along with the final proof file of the manuscript, there may be a series of errors and ambiguities in the manuscript, which are sent to the author in the form of comments along with the proof version of the manuscript. The corresponding author is obliged to clarify and resolve these problems and ambiguities in the specified time.

5. **After publication on the journal's website**

After announcing the initial acceptance, the information of the article without its content will be indexed in the Articles in the Press section of the website. After including the article in the issue selected by the journal, the desired article will be indexed in the Current Issue unit along with Vol, No, and pp. Also, the electronic file of the article can be introduced in all scientific references through the DOI link. The important point is that, after acceptance and indexing, the names of the authors cannot be changed, that is, it will not be possible to add, delete, or change the order of the names of the authors and their organizational affiliations.

Cooperative Publication Organization

Renewable Energy Research Institute of Arak University
http://araku.ac.ir/web/riren

Iranian Wind Energy Association
https://www.irwea.org/fa/

Indexing Databases and Social Networks

Google Scholar: https://scholar.google.com/citations?user=47bsJFoAAAAJ&hl=en

Linkedin: https://www.linkedin.com/in/jgeri-arak-university-0818872b9

Academia:https://independent.academia.edu/JournalofGreenEnergyResearchandInnovationJGERI

PaperHive: https://paperhive.org/users/jgeri

GrowKudos: https://www.growkudos.com/profile/j._green_energy_res._innov._jgeri

MyScineceWork: https://www.mysciencework.com/profile/j.green.energy.res.innov.jgeri

SciExplore: https://sciexplore.ir/profiles/author/987-081-740

Magiran: https://www.magiran.com/magazine/8484

Contents

Journal of Green Energy Research and Innovation

Improving the Technical and Economic Indexes of Distribution Network by Three-Stage Enhanced Imperialist Competitive Algorithm

Babak Rostami, Javad Ebrahimi, Zeinab Sabzian Molaee, Vahid Davatgaran, Seyed Arash Alavi

Highlight

- Location and sizing of renewable resources
- Using Enhanced Imperialist Competitive Algorithm
- Carrying out the proposed design on a practical feeder

Graphical Abstract

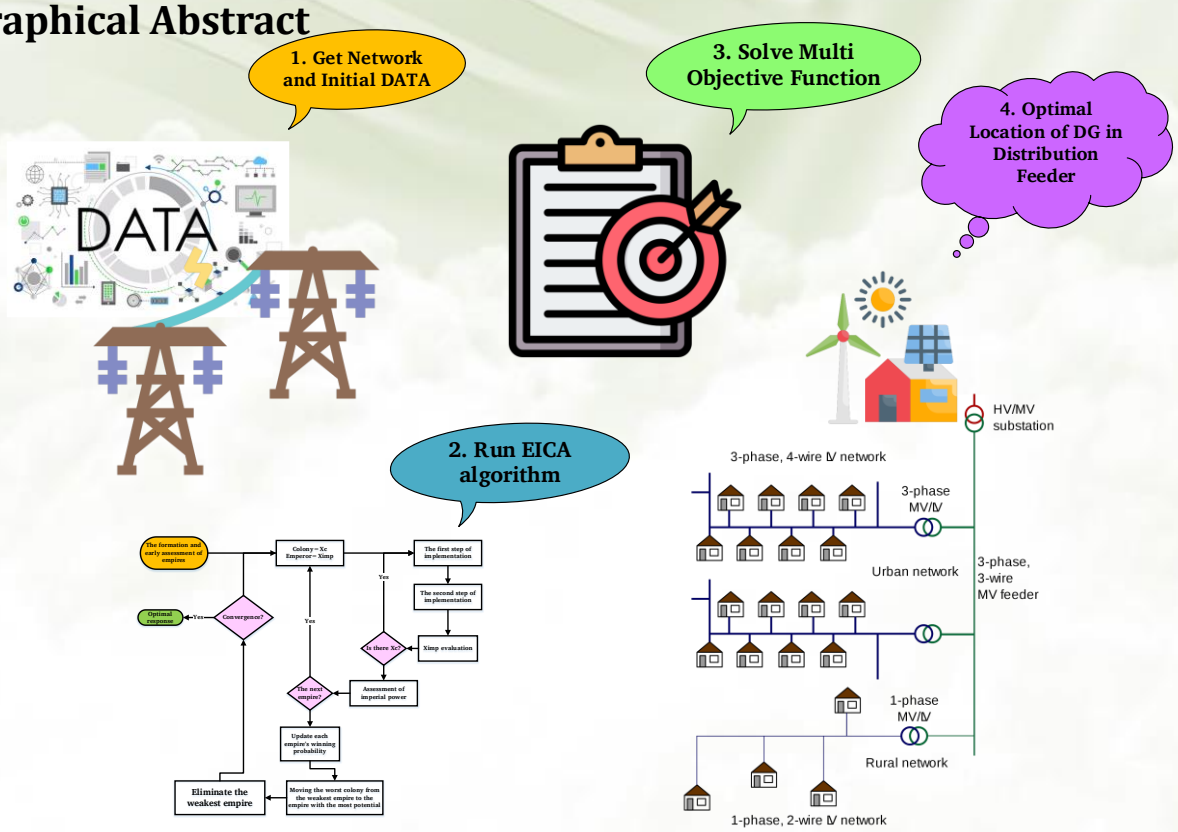

Use your device to scan and read the article online

Citation

B. Rostami, J. Ebrahimi, Z. Sabzian Molaee, V. Davatgaran, and S. A. Alavi, "Improving the Technical and Economic Indexes of Distribution Network by Three-Stage Enhanced Imperialist Competitive Algorithm," *Journal of Green Energy Research and Innovation*, vol. 1, no. 3, pp. 1-15, 2024.

https://doi.org/10.61186/jgeri.1.3.1

JGERI Journal of Green Energy Research and Innovation

Online ISSN: 3041-9018

Journal of Green Energy Research and Innovation

Journal Homepage: www.jgeri.araku.ac.ir

Improving the Technical and Economic Indexes of Distribution Network by Three-Stage Enhanced Imperialist Competitive Algorithm

Babak Rostami[1], Javad Ebrahimi[2]*, Zeinab Sabzian Molaee[3], Vahid Davatgaran[4], Seyed Arash Alavi[5]

[1] *Bakhtar Regional Company, Arak, Iran.*
[2] *Department of Education and Training of Isfahan, District 4 Management, Isfahan, 81458-13331, Iran.*
[3] *Department of Electrical Engineering, Afarinesh University, Borujerd, Lorestan, Iran.*
[4] *Department of Electrical Engineering, Technical and Vocational University (TVU), Tehran, Iran.*
[5] *School of Electrical and Electronic Engineering University College Dublin, Dublin, Ireland.*

* ***Corresponding Author:*** *engineer.jebrahimi@gmail.com*

ARTICLE INFO

Keywords:
Optimal location,
Distributed generation source,
Enhanced imperialist competition algorithm.

Article history:
Received: 24 January 2024;
Revised: 24 February 2024;
Accepted: 01 March 2024;

Article type:
Research Article

ABSTRACT

Restructuring the distribution system in the presence of distributed generation (DG) sources is an effective solution to reduce the cost of power generation and improve the technical and economic parameters of networks. This paper models the optimal design of the location and capacity of DGs in a distribution system as a multi-objective optimization problem. The technical parameters of the problem include network losses, voltage stability index, and voltage profile improvement. Moreover, the economic parameters of the problem are the capital and operation costs of the system. The optimization problem presented in this paper is of mixed-integer nonlinear programming (MINLP) type, so the enhanced imperialist competition algorithm (EICA) is adopted to minimize the objective function. In this algorithm, adding a new implementation phase to the ICA increases searchability and thus enhances the algorithm's efficiency over ICA. The proposed method is first implemented on a standard IEEE 33-bus system. Then, a real network is incorporated to optimize the technical and economic parameters. The analysis and comparison of the results demonstrate the efficacy of the suggested algorithm in the optimal design of the system compared to the original ICA .In this article, we are finally able to bring the voltage profile and voltage stability index of the "Rahdarkhaneh" distribution feeder close to 1 pu and significantly reduce the network losses.

1. Introduction

Population growth, economic development, and industrialization of countries have increased the consumption of electrical energy, making it necessary to develop and expand distribution systems and increase investments in this industry. The expansion of distribution systems results in escalated losses, voltage drops, and, thus, a decrease in node voltage stability and load imbalance. Power loss has always been a considerable amount due to the large scale of the distribution network, low X/R ratio, and voltage drop along the path of distribution network feeders, so that it is estimated that more than 13%

of the total power produced in the networks is wasted in distribution networks [1]. In recent years, various measures have been taken to optimize and shift the distribution networks from the traditional structure to the new structure, and DGs have played an essential role in these changes and the new structure [2-5].

1.1. Motivation

DGs provide many advantages for both consumers and distribution companies. If these sources are optimally located, the loss will significantly be reduced, the voltage profile will improve, and by installing DG in weak buses, the operation of the distribution system will perhaps be stabilized. Also, government incentives, low cost of energy transmission, low investment risk, and high efficiency have highlighted the economic importance of DGs in recent years. On the other hand, misplacement of DGs in the network causes problems, such as increasing losses, overvoltage, or voltage drop in the network, and increasing the costs of energy generation and transmission. Hence, researchers have widely discussed optimizing the location and capacity of DGs in the distribution system.

1.2. Literature review

So far, numerous researches have been carried out to optimize the operation of DGs in distribution systems. Most of these studies have used metaheuristic methods to solve the problem of optimizing the location and size of these resources in power systems. For example, authors in [3-5] used mixed particle swarm optimization, multi-objective particle swarm optimization, and the coyote optimization algorithm to minimize power losses and improve the voltage profile in the distribution network, respectively. Also, the optimal location of DGs in an unbalanced distribution network was found by using a genetic algorithm [6]. The differential algorithms, firefly algorithm, and gray wolf algorithm are other methods employed in [7-12] to find the optimal location of DGs, respectively. On the other hand, studies have pursued various objectives in locating DGs. For instance, the effect of installing photovoltaic (PV) DG on reducing losses and improving the voltage profile in a real rural distribution system in Yogyakarta, Indonesia was investigated in [10]. The voltage and reactive power control methods using PVs on a standard 33-bus system were evaluated in [11]. The simultaneous installation of DGs and DSTATCOM in distribution networks to minimize power loss and voltage deviation and maximize the voltage stability index was introduced [12] using the Lightning Search Algorithm (LSA). Also, increasing the system's reliability has been a concern of researchers in the optimal design of the location and capacity of DGs [13]. Four heuristic algorithms for reducing distribution network losses in the presence of DGs were compared in [14]. In some studies, the problem of restructuring and reconfiguring the distribution network has been solved to reduce power losses and improve the reliability index [15-18]. However, many studies on locating DGs in the distribution system have only examined the network's technical parameters in the objective function. For example, the problem of locating DGs to reduce power losses was implemented in [5] and [7]. Authors in [2] discussed the economic aspects of the presence of DGs in the network with the objective function of maximum saving and improvement of the voltage profile. Also,

in most articles, studies have been conducted only on standard IEEE networks, while in a few cases, DG location has been done on the real case [10, 13, 19-23]. On the other hand, using a powerful search algorithm to find the optimal solution needs to be considered.

1.3. Research gap

Therefore, to overcome the shortcomings in the research related to the optimal allocation of DGs in the distribution system, this paper presents a new optimal location and sizing of DGs. The method is a nonlinear multi-objective optimization problem in which, in addition to the technical parameters, the economic parameters of the system are also examined. Moreover, the objective function is minimized by the EICA algorithm, which improves the efficiency of the algorithm by adding two separate steps to the conventional ICA.

1.4. Contributions and Novelties

The research contributions are as follows:

1- Locating scattered production resources by a new EICA algorithm

2- Solving the problem of location and capacity of DG in three different modes on a real feeder

3- Dramatically improving the technical and economic parameters of the network

The rest of the paper is organized as follows. Section 2 is dedicated to the formulation and layout of the problem. Section 3 describes the solution method. Section 4 presents the analysis of the results, and finally, Section 5 provides the conclusion.

2. Problem formulation

This section presents the formulation of a comprehensive DG location problem. The objective function considered here includes technical and economic functions, taking into account network constraints, expressed as cost minimization.

2.1. Objective function

The proposed method's objective function is formulated as a multi-objective nonlinear programming (NLP) function. From a technical point of view, reduction of losses, improvement of voltage profile, and enhancement of grid voltage stability are considered. DG investment cost, DG repair and maintenance cost, and DG power generation cost are the economic aspects of the optimization problem [26]. Therefore, the total objective function is formulated as Equation (1):

$$\text{Min}(f)=F_{\text{TOTAL-COST}}+K_1 f_v+K_2 f_{\text{VSI}} \quad (1)$$

Where coefficients K_2 and K_1 are weighting coefficients for the contribution of each voltage stability index and voltage profile in the objective function, respectively, and $F_{\text{TOTAL-COST}}$ is the total cost function calculated by Equation (2) [28, 30-32]:

$$F_{\text{TOTAL-COST}}=F_{\text{installation}}+F_{\text{maintenance}}+F_{\text{operation}}+F_{\text{Reduction-loss}} \quad (2)$$

Where $F_{\text{installation}}$, $F_{\text{maintenance}}$, $F_{\text{operation}}$, and $F_{\text{Reduction-loss}}$ are the costs of investment and installation, repair and maintenance, power generation, and reduction of the cost of purchased power calculated by Equation (3)-(6), respectively.

$$F_{installation}=\sum_{i=1}^{N_{DG}}.\sum_{j=1}^{C_{DG}} COST_{installation,ij} \quad (3)$$

$$F_{maintenance}=\sum_{i=1}^{N_{DG}}.\sum_{j=1}^{C_{DG}} COST_{main,ij} \times \sum_{t=1}^{T}((1+inf\,R)/(1+int\,T))^{t} \quad (4)$$

$$F_{operation}=\sum_{i=1}^{N_{DG}}.\sum_{j=1}^{C_{DG}} T_J \times G_{DG,ij} \times G_{cost,ij} \times \sum_{t=1}^{T}((1+inf\,R)/(1+int\,T))^{t} \quad (5)$$

$$F_{Reduction\text{-}loss}=T_j \times C_{energy\text{-}market} \times (Loss+\sum_{n=1}^{num} P_{load}- \sum_{n=1}^{NDG} C_{DG}) \times \sum_{t=1}^{T}((1+inf\,R)/(1+int\,T))^{t} \quad (6)$$

where (inf R), (inf T), (T), and (T_J) denote the inflation rate, interest rate, time horizon, and duration of DG power generation in one year, respectively. Also, f_v is the voltage regulation index determined by Equation (7):

$$f_v=\sum_{i=1}^{Nn}(V_i-V_{rate})^2 \quad (7)$$

Also, parameter f_{VSI} is the voltage stability index in the distribution network, which is defined as Equation (8):

$$f_{VSI}=\frac{1}{\min(SI(n_i))} \qquad i=1...,N_n \quad (8)$$

This index for the evaluation of all network nodes is mentioned in [16] and [24] as given in Equation (9), where SI is the voltage stability index in the *i*th bus. This value must be positive for all buses for the stable operation of the distribution system.

$$SI(n_i)=|V_{i-1}|^4-4[P_iR_{i-1}+Q_iX_{i-1}]|V_{i-1}|-4[P_iR_{i-1}+Q_iX_{i-1}]^2 \quad (9)$$

2.2. Problem constraints

The constraints of the optimization problem are described below:

2.2.1. Power balance constraint

The presence of DG in the network should satisfy the condition of active and reactive power balance in all network buses. Network buses are satisfied as Equation (10) and (11) [34, 35]:

$$P_{gi}-P_{di}-V_i\sum_{j=1}^{N}V_jY_{ij}\cos(\delta_i-\delta_j-\theta_{ij})=0 \quad (10)$$

$$Q_{gi}-Q_{di}-V_i\sum_{j=1}^{N}V_jY_{ij}\sin(\delta_i-\delta_j-\theta_{ij})=0 \quad (11)$$

2.2.2. Voltage limits

The presence of the DG in the network should maintain bus voltages within their allowable range, as given in Equation (12) [36]:

$$V_i^{min}<V_i<V_i^{max} \quad , \quad i=1...,N_i \quad (12)$$

2.2.3. Lines capacity limits

The limits of line capacity are given in Equation (13):

$$|S_i|\leq|S_i^{max}| \quad , \quad i=1,...,N_b \quad (13)$$

2.2.4. Generators' power generation limits

The limit on generation units' output power is provided by Equation (14):

$$P_{gi}^{min}<P_{gi}<P_{gi}^{max} \quad (14)$$

The paper adopts the forward-backward sweep method [17, 25, 33] to solve the problem described in Equation (10)-(14).

3. Methodology

The DG optimal location problem presented in this research is a multi-objective optimization problem that simultaneously considers the optimization of economic and technical parameters of the network. The proposed method is formulated as a nonlinear problem solved by metaheuristic methods in MATLAB software. Therefore, EICA [28-30], a new optimization strategy based on human socio-political evolution, is used in this paper to solve the proposed problem. In the following, a brief description of this algorithm is provided, and then the improvement of ICA is discussed using two separate solutions. EICA adds a new implementation step to standard ICA. Through this implementation, a country (neighbor) is randomly selected for each colony in each empire. If the neighbor is better, the colony moves to the neighbor in the same empire, and if the neighbor is weaker, the colony moves away from its neighbor. Also, the newly created colony replaces the current colony if it is better. Therefore, the efficiency of the algorithm is expected to improve. The proposed problem is solved by EICA through the following steps:

Step 1: Initialization of variables

After recalling information on loads and lines, the DGs' size and location are randomly selected. Power flow is performed to minimize Equation (1) to determine the value of the imperialist and colonies of the empires. Countries are created with a random position (Npop) and distributed by the empire (Nimp = Npop/5). The status of all the countries is evaluated, and the worthiest country is determined as the emperor.

Step 2: For each empire, step 3 is repeated.

Step 3: For each colony in the current empire, steps 4 to 6 are repeated.

Step 4: Implementation of Phase I: Every colony except the emperor is moved by Equation (15):

$$X_{c,new}=X_c+(4\times rand-1)+(X_{imp}-X_c) \quad (15)$$

$X_{c,new}$ is evaluated, and if it is better than X_c, it replaces X_c.

Step 5: Implementation of Phase II: A neighboring colony X_{Nh} is randomly selected. If X_{Nb} is better than X_c, S = +1; otherwise, S = -1. Colony $X_{c,new}$ is created according to Equation (16):

$$X_{c,new}=X_c+ rand\times s +(X_{Nb}-X_c) \quad (16)$$

$X_{c,new}$ is evaluated, and if it is better than Xc, it replaces X_c.

Step 6: If there is a colony with a lower cost than the imperialists, it trades its position within the corresponding empire.

Step 7: Total power (T_{imp}), normalized total power (NT_{imp}), and probability (P_{imp}) for all empires are calculated by Equation (17)-(19):

$$T_{imp}=fitness(X_{imp})+k\times\frac{\sum_{i=1}^{N_{imp}} fitness(X_{imp})}{2N_{imp}} \quad (17)$$

$$NT_{imp}=T_{imp}-max(T_{imp}) \quad (18)$$

$$P_{imp}=\left|\frac{NT_{imp}}{\sum_{i=1}^{N_{imp}} NT_i}\right| \quad (19)$$

Step 8: Transfer the worst colony from the weakest empire to the empire with the highest probability of winning based on (P_{imp}).

Step 9: Destroy the weak empires.

Step 10: Repeat **Step 2** until the termination criterion, i.e., reaching the maximum number of iterations (MaxIter) or a certain number of objective function evaluations, is met. Figure 1 shows the above steps in the EICA algorithm.

4. Results

This section presents the analysis of optimizing the DG's location and capacity in the distribution network using the proposed method in two test systems. This research was designed in four scenarios for each test system, where the number of DGs differed in each scenario. The proposed optimization method was solved for each scenario using both the ICA and EICA algorithms.

4.1. Standard IEEE 33-bus system

To evaluate the presented method, an IEEE standard 33-bus system given in [19] and [27] was studied as the first test system. The simulation results are given in Tables 1-4, while the voltage profile is illustrated in Figure 2. The location and power factor of DGs were different among the scenarios. Installation, maintenance, and operation costs were assumed to be the same in the two algorithms.

According to the values given in Tables 1-4, it can be seen that after optimizing the location and capacity of DGs in the 33-bus network, the technical objectives of the problem were placed in favourable conditions.

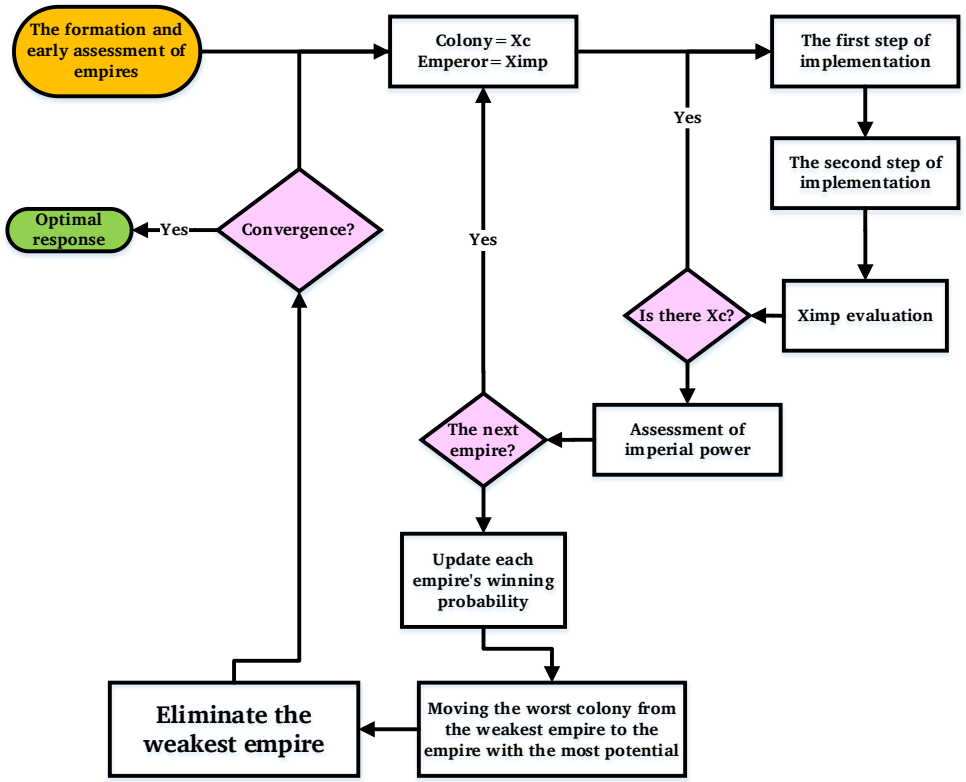

Figure 1. The flowchart of EICA.

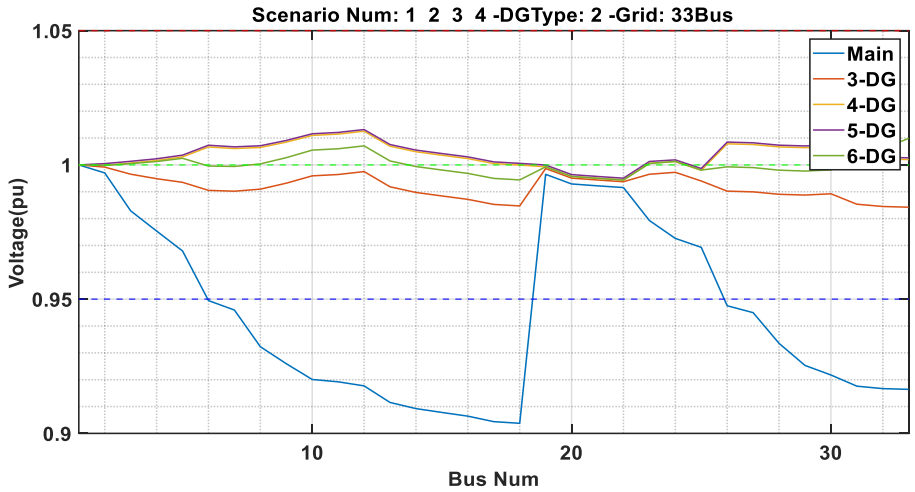

(a) Voltage profile in EICA

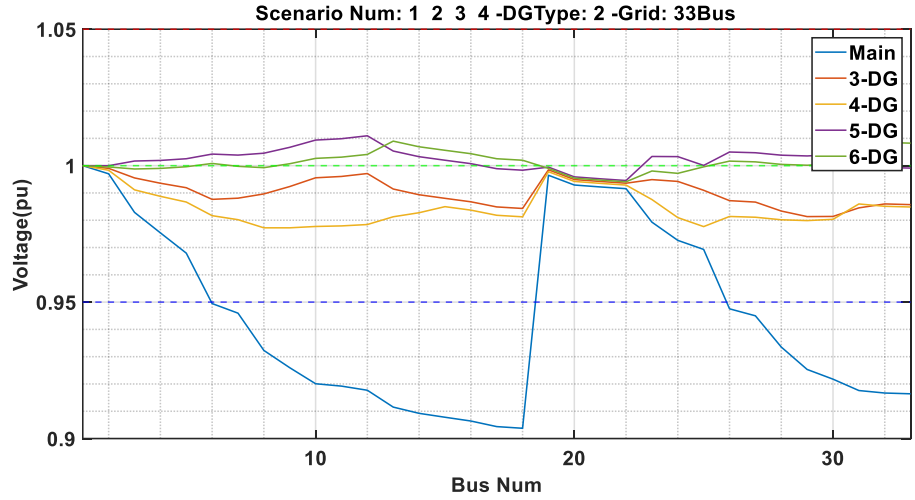

(b) Voltage profile in ICA

Figure 2. Voltage profile of the 33-bus system.

Table 1. DG capacity (KVA) for the 33-bus system.

DG No.	Scenario 1		Scenario 2		Scenario 3		Scenario 4	
	ICA	EICA	ICA	EICA	ICA	EICA	ICA	EICA
DG1	1000	1000	1000	1000	1000	1000	1000	1000
DG2	982	1000	1000	1000	1000	1000	1000	1000
DG3	915	1000	856	1000	947	1000	828	1000
DG4	-	-	762	1000	588	1000	847	1000
DG5	-	-	-	-	736	1000	965	1000
DG6	-	-	-	-	-	-	653	1000

Table 2. DG power factor for the 33-bus system.

DG No.	Scenario 1		Scenario 2		Scenario 3		Scenario 4	
	ICA	EICA	ICA	EICA	ICA	EICA	ICA	EICA
DG1	0.82	0.9	0.8	0.8	0.8	0.92	0.96	0.8
DG2	0.98	0.8	0.98	0.93	0.9	0.88	0.8	0.88
DG3	0.98	0.9	0.98	0.88	0.95	0.93	0.98	0.99
DG4	-	-	0.95	0.91	0.91	0.8	0.96	0.89
DG5	-	-	-	-	0.94	0.91	0.96	0.99
DG6	-	-	-	-	-	-	0.98	0.88

Table 3. DG location (bus number) for the 33-bus system.

DG No.	Scenario 1		Scenario 2		Scenario 3		Scenario 4	
	ICA	EICA	ICA	EICA	ICA	EICA	ICA	EICA
DG1	12	12	31	30	30	2	33	33
DG2	32	30	33	12	12	26	32	12
DG3	24	24	31	26	24	12	26	5
DG4	-	-	15	24	23	30	25	33
DG5	-	-	-	-	26	24	13	33
DG6	-	-	-	-	-	-	32	24

Table 4. Economic parameters of the system (k$) for the 33-bus system.

Parameter	Base	Scenario 1		Scenario 2		Scenario 3		Scenario 4	
		ICA	EICA	ICA	EICA	ICA	EICA	ICA	EICA
Installation cost	-	954	954	1272	1272	1590	1590	1908	1908
Repair cost	-	848	848	1131	1131	1414	1414	1697	1697
Operation cost	-	3395	3515	4239	4687	5005	5858	6202	7030
Loss cost	418	71	31	82	27	26	27	33	35
purchase cost of	13509	2974	2600	352	-	-	-	-	-
Loss reduction profit	-	346	387	336	391	392	390	384	383
Purchase reduction profit	-	10535	10909	13157	14545	15533	18181	19249	21818
Gross profit	-	10882	11296	13493	14963	15925	18572	19634	22201
Net profit	-	5684	5978	6850	7846	7916	9709	9826	11566

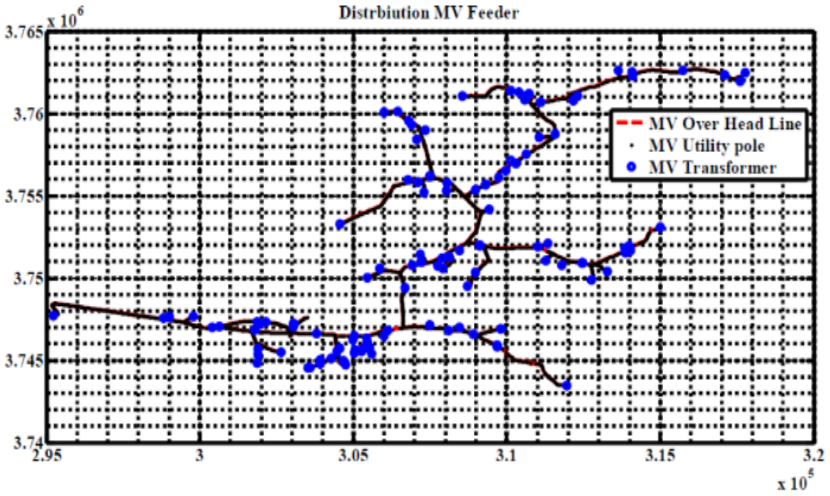

Figure 3. Diagram of the 133-bus system (Rahdarkhaneh feeder).

Thus, the two algorithms stabilized the voltage within the allowed range, and EICA provided a smoother voltage profile.

4.2. The 133-bus system

The actual 133-bus road distribution company located in the city of Borujerd, Iran, was selected as the second test system according to Figure 3. The simulation results are reported in Tables 5-8, while the voltage profile is illustrated in Figure 4. DGs' installation location and power factor differed in different scenarios, and the costs of installation, repairs, and operation in each scenario were assumed to be the same in the two algorithms.

Table 5. DG capacity (kVA) for the 133-bus system.

DG No.	Scenario 1		Scenario 2		Scenario 3		Scenario 4	
	ICA	EICA	ICA	EICA	ICA	EICA	ICA	EICA
DG1	1000	1000	1000	1000	1000	1000	1000	1000
DG2	914	1000	1000	1000	1000	1000	1000	1000
DG3	909	1000	938	1000	752	994	841	911
DG4	0	0	839	1000	935	1000	783	998
DG5	0	0	0	0	729	853	765	337
DG6	0	0	0	0	0	0	722	1000

Table 6. DG power factor for the 133-bus system.

DG No.	Scenario 1		Scenario 2		Scenario 3		Scenario 4	
	ICA	EICA	ICA	EICA	ICA	EICA	ICA	EICA
DG1	0.83	0.84	0.8	0.89	0.81	0.88	0.98	0.88
DG2	0.99	0.99	0.98	0.99	0.99	0.89	0.91	0.81
DG3	0.99	0.88	0.99	0.88	0.88	0.97	0.97	0.87
DG4	0	0	0.99	0.88	0.97	0.88	0.98	0.88
DG5	0	0	0	0	0.99	0.92	0.88	0.99
DG6	0	0	0	0	0	0	0.99	0.99

Table 7. DG location (bus number) for the 133-bus system.

DG No.	Scenario 1		Scenario 2		Scenario 3		Scenario 4	
	ICA	EICA	ICA	EICA	ICA	EICA	ICA	EICA
DG1	124	93	131	7	130	40	132	127
DG2	132	7	133	2	133	51	75	2
DG3	132	127	131	127	133	2	127	51
DG4	0	0	113	93	133	20	127	93
DG5	0	0	0	0	130	51	122	127
DG6	0	0	0	0	0	0	129	3

Table 8. Economic parameters (k$) of the 133-us system.

Parameter	Base	Scenario 1		Scenario 2		Scenario 3		Scenario 4	
		ICA	EICA	ICA	EICA	ICA	EICA	ICA	EICA
Installation cost	-	954	954	1272	1272	1590	1590	1908	1908
Repair cost	-	848	848	1131	1131	1414	1414	1697	1697
Operation cost	-	3307	3515	4426	4687	5174	5679	5988	6164
Loss cost	645	77	25	61	23	55	21	32	27
purchase cost of	9025	0	0	0	0	0	0	0	0
Loss reduction profit	-	568	621	582	622	590	624	614	618
Purchase reduction profit	-	10264	10909	13736	14545	16058	17624	18584	19074
Gross profit	-	10832	11530	14320	15168	16648	18249	19199	196921
Net profit	-	5722	6212	7490	8077	8469	9566	9605	9941

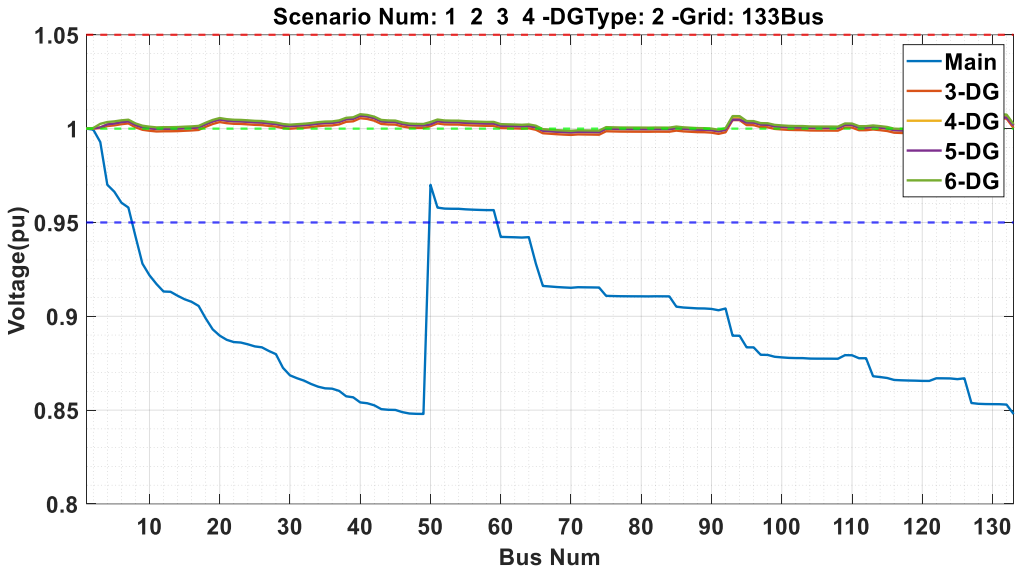

(a) Voltage profile in EICA

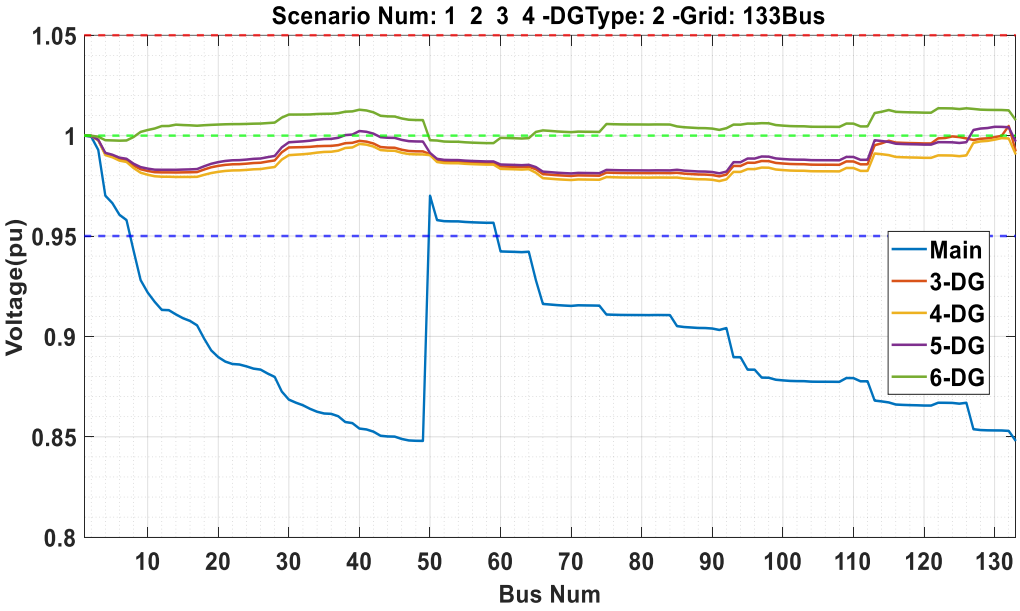

(b) Voltage profile in ICA

Figure 4. Voltage profile of the 133-bus system.

In the voltage stability index curve, despite the optimal performance of the two algorithms, the EICA solution in Scenario 4 recorded a flat graph close to one. Finally, solving the problem using both ICA and EICA algorithms in the worst scenario reduced the network loss by 41 and 17.5 kW, respectively, reflecting the ability of the EICA solution.With the optimal location of DGs using the ICA and EICA algorithms, the cost of network losses ($417,000) was reduced by 94% in the best case. The purchase of energy deficiency from the upstream network was zero in three scenarios in the EICA algorithm and two scenarios in the ICA algorithm, so the net profit was higher in these scenarios. The profit from loss reduction, the profit from energy purchase reduction, gross profit, and net profit from scenarios 1 to 4 were ascending, showing better results of solving EICA in the optimization problem. Also, despite the faster convergence of the ICA algorithm, the optimal convergence value was lower in the EICA algorithm.

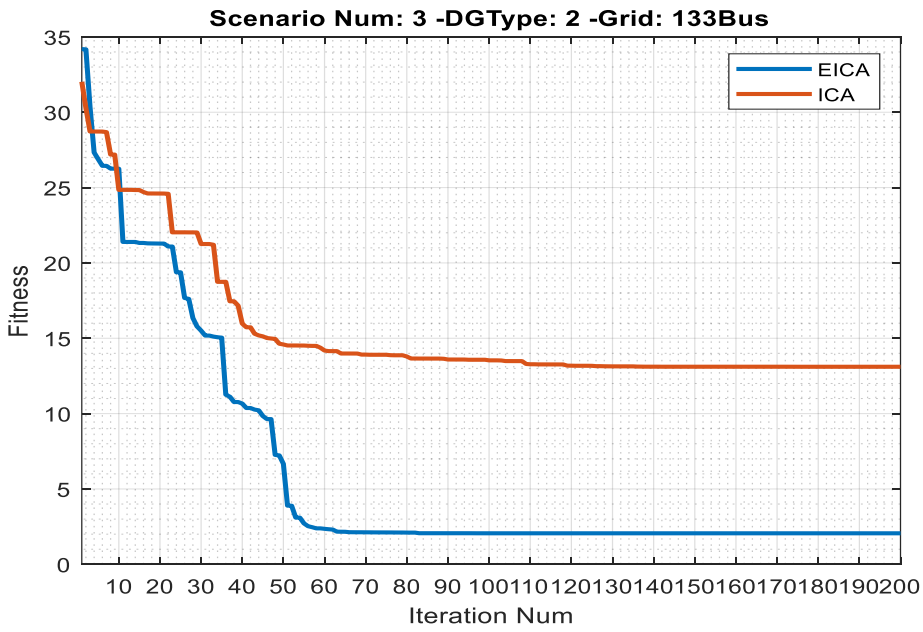

Figure 5. Convergence curve of both algorithms in Scenario 3 on the 133-bus system.

In addition, applying the proposed optimization method to the 133-bus network and comparing the results in Tables 5-8 shows that the EICA solution and the ICA solution stabilized the voltage in the nominal range in four scenarios, and EICA recorded a completely smooth voltage profile in all buses. Also, according to the network stability index curve, the EICA solution was significantly superior to the ICA, and the four scenarios presented a flat graph close to one in terms of stability.

The optimal location of DGs reduced network losses by, on average, 314 kW, and the cost of losses in the EICA solution was reduced by 96%. In solving ICA, the average loss reduction was 91%. Moreover, the installation and repair costs were proportional to the number of DGs in scenarios 1 to 4, and by adding a new DG, $600,000 would be added to the costs.

In solving the optimization problem by the two algorithms, the cost of purchasing energy shortage from the upstream network became zero, so the profit due to the reduction of losses, the profit of reducing energy purchase, and the gross profit increased from scenarios 1 to 4, respectively. Also, the net profit in the EICA solution was, on average, $600,000 more than that in the ICA solution due to more optimal DG placement. Although the EICA solution converged faster than the ICA solution, it had a lower optimal convergence value than the ICA algorithm.

Therefore, by summarizing the mentioned items, it is concluded that:

1) The EICA algorithm recorded a good performance in terms of the optimal location of DG in the distribution network.

2) Multi-objective DG location optimized the technical and economic parameters of the distribution system.

3) The significant reduction in loss costs and not needing to purchase energy from the upstream network in the real network showed the effectiveness of the proposed method in reducing system costs and increasing net profit.

5. Conclusion

This paper focused on determining the location and capacity of DGs as a multi-objective MINLP problem solved in MATLAB. The presented optimization problem was solved using the EICA algorithm for two test systems. First, the optimal location of DG was implemented on a standard 33-bus system to evaluate the proposed method. Then, the presented method was used to optimize a real network's technical and economic parameters. The results were compared with a standard ICA solution to show the better performance of the EICA algorithm. The results demonstrated that the proposed method effectively reduced the costs of the system, including the cost of losses and the cost of purchasing energy, compared to the other methods. Also, multi-objective optimization made the network technical parameters, such as voltage profile, network voltage stability index, and network losses, reach the desired value in addition to the system costs. According to the simulation results and the analysis of the results for different scenarios, the proposed method can be of interest to distribution network operators. The important results obtained in this article in summary are:

1- Reducing network losses
2- Reducing installation costs
3- Improvement of feeder voltage profile and stability

6. Future works

In the continuation of this research, future researchers are suggested to work on the following topics:
1- Positioning considering uncertainty
2- Positioning in the presence of electric vehicles
3- Considering the effect of climate change on the production of renewable resources

References

[1] H. N. Ng, M. M. A. Salama, and A. Y. Chikhani, "Classification of Capacitor Allocation Techniques," *IEEE Trans on Power Delivery*, vol. 15, no. 1, pp. 387-392, 2000.
[2] V. Rafi, and P. K. Dhal, "Maximization Savings in Distribution Networks with Optimal Location of Type-I Distributed Generator Along with Reconfiguration Using PSO-DA Optimization Techniques," *Materials Today: Proceedings*, vol. 33, pp. 4094-4100, 2020.
[3] H. Makvandi, M. Abasi, et al., "Design of New Intelligent Islanding Detection Scheme in Multi-Machine Power Systems to Prevent Wide-Area Blackouts," *12th Smart Grid Conference (SGC)*, pp. 1-7, 2022.
[4] S. Essallah, and A. Khedher, "Optimization of Distribution System Operation by Network Reconfiguration and DG Integration Using MPSO Algorithm," *Renewable Energy Focus,* vol. 34, pp. 37-46, 2020.
[5] M. Z. Malik, M. Kumar, et al., "Strategic Planning of Renewable Distributed Generation in Radial Distribution System using Advanced MOPSO Method," *Energy Reports*, vol. 6, pp. 2872-2886, 2020.
[6] M. Abasi, A. Saffarian, M. Joorabian, and S. G. Seifossadat, "Location of Double-Circuit Grounded Cross-Country Faults in GUPFC-Compensated Transmission Lines Based on Current and Voltage Phasors Analysis," *Electric Power Systems Research,* vol. 195, 107124, 2021.

[7] M. Abasi, A. Rohani, F. Hatami, M. Joorabian, and G. B. Gharehpetian, "Fault Location Determination in Three-Terminal Transmission Lines Connected to Industrial Microgrids Without Requiring Fault Classification Data and Independent of Line Parameters," *International Journal of Electrical Power & Energy Systems,* vol. 131, 107044, 2021.

[8] T. T. Nguyen, T. T. Nguyen, N. A. Nguyen, and T. L. Duong, "A Novel Method Based on Coyote Algorithm for Simultaneous Network Reconfiguration and Distribution Generation Placement," *Ain Shams Engineering Journal*, vol. 12, no. 1, pp. 665-676, 2021.

[9] S. Biswa, S. K. Goswami, and D. Bhattacharya, "Optimal Placement of Distributed Generation in an Unbalanced Radial Distribution System Considering Load Variation," *2019 IEEE Region 10 Symposium (TENSYMP),* pp. 173-178, 2019.

[10] L. M. Belmino, F. S. Soares, et al., "Placement and Sizing of Distributed Generation in Distribution System," *2019 IEEE PES Innovative Smart Grid Technologies Conference - Latin America (ISGT Latin America),* pp. 1-6, 2019.

[11] M. Abasi, A. T. Farsani, A. Rohani, and A. Beigzadeh, "A Novel Fuzzy Theory-Based Differential Protection Scheme for Transmission Lines," *International Journal of Integrated Engineering,* vol. 12, no. 8, pp. 149-160, 2020.

[12] S. M. Sadeghi, M. Daryalal, and M. Abasi, "Two-Stage Planning of Synchronous Distributed Generations in Distribution Network Considering Protection Coordination Index and Optimal Operation Situation," *IET Renewable Power Generation,* vol. 16, no. 11, pp. 2338-2356, 2022.

[13] M. Abasi, M. Joorabian, A. Saffarian, and S. G. Seifossadat, "An Algorithm Scheme for Detecting Single-Circuit, Inter-Circuit, and Grounded Double-Circuit Cross-Country Faults in GUPFC-Compensated Double-Circuit Transmission Lines," *Electrical Engineering*, vol. 104, pp. 2021-2044, 2022.

[14] A. Siadatan, P. Farhadi, B. Taheri, and M. Sedaghat, "Optimal Placement of Various Distributed Generations in Distribution Systems using Firefly Algorithm," *2018 4th International Conference on Electrical Energy Systems (ICEES),* pp. 309-314, 2018.

[15] A. Rohani, M. Abasi, A. Beigzadeh, M. Joorabian, and G. B. Gharehpetian, "Bi-Level Power Management Strategy in Harmonic-Polluted Active Distribution Network Including Virtual Power Plants," *IET Renewable Power Generation*, vol. 15, no. 2, pp. 462-476, 2021.

[16] M. Abasi, N. Heydarzadeh, and A. Rohani, "Broken Conductor Fault Location in Power Transmission Lines using GMDH Function and Single-Terminal Data Independent of Line Parameters," *Journal of Applied Research in Electrical Engineering,* vol. 1, no. 1, pp. 22-32, 2022.

[17] F. S. Gazijahani, and J. Salehi, "Robust Design of Microgrids with Reconfigurable Topology Under Severe Uncertainty," *IEEE Transactions on Sustainable Energy*, vol. 9, no. 2, pp. 559-569, 2018.

[18] A. Sefidgar-Dezfouli, and V. Davatgaran, "Smart Microgrid Optimal Scheduling with Stable and Economic Islanding Capability using Optimal Load Contribution as Spinning Reserve," *International Transactions on Electrical Energy Systems*, vol. 30, no. 11, p.e12566, 2020.

[19] S. A. Shirmardi, M. Abasi, et al., "Designing an Energy Managing System for Distributed Dispersion in Smart Microgrids Based on Environmental Constraints," *12th Smart Grid Conference (SGC), pp.* 1-6, 2022.

[20] J. P. Oliveira, A. B. Rodrigues, and M. G. da Silva, "Probabilistic Evaluation of Voltage Control and Reactive Power Techniques with Photovoltaic Distributed-Generation," *2018 Simposio Brasileiro de Sistemas Eletricos (SBSE)*, pp. 1-6, 2018.

[21] H. Makvandi, M. Abasi, et al., " Design of New Intelligent Islanding Detection Scheme in Multi-Machine Power Systems to Prevent Wide-Area Blackouts" 12th Smart Grid Conference (SGC), 2022. IEEE Index.

[22] M. Abasi, A. T. Farsani, A. Rohani, and M. A. Shiran, "Improving Differential Relay Performance during Cross-Country Fault Using a Fuzzy Logic-Based Control Algorithm," *5th Conference on Knowledge Based Engineering and Innovation (KBEI)*, pp. 193-199, 2019.

[23] Y. Thangaraj, and R. Kuppan, "Multi-Objective Simultaneous Placement of DG and DSTATCOM Using Novel Lightning Search Algorithm," *Journal of Applied Research and Technology*, vol. 15, no. 5, pp. 477-491, 2017.

[24] A. V. Pombo, J. Murta-Pina, and V. F. Pires, "A Multiobjective Placement of Switching Devices in Distribution Networks Incorporating Distributed Energy Resources," *Electric Power Systems Research*, vol. 130, pp. 34-45, 2016.

[25] A. M. Ibrahi, and R. A. Swief, "Comparison of Modern Heuristic Algorithms for Loss Reduction in Power Distribution Network Equipped with Renewable Energy Resources," *Ain Shams Engineering Journal,* vol. 9, no. 4, pp. 3347-3358, 2018.

[26] J. Ebrahimi, and M. Abedini, "A Two-Stage Framework for Demand-Side Management and Energy Savings of Various Buildings in Multi Smart Grid Using Robust Optimization Algorithm," *Journal of Building Engineering*, vol. 53, 104486, 2022.

[27] M. Chakravorty, and D. Das, "Voltage Stability Analysis of Radial Distribution Networks," *International Journal of Electrical Power & Energy Systems*, vol. 23, no. 2, pp. 129-135, 2001.

[28] M. Sadeghi, M. Abasi, "Optimal Placement and Sizing of Hybrid Superconducting Fault Current Limiter to Protection Cordination Restoration of the Distribution Networks in the Presence of Simultaneous Distributed Generation," *Electric Power Systems Research*, vol. 201, 107541, 2021.

[29] M. Abasi, M. Joorabian, A. Saffarian, and S. G. Seifossadat, "A Comprehensive Review of Various Fault Location Methods for Transmission Lines Compensated by FACTS Devices and Series Capacitors," *Journal of Operation and Automation in Power Engineering*, vol. 9, no. 3, pp. 213-225, 2021.

[30] M. Shahrouzi, and A. Salehi, "Enhanced Imperialist Competitive Algorithm for Optimal Structural Design," *Scientia Iranica*, vol. 28, no. 4, pp. 1973-1993, 2021.

[31] E. Chegeni, M. Zandieh, and J. Ebrahimi, "Attitude Control of Satellite with Pulse-Width Pulse-Frequency (PWPF) Modulator using Generalized Incremental Predictive Control," *Majlesi Journal of Electrical Engineering*, vol. 8, no. 3, pp. 25-31, 2014.

[32] H. Makvandi, M. Abasi, et al., "Design of an Optimal STATCOM Controller to Enhance Dynamic Stability of the Smart Grid," *2023 27th International Electrical Power Distribution Networks Conference (EPDC)*, pp. 94-101, 2023.

[33] J. Ebrahimi, and M. Abasi, "Design of a Power Management Strategy in Smart Distribution Networks with Wind Turbines and EV Charging Stations to Reduce Loss, Improve Voltage Profile, and Increase Hosting Capacity of the Network," *Journal of Green Energy Research and Innovation*, vol. 1, no. 1, pp. 1-15, 2024.

[34] M. Khalifeh, S. S. Mortazavi, M. Joorabian, and V. Davatgaran, "Studding Two Indices of Voltage Stability in Reliability Constrained Unit Commitment in a Day-Ahead Market," *21st Iranian Conference on Electrical Engineering (ICEE)*, pp. 1-6, 2013.

[35] V. Davatgaran, S. S. Mortazavi, M. Saniei, and M. Khalifeh, "Different Strategies of Interruptible Load Contracts Implemented in Reliability Constrained Unit Commitment," *21st Iranian Conference on Electrical Engineering (ICEE),* Iran, pp. 1-6, 2013.

[36] M. Abedini, R. Eskandari, J. Ebrahimi, M. H. Zeinali, and A. Alahyari, "Optimal Placement of Power Switches on Malayer Practical Feeder to Improve System Reliability Using Hybrid Particle Swarm Optimization with Sinusoidal and Cosine Acceleration Coefficients," *Computational Intelligence in Electrical Engineering*, vol. 11, no. 2, pp. 73-86, 2020.

Declaration of Competing Interest

The authors declare that they have no known competing financial interests or personal relationships that could have appeared to influence the work reported in this paper. The ethical issues, including plagiarism, informed consent, misconduct, data fabrication and/or falsification, double publication and/or submission, redundancy, have been completely observed by the authors.

Credit Authorship Contribution Statement

Babak Rostami: Data curation, Funding acquisition, Methodology, Resources, Validation, Visualization. **Javad Ebrahimi:** Formal analysis, Project administration, Resources, Software, Supervision, Roles/Writing original draft, Writing-review & editing. **Zeinab Sabzian-Molaee**: Data curation, Methodology, Project administration, Supervision, Validation. **Vahid Davatgaran**: Investigation, Resources, Visualization. **Seyed Arash Alavi**: Formal analysis, Visualization.

Bibliography

Babak Rostami was born in Iran, in 1986 He received his M.Sc. degrees in Electrical Engineering (Power system) from Afarinesh Higher Education Institute of Borujerd, in 2021. He is currently working as power transmission shift operation expert in Bakhtar Regional Company. His current research interest includes power system operation, distributed generation and microgrids.

Javad Ebrahimi was born in Iran, in 1988. He received his Ph.D. degrees in Electrical Engineering from Khomeinishahr Branch, Islamic Azad University, Khomeinishahr/Isfahan, Iran, in 2020. He is currently working as a technical teacher in Technical and Vocational Academy of Isfahan province. Also, he taught for 10 years at Borujerd Islamic Azad University and Ayatollah Borujerd University. he has published 10 research paper, 8 conference paper and 1 industrial research project. His current research interest includes power quality, smart Grid, demand side management and microgrids.

Zeinab Sabzian-Molaee received the B.Sc. degree in power system engineering from Tabriz University, Tabriz, Iran, in 2008. She received the M.Sc. and Ph.D. degrees from Islamic Azad University, Iran, in 2014 and 2022, respectively. Her research interests include power system planning, hybrid ac–dc distribution systems, and renewable distributed generation.

Vahid Davatgaran was born in 1987 in Iran. He received his B.Sc., M.Sc., and Ph.D. degrees in Electrical Engineering (Power Systems) from Shahid Chamran University of Ahvaz, Iran, in 2010, 2013, and 2019, respectively. He is currently an assistant professor at Department of Electrical Engineering, Technical and Vocational University (TVU), Tehran, Iran. His fields of interest include operation and planning of power systems, microgrids and renewable energies, smart grids, and reactive power control in power systems

Seyed Arash Alavi, a senior energy policy researcher at University College Dublin, holds a Ph.D. and bachelor's degrees from Shahid Chamran University, along with a master's degree from Khaje Nasir Toosi University of Technology, all in Electrical Engineering with a focus on Power Systems. His research currently centers on decarbonizing the electricity sector through the integration of renewable energies into the power systems. Additionally, he explores the electrification of heat and transportation by incorporating low-carbon technologies such as heat pumps (HPs) and electric vehicles (EVs).

Journal of Green Energy Research and Innovation

Impact of Spinning Reserve on Frequency Control in a Hybrid Power Plant Including Renewable Energy

Saeed Jamshidi, Hossein Bagheri, Saeed Hasanvand, Mohammad Esmaeil Hassanzadeh, Arash Rohani

Highlight

- Designing a secondary control for several diesel generators and BESS to participate in frequency control.
- Considering the effect of a BESS as a spinning reserve to control a microgrid's frequency
- Proposing the secondary control to deal with frequency deviation and accelerate the operation of spinning reserve.

Graphical Abstract

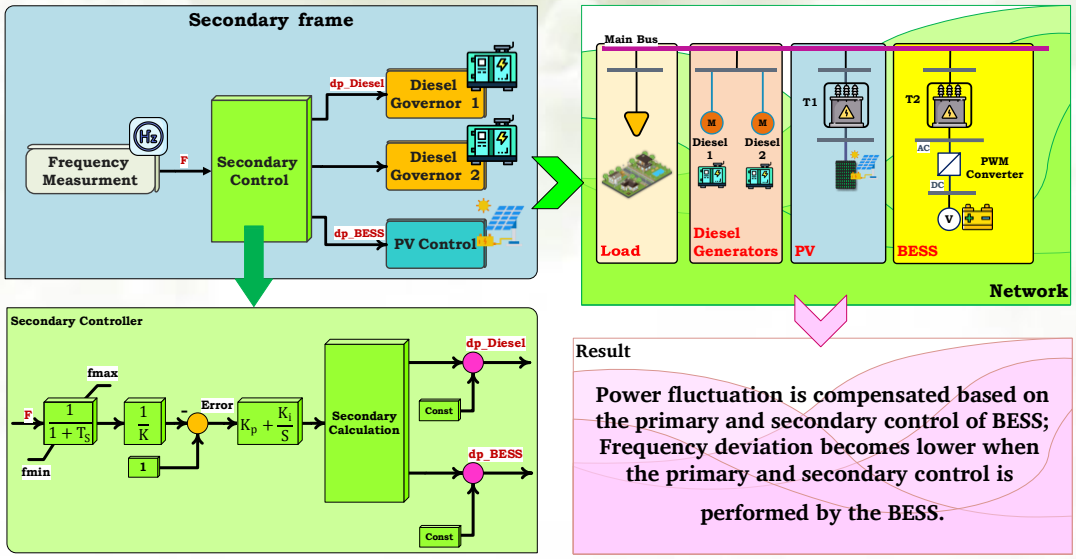

Use your device to scan and read the article online

Citation

S. Jamshidi, H. Bagheri, S. Hasanvand, M. E. Hassanzadeh, and A. Rohani, " Impact of Spinning Reserve on Frequency Control in a Hybrid Power Plant Including Renewable Energy," *Journal of Green Energy Research and Innovation*, vol. 1, no. 3, pp. 16-29, 2024.

https://doi.org/10.61186/jgeri.1.3.16

JGERI Journal of Green Energy Research and Innovation

Online ISSN: 3041-9018

Journal of Green Energy Research and Innovation

Journal Homepage: www.jgeri.araku.ac.ir

Impact of Spinning Reserve on Frequency Control in a Hybrid Power Plant Including Renewable Energy

Saeed Jamshidi [1], Hossein Bagheri [1], Saeed Hasanvand [1]*, Mohammad-Esmail Hasanzadeh [1], Arash Rohani [2]

[1] *Department of electrical engineering, Firouzabad Higher Education Center, Shiraz University of Technology, Shiraz, Iran.*
[2] *Power Systems Engineer at APD Engineering, Perth WA 6000, Australia.*

* ***Corresponding Author:*** *s.hasanvand@sutech.ac.ir*

ARTICLE INFO

Keywords:
Primary frequency control,
Secondary frequency control,
Microgrid,
Spinning reserve.

Article history:
Received: 09 January 2024;
Revised: 06 April 2024;
Accepted: 08 April 2024;

Article type:
Research Article

ABSTRACT

In this paper, the effect of a battery energy storage system (BESS) as a spinning reserve is considered to control the frequency of a microgrid consisting of a diesel generator, photovoltaic, BESS, and electrical loads. In this stand-alone microgrid, the output power of diesel generators and the BESS are subject to variations to compensate for power fluctuations caused by the load and output power of photovoltaic. Therefore, secondary control, in addition to the primary control, has been proposed to deal with frequency deviation and accelerate the operation of spinning reserve. The scheme is simulated in a hybrid power plant, where results show the effectiveness of the secondary control on frequency deviation damping of the microgrid, thus improving dynamic stability.

1. Introduction

In the past, frequency has not been a major problem for most power systems due to low electricity demand in comparison to power resources. Recently, for economic and environmental reasons, power systems have operated at their maximum capacity and near their boundaries, which may affect frequency stability. Therefore, in addition to providing a reliable power supply, the technologies of new power generation controllers should be more efficient and upgraded to control the basic parameters of the network, such as frequency [1-3]. Due to the need to supply remote areas, smaller stand-alone power grids have no access to interconnected networks to deliver electricity and feed the load. Connecting these areas to the main grid is a time-consuming and costly project, or in some cases physically impossible, where sensitive protection devices need to be devised to prevent devastating faults [4]. These grids usually supply their energy through a distributed generation system, called a microgrid. Electricity in microgrids is traditionally generated using diesel fuel. The high cost of such generation of electrical energy and its

environmental problem have encouraged the utilization of renewable energy resources [5-7]. These resources have many advantages for power systems, but their output power is uncertain and probabilistic. Therefore, the widespread integration of power systems faces some challenges. On the other hand, spinning reserve (SR) is one of the most important ancillary services to maintain system reliability during hazardous events. In microgrids, due to the presence of renewable sources with uncertain output, the frequency of the system experiences more oscillation than usual; so, they should be controlled so that network frequency and stability are kept within acceptable boundaries. A developing network is divided into primary, secondary, and tertiary control hierarchy, which focuses on power delivery and frequency control by balancing generation and load. Increased penetration of renewable energy to 50% of the total energy requires new solutions to maintain the stability of such a system [8].

Power systems integrated with intermittent renewable power generation require more advanced control, as well as an SR to maintain the stability of basic parameters such as voltage and frequency. This SR can be supplied by generation on the demand side [9]. Another solution is to use optimal control for power resources in microgrids. This method is becoming more important today due to the lack of SR [10]. Hybrid power plants are an optimal approach for remote networks [11]. Increasing the penetration of renewable energy such as photovoltaic is leading to more fluctuations in the grid frequency. Storage systems with a combined heat pump can participate in frequency treatment [12]. Other cases of energy storage technologies e.g. batteries [13], and flywheels [14], can also help frequency control in a microgrid. However, these technologies are complex and costly, and their effects on operating and maintenance costs have not yet been entirely evaluated [15]. In the case of events such as load failure or generation shortage, system stability will be affected and may lead to a critical situation. As a result, energy storage devices help the enhancement of the stability of microgrids. Among the main energy storage devices are battery energy storage systems (BESS), flywheels, and capacitive units [16-18]. The benefits of installing renewable energy resources are reduced if the SR is fully allocated to them. One solution is adopting inverters for storage systems and applying proper control. Therefore, a combination of renewables and storage systems performs the roles of primary and secondary frequency control and shares the total SR [19]. A frequency control method using the fuzzy PI controller is proposed in [20] to ensure active power balance and frequency fluctuations damping in a microgrid power system. The integration of BESS with such a system compensates for the fluctuations of renewable energy output to have an acceptable frequency response. Reference [21] provides a multitasking program for a large-scale BESS that stores excess PV energy and provides a secondary control strategy. In [22], during high fluctuation power, the BESS adjusts the output of PV to ensure that the net power injected from the PV/BESS system into the grid is smooth. For this purpose, an improved dynamic BESS model with charge controller feedback is proposed. Additional BESS capacity may be available to improve the efficiency of the energy storage system. This means that the frequency correction reserves by this approach are more economical [23]. The frequency control service is given significant

importance, and a concise overview of the interconnections between energy storage, energy production, and energy consumption components may be found in reference [24]. Furthermore, a comprehensive evaluation of BESS grid applications in the last decade is employed to gauge advancements in technological and economic research, as well as the health condition and charge level. This work introduces a novel approach to examining the duty cycle of BESS applications. It enhances the understanding of BESS operations and facilitates their integration with technical and economic operations [24]. This is achieved by performing a comprehensive evaluation of the grid application and integrating the BESS. The review study [25] encompasses comprehensive and impactful research that specifically examines the current advancements in hybrid PV-BESS systems. This report additionally encompasses a meticulous evaluation of the research projects that were carried out with hybrid PV-BESS systems. The review examines the merits and limitations of these investigations, together with the limitations they may encounter, and the possibility for further enhancement. The study [26] investigates, evaluates, and classifies the uses of BESSs based on the time constants associated with each application. The literature [27] aims to investigate the power quality problems arising from wind turbines in the electrical system, and how BESS can mitigate or minimize these disruptions in the network. Wind power, thermal power, and hydropower all contribute to system frequency regulation. The technique described in [28] allocates reserve capacity among these three power sources. In multi-objective chance constraint programming, the optimization goals of the economics and frequency stability are considered. The research presented in [29] proposes the integration of an energy storage system (ESS) into the control loop to regulate the frequency in cases of network instability or when the average frequency between connected areas deviates from zero.

According to the literature, frequency control is one of the most important issues in power systems especially in microgrids including renewable resources. Considering the advantages and disadvantages of frequency control methods, this paper proposes a hybrid control system including BESS and secondary control for SR in a microgrid.

Due to frequency deviation, the secondary control decides how much the diesel generator and BESS output will change. The effect of secondary control on the diesel generator due to mechanical parts increases response time, fuel consumption, and cost, but there is no problem with reducing inertia. On the other hand, the effect of secondary control on the battery is very effective in improving the frequency but low inertia may cause some problems. Thus, the proposed method considers these two resources for SR with the following features:

- The secondary control for several diesel generators and BESS is designed to participate in frequency control.
- In this paper, the BESS acts as a spinning reserve, in which:

  A. Daily load profile is more realistic and peak load day is considered (summer day load profile).

  B. Diesel generators have less fluctuation and do not have a high peak at outage time.

C. The frequency fluctuations are decreased as a result of applying the proposed control system.

2. Modeling and formulation

2.1. Primary control and governor

The governor is the primary control of a generator that controls the active power output of a generator. After a load change, the governor immediately changes the diesel torque and its generation to supply the load. It causes an imbalance between mechanical torque and electrical torque in the generator shaft. So, the rotor velocity and the frequency are changed. On the other hand, the primary controller of BESS is integrated with its controller to regulate the output power and the frequency. The primary controller regulates the frequency around the nominal value after a short time by changing the load which has been shown in Figure 1. The frequency deviation is proportionate to the amount of load increase/decrease and the control parameters of primary control which was configured in the governor of diesel generators or BESS frequency controller.

As indicated in Figure 2, the modified output power of a diesel generator or BESS can be computed due to Equation (1):

$$P_i' = P_i + \Delta P_i \quad (1)$$

P_i': is the modified active power of the power source *i*.

P_i: is the initial active power value of power source *i*.

ΔP_i: is the active power change in the power source according to primary control.

ΔP_i: is determined by the total frequency deviation and the corresponding primary control gain K_{pf_i} (i.e. the inverse of the droop value)

$$\Delta P_i = \Delta f * K_{pf\_i} \quad (2)$$

K_{pf_i} : is the primary control gain of generator i: [MW/HZ];

Δf: is the total frequency deviation.

Δf can be calculated as follows:

$$\Delta f = \frac{\Delta P_{Tot}}{\sum K_{pf}} \quad (3)$$

$\sum K_{pf}$: is the summation of the primary control gain of all generators and BESS;

ΔP_{Tot}: is the total active power change by the primary control.

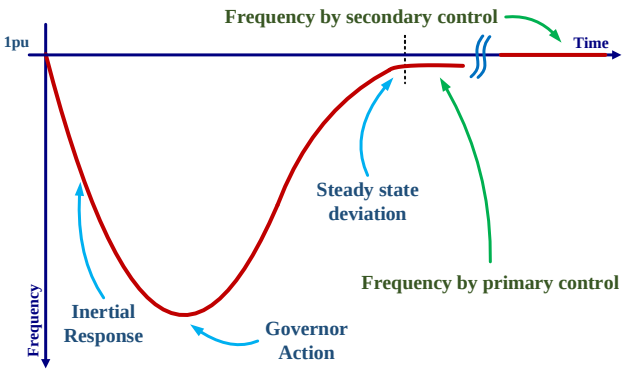

Figure 1. Frequency deviation followed by load increase [6].

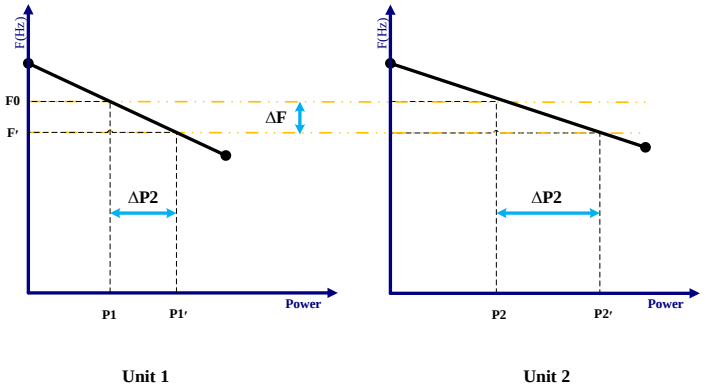

Figure 2. Dividing the power by units parallel to specific droop.

2.2. Secondary control

As a result, at the primary control, a change in the load of the grid causes the steady-state frequency deviation. Restoring the frequency value to the nominal value and eliminating the error requires supplementary control action. Secondary control adjusts power supply set points to keep the frequency at the nominal value. The secondary control operates much slower than the primary control and compensates for the frequency deviation after the operation of the primary control. The secondary control can be considered as an SR that can deliver the required active power to the grid for frequency error correction [2].

3. Case study and its components

The understudy network is an islanded microgrid that consists of two diesel generators that supply the network load, BESS, and a PV power plant. Diesel generators have similar settings and their active power generation values at nominal power are 0.85 (MW) on average. Output power for PV and BESS are 2.84 and 3 MVA respectively [2]. Table 1 tabulates the list of generation units adopted in the system, and provides their capacity. Single-line diagram of these units and configuration of the main bus, load, diesel generators, PV, and BESS are illustrated in Figure 3.

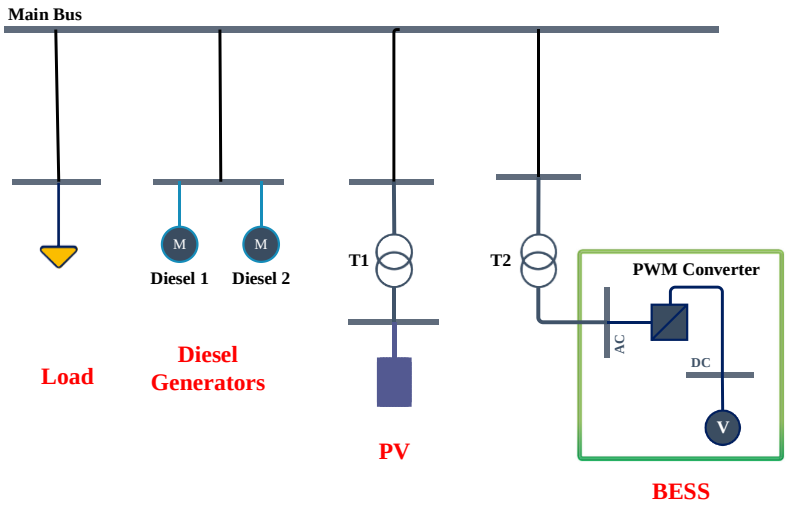

Figure 3. Single-line diagram of a hybrid power plant.

Table 1. Generation units of the system.

5- Main components	4- Capacity	3- Unit
8- Diesel generator × 2	7- 1.02	6- [MVA]
11- PV	10- 2.8	9- [MWp]
14- BESS	13- 23	12- [MWh]

3.1. Secondary controller model

The secondary controller includes five slots which are shown in Figure 4. The first left slot is the frequency measurement, which provides the frequency in the reference bus and sends the signal to the secondary controllers. The second left slot is the secondary controller which receives the measured frequency and sends the control signals to keep the frequency at the nominal value. The third slot is the controller of the BESS. And the last two slots are the diesel governor models [2].

The control signal (dp_sec) as an active power is added to the initial set point of the control models. The model of diesel governors and BESS controller need to be adjusted by adding one input of (dp_sec) to each one, and its value has been used utilizing new summation points to the original power set point of each model.

The secondary controller is the sub-system, which is attached to the secondary slot model. The input of this sub-system is the frequency, which is provided by the frequency measurement device. The output is active power change, which is sent to the governors

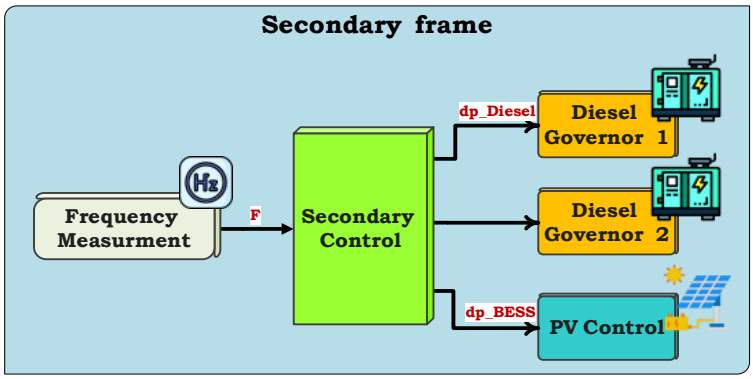

Figure 4. Composite frame model of the secondary controller.

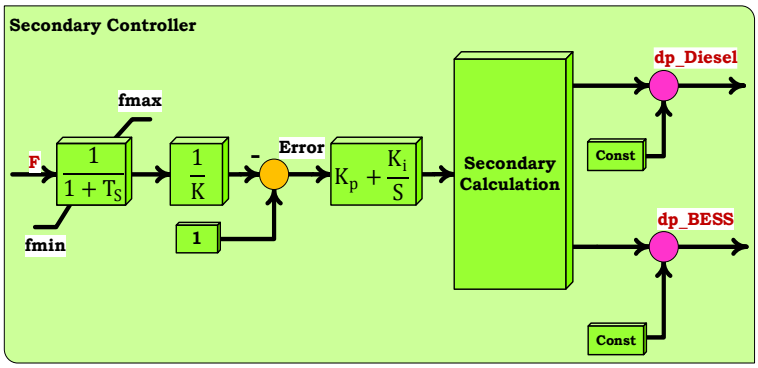

Figure 5. The secondary controller designed with seven blocks.

of the diesel generators (dp_Diesel), and the power controller of the BESS (dp_BESS). The secondary controller is designed by seven blocks (Figure 5) and described as follows:

1. Time delay: represents the reaction of the secondary control compared to the primary control.
2. Gain 1/f: returns the value of the frequency from Hz to per unit value.
3. Constant signal: the set value of the frequency which is 1 [pu].
4. Primitive controller type PT1: has been obtained from the global library of PowerFactory, which has the transfer function of 1/(K+sT).
5. Signal divider: it divides the control signal between the attached blocks to determine their contribution to the secondary control. This block has a main role in secondary control.
6. Constant signal: changes per unit to (MW) value.
7. Constant signal: changes per unit to (MW) value.

The secondary control for active power is distributed between the diesel generators and BESS according to Equation (4) [5]:

$$Kp_j = P_{disp,j} / \sum_{i=0}^{i=n} P_{disp,i} \quad (4)$$

K_{pj}: is the power-sharing factor of the secondary control for the power source (j).

$P_{(disp,\,j)}$: is the dispatch power of the power source to be applied in secondary control.

n: is the number of the attached power sources in the secondary controller.

$$P_j = P_{primary,j} + Kp_j . dP_{secondary} \quad (5)$$

P_j: is the output power of the power source.

$P_{(primary,\,j)}$: is the output power of the power source, which is defined by the primary controller.

$dP_{secondary}$: is the total power change demanded by the secondary controller.

3.2. Load and PV profile

The load profile is an estimation of the total energy required by the power system or subsystem over a given period (hours, days, and so on). In this simulation, the load profile is daily (24 hours) and depicted in Figure 6.

The output power of PV modules is a function of solar radiation. PV is simulated as a negative charge. Therefore, it is similar to the load in the system, but the parameters have negative values. The PV output power characteristics are modeled for a sunny day and shown in Figure 7.

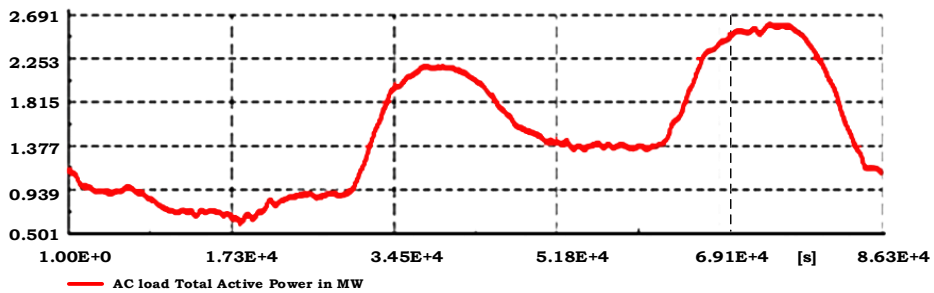

Figure 6. Load profile for the simulated day.

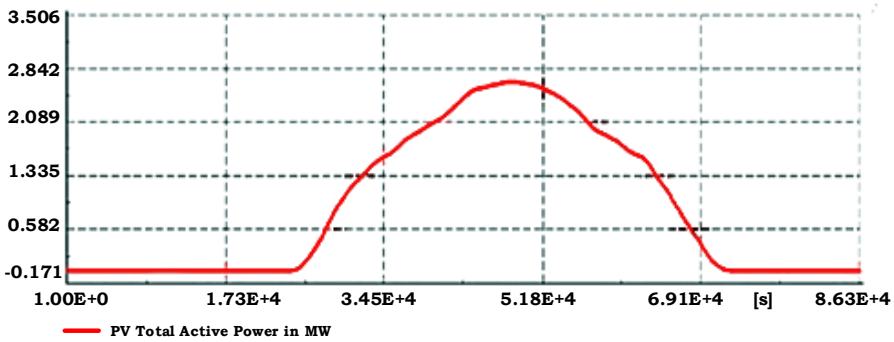

Figure 7. PV power profile for the simulated day.

4. Simulation

Primary and secondary controls in this paper are used to control active power and frequency. in the studied microgrid BESS, diesel generators, and PV are considered as energy resources. PV plant injects all accessible energy into the network by solar radiation, thus the primary and secondary control on the PV plant control section cannot be applied. In this study, the first diesel generator is disconnected from the network when the PV plant is operated at 6:30 a.m. and reconnects at 8 p.m. The total operating time is 10.5 hours. On the other hand, the second diesel generator disconnected at 7 am and reconnected to the network at 7:30 pm. The total operating time for the second is 11.5 hours. The network frequency fluctuates during the disconnection and connection of diesel as well as the connection time of the PV plant. To control the frequency, three strategies are introduced in this study:

Strategy 1: In the first strategy, primary control is applied to diesel generators and BESS.

Strategy 2: In the second strategy, primary and secondary control are applied to diesel generators and BESS.

Strategy 3: In the third strategy diesel generators and BESS perform primary control, but BESS participation is more for secondary control.

4.1. Output power of diesel generators

Figure 8 shows the output power for each diesel generator for all strategies. In the first strategy, because diesel generators do not participate in the secondary control, the amount of diesel output is constant, Figure 8(a). In the second strategy due to secondary control of the diesels, the output power fluctuations are visible in Figure 8(b). In this strategy, network reliability is decreased because of continuous changes in diesel generators output which reduces their lifetime. In the third strategy, due to more BESS participation, diesel generators experience fewer fluctuations, as shown in Figure 8(c). Therefore, the issue of repair and maintenance and its costs is varied due to the operation of diesel generators. This combination of secondary control consisting of BESS and diesel has better results in power and frequency fluctuations and it is more reliable and efficient.

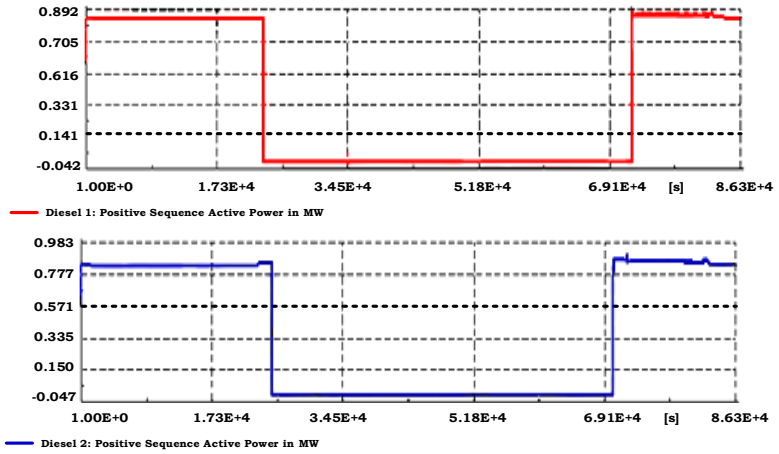

(a)

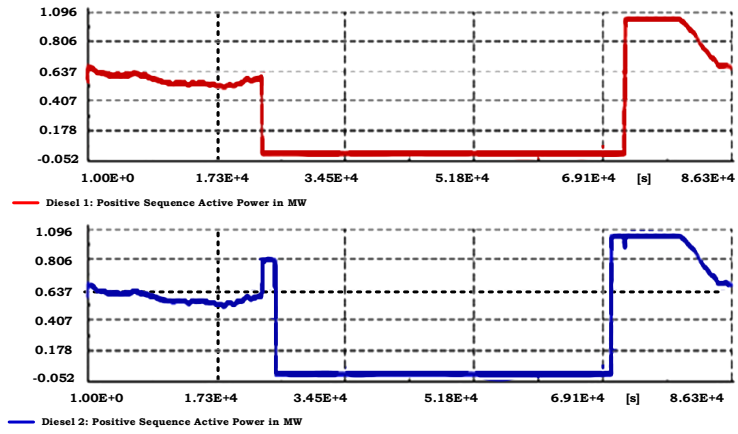

(b)

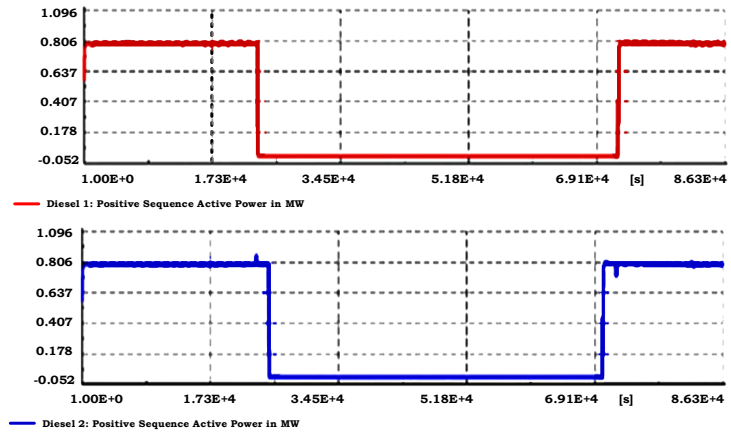

(c)

Figure 8. (a) Output power of diesel generators of strategy 1.
(b) Output power of diesel generators of strategy 2.
(c) Output power of diesel generators of strategy 3.

4.2. BESS output power

This paper aims to survey batteries' performance on spinning reserves to control frequency and increase network reliability; three important points should be investigated. The first one is the fluctuations of charge (power consumption from the network) and

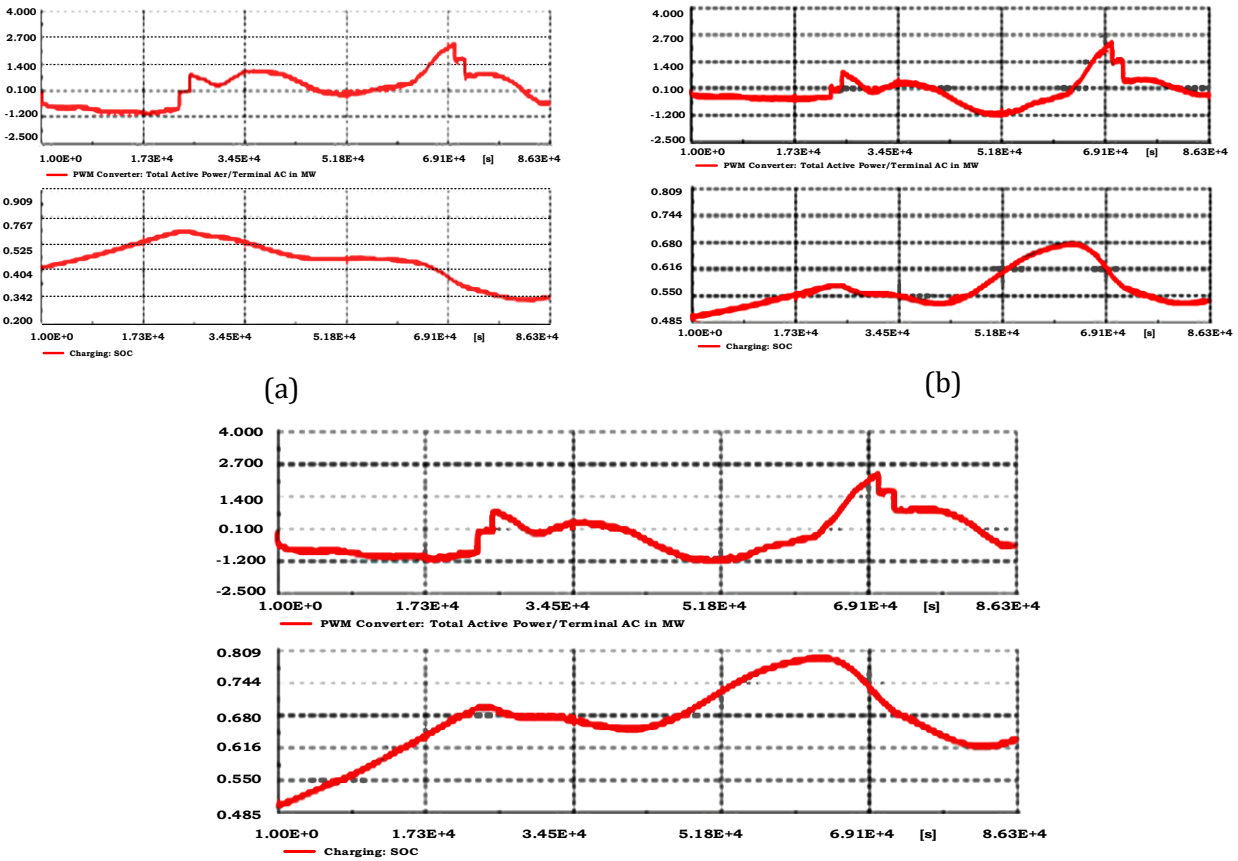

Figure 9. (a) BESS output power of strategy 1.
(b) BESS output power of strategy 2. (c) BESS output power of strategy 3.

discharge (power injection to the battery). The second one is the changes in battery state of charge (SOC), which affect battery lifetime. The third one is the reaction of the BESS control system and the secondary control) to the entry and outage events of diesel generators, load, and PV. Figure 9 indicates the fluctuating output power of BESS. These fluctuations are more evident when PV generates power during the daytime. Figure 9(a) shows constant value output for diesel, which has no role in frequency correction but the BESS control system responds quickly to these fluctuations. In Figure 9(b), after applying secondary control on diesel generators and BESS, it Causes changes in BESS production and consumption. It is quite clear that power generation and consumption are lower compared to strategy three. The charge rate of strategy three is higher than others because the output of PV and diesel generators is more than the amount of load consumption which indicates there is excess power in the network and it is better to utilize this excess power in spinning reserve. Strategy 3 minimizes fluctuations in battery charge and discharge. Comparing three strategies to describe BESS's response in network events indicates that the third strategy operates better than others. Moreover, battery SOC changes are in a respectable performance range in all three strategies [30].

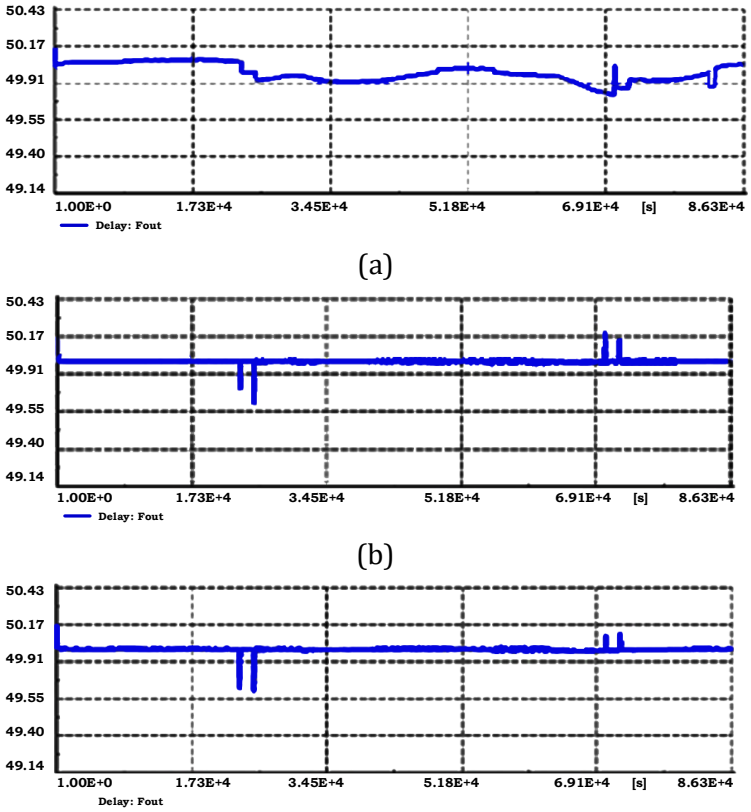

Figure 10. Frequency during a day
(a) Strategy 1. (b) Strategy 2. (c) Strategy 3.

4.3. Frequency analyzing

Frequency deviation analysis for three strategies is surveyed in this section. Figure 10 describes the frequency fluctuation of the network in 24 hours. As can be seen, when secondary control is not utilized in Figure 10(a), the frequency response after the mentioned events is not reasonable because of its fluctuations, but it is satisfactory for the third strategy as shown in Figure 10(c). The result of the second strategy is also acceptable, but the output of diesel generators changes, and as mentioned before this approach is not economical.

5. Conclusions

In this paper, secondary control is introduced for controlling frequency deviation and rapid control of the SR in an islanded microgrid. The secondary control operates in such a way that the diesel generator and BESS have participated in secondary control. Three strategies in the presence of diesel generators, PV, and BESS have been investigated and the best one has been introduced.

As a result, the outcomes of the proposed method are as follows:

- Using BESS as a SR contributes to:
  - preventing the use of diesel generators (as spinning reserves), thus reducing the variable cost of the system (including fuel and repair/maintenance) and air pollution (greenhouse gases).

- saving surplus energy of PV.
- increasing the response time of the system and thus stability.

- Power fluctuation is compensated based on the primary and secondary control of BESS; therefore, the output power of diesel generators becomes more constant and closer to the nominal value.

Frequency deviation becomes lower when the primary and secondary control is performed by the BESS.

References

[1] J. Horne, D. Flynn, and T. Littler, "Frequency Stability Issues for Islanded Power Systems," *2004 IEEE PES Power Systems Conference and Exposition*, vol. 1, pp. 299-306, 2004.

[2] M. Abasi, M. Joorabian, A. Saffarian, and S. G. Seifossadat, "A Comprehensive Review of Various Fault Location Methods for Transmission Lines Compensated by FACTS Devices and Series Capacitors," *Journal of Operation and Automation in Power Engineering,* vol. 9, no. 3, pp. 213-225, 2021.

[3] M. Sadeghi, and M. Abasi, "Optimal Placement and Sizing of Hybrid Superconducting Fault Current Limiter for Protection Coordination Restoration of the Distribution Networks in the Presence of Simultaneous Distributed Generation," *Electric Power Systems Research*, vol. 201, 107541, 2021.

[4] M. Abasi, A. T. Farsani, A. Rohani, and M. A. Shiran, "Improving Differential Relay Performance During Cross-Country Fault Using a Fuzzy Logic-Based Control Algorithm," *2019 5th Conference on Knowledge Based Engineering and Innovation (KBEI),* pp. 193-199, 2019.

[5] B. Idlbi, "Dynamic Simulation Of a PV-Diesel-Battery Hybrid Plant for OFF Grid Electricity Supply," *Kassel and Faculty of Engineering at Cairo*, 2012.

[6] D. Nikolic, M. Negnevitsky, and M. De Groot, "Fast Demand Response as Spinning Reserve in Microgrids," *Mediterranean Conference on Power Generation, Transmission, Distribution and Energy Conversion (MedPower 2016),* pp. 1-5, 2016.

[7] Z. He, J. Zhou, N. Sun, B. Jia, and H. Qin, "Integrated Scheduling of Hydro, Thermal and Wind Power with Spinning Reserve," *Energy Procedia*, vol. 158, pp. 6302-6308, 2019.

[8] A. Gitis, M. Leuthold, and D. U. Sauer, "Applications and Markets for Grid-Connected Storage Systems," *Electrochemical Energy Storage for Renewable Sources and Grid Balancing*, pp. 33-52, 2015.

[9] S. N. Palacio, K. J. Kircher, and K. M. Zhang, "On the Feasibility of Providing Power System Spinning Reserves from Thermal Storage," *Energy and Buildings*, vol. 104, pp. 131-138, 2015.

[10] H. Al Yammahi, and A. Ai-Hinai, "Intelligent Frequency Control Using Optimal Tuning and Demand Response in an AC Microgrid," *2015 International Conference on Solar Energy and Building (ICSoEB),* pp. 1-5, 2015.

[11] C. Lins, L. E. Williamson, S. Leitner, and S. Teske, "Renewable Energy Policy Network for the 21st Century (REN21)," pp. 1-31, 2014,

[12] G. Angenendt, M. Merten, S. Zurmühlen, and D. U. Sauer, "Evaluation of the Effects of Frequency Restoration Reserves Market Participation with Photovoltaic Battery Energy Storage Systems and Power-To-Heat Coupling," *Applied Energy*, vol. 260, 114186, 2020.

[13] D. Kottick, M. Blau, and D. Edelstein, "Battery Energy Storage for Frequency Regulation in an Island Power System," *IEEE transactions on energy conversion*, vol. 8, no. 3, pp. 455-459, 1993.

[14] N. Hamsic, A. Schmelter, et al., "Increasing Renewable Energy Penetration in Isolated Grids Using a Flywheel Energy Storage System," *International Conference on Power Engineering, Energy and Electrical Drives*, pp. 195-200, 2007.

[15] ABB, "ABB-PowerCorp. (2012). Low-Load Diesel (LLD) product," Abb, 2012.

[16] H. Bevrani, F. Habibi, P. Babahajyani, M. Watanabe, and Y. Mitani, "Intelligent Frequency Control in an AC Microgrid: Online PSO-Based Fuzzy Tuning Approach," *IEEE Transactions on Smart Grid*, vol. 3, no. 4, pp. 1935-1944, 2012.

[17] I. Staffell, and M. Rustomji, "Maximising the Value of Electricity Storage," *Journal of Energy Storage*, vol. 8, pp. 212-225, 2016.
[18] S. A. Pourmousavi, and M. H. Nehrir, "Real-Time Central Demand Response for Primary Frequency Regulation in Microgrids," *IEEE Transactions on Smart Grid*, vol. 3, no. 4, pp. 1988-1996, 2012.
[19] A. Dolara, F. Grimaccia, S. Leva, M. Mussetta, and E. Ogliari, "Stability Analysis and Optimal Energy Management of a Stand-Alone Hybrid Microgrid," *IEEE International Conference on Environment and Electrical Engineering and 2018 IEEE Industrial and Commercial Power Systems Europe (EEEIC / I&CPS Europe)*, pp. 1-6, 2018.
[20] X. Li, D. Hui, L. Wu, and X. Lai, "Control Strategy of Battery State of Charge for Wind/Battery Hybrid Power System," *IEEE International Symposium on Industrial Electronics*, pp. 2723-2726, 2010.
[21] A. Zeh, M. Müller, H. C. Hesse, A. Jossen, and R. Witzmann, "Operating a Multitasking Stationary Battery Storage System for Providing Secondary Control Reserve on Low-Voltage Level," *International ETG Congress 2015; Die Energiewende - Blueprints for the new energy age,* pp. 1-8, 2015.
[22] M. Z. Daud, and A. Mohamed, "A Novel Coordinated Control Strategy of PV/BES System Considering Power Smoothing," *IEEE Conference on Clean Energy and Technology (CEAT)*, pp. 416-421, 2013.
[23] G. B. M. A. Litjens, E. Worrell, and W. G. J. H. M. van Sark, "Economic Benefits of Combining Self-Consumption Enhancement with Frequency Restoration Reserves Provision by Photovoltaic-Battery Systems," *Applied Energy*, vol. 223, pp. 172-187, 2018.
[24] C. Zhao, P. B. Andersen, C. Træholt, and S. Hashemi, "Grid-connected battery energy storage system: a review on application and integration," *Renewable and Sustainable Energy Reviews,* vol, 182, 113400, 2023.
[25] M. M. Rana, M. Uddin, et al., "A Review on Hybrid Photovoltaic–Battery Energy Storage System: Current Status, Challenges, and Future Directions," *Journal of Energy Storage*, vol. 51, 104597, 2022.
[26] M. Eskandari, A. Rajabi, A. V. Savkin, M. H. Moradi, and Z. Y. Dong, "Battery Energy Storage Systems (BESSS) and the Economy-Dynamics of Microgrids: Review, Analysis, and Classification for Standardization of Besss Applications," *Journal of Energy Storage,* vol. 55, 105627, 2022.
[27] L. Pontes, T. Costa, et al., "Operational Data Analysis of a Battery Energy Storage System to Support Wind Energy Generation," *Energies*, vol. 16, no. 3, 2023.
[28] C. Xing, X. Xi, and S. Li, "A Rolling Optimization Method of Reserve Capacity Considering Wind Power Frequency Control," *Journal of Renewable and Sustainable Energy*, vol.14, no.1, 2022.
[29] M. W. Siti, N. T. Mbungu, D. H. Tungadio, B. B. Banza, and L. Ngoma," Application of Load Frequency Control Method to a Multi-Microgrid with Energy Storage System," *Journal of Energy Storage,* vol. 52, 104629, 2022.
[30] Spirit Energy "Battery Storage Knowledge Bank- Understanding Batteries," *SPRIT*, 2020.

Declaration of Competing Interest

The authors declare that they have no known competing financial interests or personal relationships that could have appeared to influence the work reported in this paper. The ethical issues, including plagiarism, informed consent, misconduct, data fabrication and/or falsification, double publication and/or submission, redundancy, have been completely observed by the authors.

Credit Authorship Contribution Statement

Saeed Jamshidi: Conceptualization, Formal analysis, Methodology, Roles/Writing - original draft. **Hossein Bagheri:** Data curation, Funding acquisition, Methodology, Software. **Saeed Hasanvand**: Conceptualization, Methodology, Supervision, Roles/Writing - original draft. **Mohammad Esmaeil Hassanzadeh:** Conceptualization, Methodology, Software, Supervision, Roles/Writing - original draft. **Arash Rohani:** Formal analysis, Resources, Roles/Writing - original draft

Bibliography

Saeed Jamshidi received his BSc. degree in electrical engineering from Firouzabad Institute of Higher Education, Iran, in 2019. His research interests include power system stability and optimization, micro-grids and renewable energies. Also, he has a professional technical certificate in industrial electricity.

Hossein Bagheri received his BSc. degree in electrical engineering from Firouzabad higher education center, Iran, in 2019, the MSc. degree from University of Tafresh, Iran, in 2021. His currently an employee of Persian Processing Energy Power (PPEP) company. His research interests include power electronics, electric machines, microgrids and renewable energy.

Saeed Hasanvand received his BSc. degree in electrical engineering from Shahid Chamran University of Ahvaz, Iran, in 2009, the MSc. degree from University of Isfahan, Iran, in 2012, and the PhD. From Shiraz University of Technology, Iran, in 2017. He is currently an assistant professor in electrical engineering at Firouzabad higher education center, Shiraz university of technology. His research interests include power system stability and optimization, micro-grids, renewable energies, FACTS devices, and power system reliability.

Mohammad Esmaeil Hassanzadeh received his MSc. and Ph.D. degrees from Shiraz University of Technology, Iran, in 2015 and 2022 respectively. He is currently an assistant professor in electrical engineering at Firouzabad Higher Education Center, Shiraz University of Technology. His research interests include power system stability and optimization, micro-grids, renewable energies, FACTS devices, and power electronics.

Arash Rohani received his B.Sc. and M.Sc. degrees in electrical engineering from Shahid Chamran University of Ahvaz, Iran, in 2009 and 2013, respectively. With 8 years of experience at the Khuzestan Regional Electric Company, he currently contributes his expertise at APD Engineering in Australia. Arash's research interests encompass power quality, protection, power system operation, and energy management.

Journal of Green Energy Research and Innovation

Sensitivity Analysis of the Problem of Contribution of Energy Storage Devices to Providing Inertia for the Primary Frequency Response

Moaiad Mohseni, Alireza Niknam Kumleh, Rezvan Keshavarzpour

Highlight

- **Providing an inertial response for ESS with fast response capability**
- **Investigating the effect of inertial response in establishing frequency response and network behavior after sudden events**
- **Considering the new model of the problem and applying the novel algorithm for this problem**

Graphical Abstract

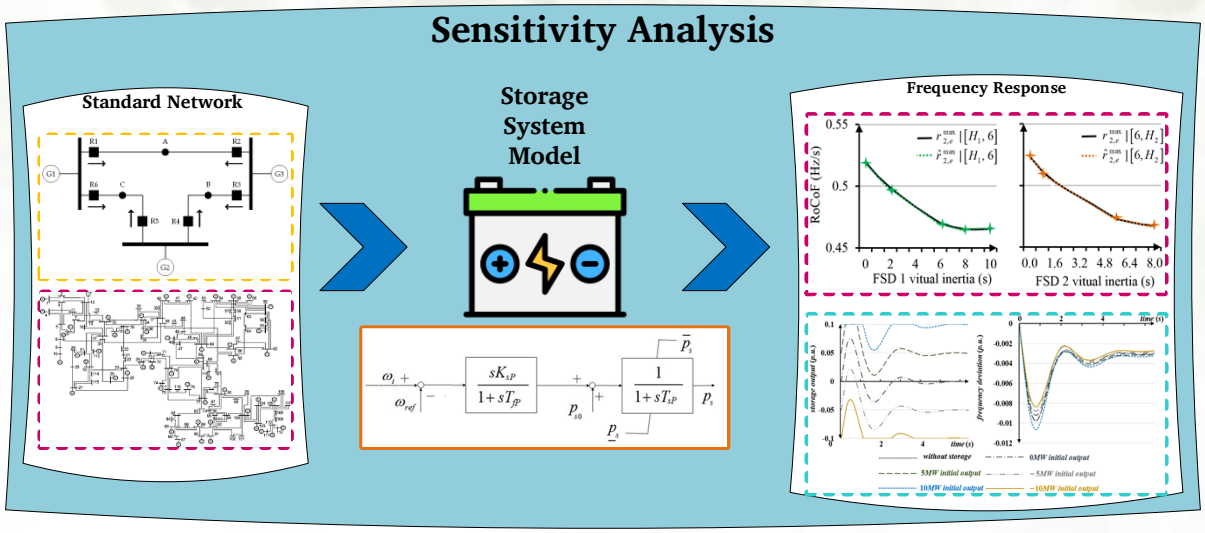

Use your device to scan and read the article online

Citation

M. Mohseni, A. Niknam Kumleh, and R. Keshavarzpour, "Sensitivity Analysis of the Problem of Contribution of Energy Storage Devices to Providing Inertia for the Primary Frequency Response," *Journal of Green Energy Research and Innovation*, vol. 1, no. 3, pp. 30-48, 2024.

https://doi.org/10.61186/jgeri.1.3.30

JGERI Journal of Green Energy Research and Innovation

Online ISSN: 3041-9018

Journal of Green Energy Research and Innovation

Journal Homepage: www.jgeri.araku.ac.ir

Sensitivity Analysis of the Problem of Contribution of Energy Storage Devices to Providing Inertia for the Primary Frequency Response

Moaiad Mohseni [1]*, Alireza Niknam Kumleh [2], Rezvan Keshavarzpour [3]

[1] *Khuzestan Regional Electric Company, Ahvaz, Iran.*
[2] *Faculty of Electrical Engineering, Amirkabir University of Technology (Tehran polytechnic), Tehran, Iran.*
[3] *National Iranian South Oil Company (NISOC), Ahvaz, Iran.*

* ***Corresponding Author:*** *moaiadmohsenii@gmail.com*

ARTICLE INFO

Keywords:
Primary frequency, response,
Energy storage,
Virtual inertia,
Sensitivity analysis.

Article history:
Received: 11 March 2024;
Revised: 12 April 2024;
Accepted: 29 April 2024;

Article type:
Research Article

ABSTRACT

Today, with the expansion of low-inertia (such as wind power plants) and non-inertia (such as photovoltaic power plants) technologies, the amount of network inertia and power related to the primary frequency response has decreased significantly. As a result, in the event of disturbances, the frequency changes with a relatively higher slope and it may violate its permissible range. To solve this problem, several methods have been presented so far that create artificial inertia by power electronic converters connected to storage devices or renewable generation. Therefore, the models make the operation of these sources similar to traditional power plants and increase their contribution to the frequency response during storage contribution events. In this paper, the sensitivity analysis of energy storage contribution to providing inertia for the primary frequency response has been carried out. IEEE 3-bus and 118-bus networks are used as test networks. MATLAB software is also adopted for optimization. The results show the impact of each storage parameter on the frequency response and how it is possible to meet the frequency response limitations of the network by managing the storage devices.

1. Introduction

Distributed generations (DGs) such as photovoltaics (PVs) and wind turbines (WTs) have expanded in recent years in power systems and some cases have replaced fossil units [1]. Renewable energy sources (RESs) are highly dependent on climate changes and high fluctuations in their output power are observed. To deal with and eliminate these fluctuations, energy storage systems (ESS) are usually used, which have many advantages such as high response speed, stable power transmission, and no dependence on climatic conditions. One of the issues regarding ESS is their optimal placement in the network, determining their optimal size, and managing their charging status in the network. Adding storage devices to the network requires an initial investment cost, but with its optimal design and management, the total costs of network operation can be reduced. Many studies have been presented in the field of optimal design of ESS. Reference [2] reviewed these methods and their design criteria. Reference [3] provided a review of battery

technology for energy storage. ABB company has designed a storage system and a special converter for it, which provides inertial response in power systems with high reliability. The speed of this system is very high and its ability to reduce frequency deviations has been well proven [3]. In reference [4], storage batteries were used to provide the primary frequency response. In fact, the combined storage system including a battery and a supercapacitor was used to provide the primary frequency response of an isolated microgrid. The principles of providing primary frequency response using storage devices are based on the management and planning of coordinated charging of storage devices. Reference [5] suggested the implementation of a market for frequency response reserve (FRR) in the future grid, specifically targeting generators and load resources equipped with under-frequency relays. The purpose of [6] was to investigate the notion of orientational smoothing in conjunction with the frequency management of deloaded photovoltaic (PV) systems to enhance self-balancing, decrease reliance on battery energy storage systems (BESS), and guarantee a consistently higher availability of regulatory reserves. Study [7] optimized temporary main frequency control parameters during rotor speed recovery using an analytically determined technique to limit secondary frequency deviation induced by DFIG inertial control. Optimized parameters included termination time and active power. Literature [8] focused on the current research trend that aims to increase the participation of wind turbine generators in rapidly regulating the grid frequency (inertia emulation), in addition to conventional power system alternators. Reference [9] presented an adaptive primary frequency support technique for clusters of electric vehicles (EVs) that are limited by the operation region specified by their charging behavior. In reference [10], a DC microgrid was investigated from the point of view of secondary frequency response. This microgrid included RESs and the use of energy storage improved the operation of the microgrid. Energy storage is one of the important components of microgrids that reduce the fluctuations of DGs and improve the operating conditions of the grid both in islanded and grid-connected conditions. In reference [11], integration of ESS units was adopted to provide the secondary frequency response of power systems. In the future, small storage units will be integrated to create a frequency response control service. The method of load frequency control was described in [12] using ESS. In literature [13], the tertiary control of a set of microgrids was presented. In that study, voltage, and frequency control were presented to restore these parameters to their desired nominal value in a set of islanded microgrids. This method is activated when the existing methods for controlling energy storage and generators do not work successfully. This method performs well as a strong support in networks containing a high level of DGs. In reference [14] a storage battery was used to control the voltage and frequency of microgrids. In that study, storage devices with high response speed were incorporated. The results showed that voltage and frequency were able to follow their reference signals suitably. A variety of adaptive control methods for WTs have also been provided, among which the pitch angle control and the rotor speed control have been provided. The results prove that the adaptive control method provides considerably better results than other frequency control methods. From the point of view of the rate of

change of frequency (RoCoF), frequency drop, and reduction of frequency deviation in steady state have been provided. The stepping method of inertial control can reduce the RoCoF, but it leads to a secondary frequency drop [15]. The traditional networks contain a high capacity of synchronous generators (in the form of hydropower, thermal, gas, coal, combined cycle, or nuclear) with high inertia. The high inertia prevents severe frequency deviations in the case of events. Therefore, in the past, the behavior of primary or secondary frequency response was not crucial [16]. Hydroelectric, nuclear, and fossil fuel-based units are naturally effective in providing primary frequency response in two ways. First, due to the high mechanical and kinetic energy of these generation units, these generators provide a high level of inertia response for the grid whenever they are connected to the grid. Second, the inherent characteristic of these units is that they are usually kept connected for a long time, and this leads to a longer persistence of inertia in the network [17]. The emergence of clean energies and their high penetration level in the power system can be considered the main factor of the emergence of frequency response limitations in power system problems. Frequency recovery, the discussion on the frequency stability of the network against disturbances, and the adjustment of the frequency response of the network against sudden incidents of the network are among the priorities of recent research on the operation of power systems. Also, the solutions to increase the penetration level of DGs in the system and the approaches to provide as much inertia as possible are among the most important recent challenges of the frequency response studies of the power system. The effects related to the uncertainty of the behavior of these DGs in the frequency of their power system are technically and economically important [18]. Another economic effect of frequency response limitations in network operation is that the network operator must adjust and plan DGs in such a way that at any moment there are units connected to the network that guarantee sufficient frequency response for a network. New planning of power plant units by considering frequency limitations means adding extra costs of network operation [19]. In reference [20], the effect of energy storage in improving the stability of the frequency response was considered. It was shown that the presence of an ESS device of 1 to 2 MWh next to a 10 MW wind farm can provide the possibility of automatic central control during 29 days of the month. Also, the investigation of the capabilities of ESS in the implementation of automatic central control in the wind research park was considered. Reference [21] reviewed the ESS technology and the progress made in this field. It was mentioned that with the current state of the electricity market, it is difficult for ESS units to compete with traditional electricity generation units. In reference [22] determined the optimal capacity of network storages and optimal control of these systems to provide network frequency improvement. Frequency deviations of power systems, which are usually caused by the fluctuations of grid-connected wind generators, are one of the main factors limiting the penetration of distributed RESs. Reference [23] investigated the effect of frequency response limitations in network operation and in the presence of energy storage. Considering the limitation of the RoCoF in planning the generation of power plants and the use of energy storage can have a great impact on the frequency behavior of the

network. In reference [24], the placement and determination of the optimal size of ESS to control the primary frequency response of an isolated section of the Mexican power grid was presented. The paper showed that the increase in the level of penetration of DGs leads to problems with network frequency. In order to provide the desired frequency response, energy storage batteries were used. In reference [25], the benefits of using energy storage in the market of providing fast frequency response in the national network of England were evaluated. Using equipment with fast response speed can reduce the power imbalance between supply and demand. A real-time strategy for controlling storage devices was presented. Controlling the charge level of energy storage has a significant effect on the life of the storage. In reference [26], ESS was used to prevent under-frequency load shedding. The under-frequency load shedding is one of the temporary measures to prevent the frequency violation at a value lower than the set limit. This action is taken to restore the network to a safe state. By using energy storage and power electronics converters [27], power can be quickly injected into the network, and frequency deviations can be avoided when a power imbalance occurs in the network. In reference [28], lithium-ion batteries were adopted as a tool for fast power transfer in sudden events and stabilization of frequency response. This reference showed how these storage batteries should be installed and utilized in the network. Also, in this research, the charging level of ESS after passing the transient frequency states was optimized. Determining the charge level of energy storage has a significant effect on increasing the life of these equipment. In reference [29], the simultaneous contribution of WTs and ESS to the electricity market to provide frequency response was discussed. In literature [30], the design of the frequency droop controller in hybrid electric vehicles to control the primary frequency response was analyzed. To better understand the primary frequency response control in the presence/absence of ESS, special designs are proposed in this paper and the stability margin of each of these designs is determined. RES and ESS have little or no inertia. Increasing the penetration level of these sources has led to a decrease in network inertia and an increase in the probability of frequency deviation or sudden network collapse. The inertia of the network was not very important in the past, but today, with the penetration of DGs and the change in the dynamic characteristics of the network, the discussion of providing the inertial response and the primary frequency response has received much attention from scholars. One of the most novel approaches to increase network inertia is to utilize the control methods of power electronic converters to show behavior similar to synchronous machines, called virtual inertia, in these sources. This study intends to provide an inertial response for ESS to maintain the frequency stability of the network against the occurrence of sudden events.

The contribution of this paper is to provide an inertial response for ESS with fast response capability. Also, investigating the effect of providing this response in establishing frequency response and network behavior after sudden events is considered among other contributions of this work. Considering the new model of the problem and applying the novel algorithm for this problem are other innovations of current research. Other parts of the paper are structured as follows. In Section 2, the description of the

proposed model is presented. In Section 3, simulations are performed, and a summary of the results is presented in Section 4.

2. Modeling and problem formulation

2.1. Providing the virtual inertia

Inertia response can be created by using fast storage devices because these devices can be charged or discharged at their maximum nominal rate in less than 1 ms. This section of the paper focuses on the primary frequency response, which is dedicated to a period of tens of seconds. Without any specific control strategy, the output level of energy storages (p_s in per-unit or p.u. and P_s in MW) remains at its initial value (i.e., p_{s0} or P_{s0}) after some time (several seconds) after the event. Therefore, fast ESS does not contribute to the transient stability of the network. A method is presented to control the ESS so that they can create virtual inertia H_s in the network. The main idea of this design focuses on controlling the output power of the storage device so that it adjusts its output power based on the local frequency of each of the storage devices. If the local frequency in terms of per-units is f_i and the nominal frequency of the network is $f_B = 60$ Hz, then the corresponding virtual rotation speed is denoted by $\omega_i = 2\pi f_i$ and the nominal rotation speed is expressed by $\omega_B = 2\pi f_B$; therefore, Equations (1) and (2) are established.

$$\Delta p_s = p_s - p_{s0} = -2H_s \Delta\dot{\omega}_i \quad (1)$$

$$\Delta p_s \in \left[\underline{p_s} - p_{s0}, \bar{p}_s - p_{s0}\right] \quad (2)$$

It can be seen that the control signal completely depends on the local frequency. Virtual inertia can be represented by $H_s = \frac{J_s(\omega_B)^2}{2S_B r^2}$ (in seconds) where J_s is in MWs. Therefore, the virtual kinetic energy of the storage device is $E_s = \frac{1}{2}J_s\omega_s^2$ and the virtual mechanical frequency is $\omega_s = \frac{\omega_i\omega_B}{r}$, and r shows the virtual poles of the device. Therefore, the relations can be rewritten as Equation (3):

$$-\Delta P_s = \dot{E}_s = J_s\omega_s\dot{\omega}_s \Leftrightarrow -\Delta p_s = 2H_s\omega_i\dot{\omega}_i \approx 2H_s\dot{\omega}_i \quad (3)$$

Control signals can be measured on the generator side (rotation speed) or the network side (connection point frequency). To achieve real results, storage dynamics, response time, and communication delay are also considered in the simulation. In this paper, ESS is equipped with a dynamic response adjustment controller. The local frequency ω_i can be adjusted using the active power output of the storage control module and the connection point voltage using the reactive power of this module. In this paper, a simplified dynamic model of the storage system is presented, which has two lagging-phase blocks with time constants T_{fP} and T_{sP}. Therefore, the inertial response provided by the module is equal to $K_{sP} = -2H_s\omega_i^2$. This study assumes that the grid power plants are divided into two categories: thermal power plants and gas power plants. Each of these plants has its characteristics and is of special importance from the point of view of dependence on natural gas. It is also assumed that the management of unit commitments will be divided into two parts [31]. The first part (upstream) is related to daily planning (or day-ahead

planning) to comply with the restrictions related to daily energy exchange contracts and the general status of power plants in terms of start/shutdown or initialization (binary variables of the problem) should be specified. The second part (downstream) is related to daily operation (same day) in which any uncertainty or fluctuations are answered in the form of adjusting the power generation of power plants (real continuous variables). In this stage, uncertainty has shown itself and usually, the final result of this stage is obtained based on mathematical expectation of probable events. In this paper, uncertainty is considered on the limits of gas supply lines. Also, to understand the effect of natural gas pricing on the problem, separate case studies will be examined. In the following, the mathematical model of the problem is discussed and then the stochastic form of the problem is presented. Figure 2 shows the output power of the storage device and the frequency deviation in different values of the virtual inertia of the storage devices. The higher the virtual inertia, the better the frequency response of the system. Also, higher values of virtual inertia require higher charging and discharging capacity of ESS.

It can be seen in Figure 3 that if the storage capacity is less than 30 MW, by increasing the charging and discharging capacity, the advantages of virtual inertia in improving the primary frequency response will be reduced.

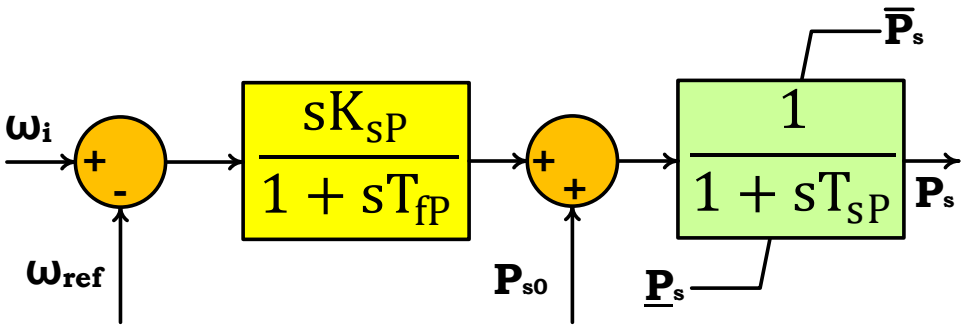

Figure 1. Simplified structure of the grid-connected storage system.

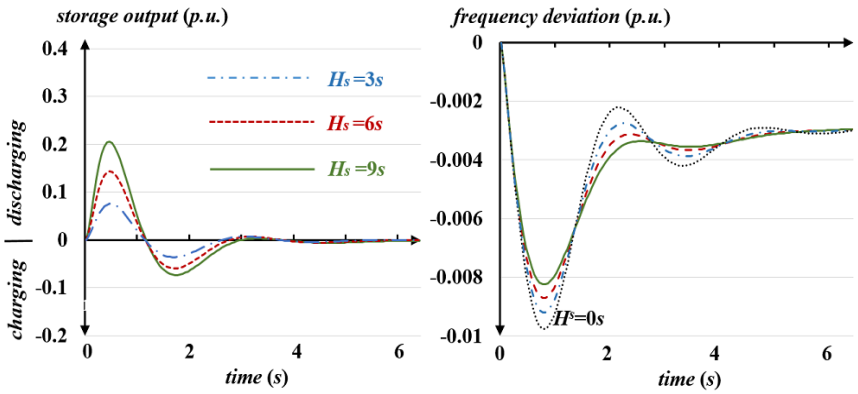

Figure 2. The effect of virtual inertia on the frequency response of the power system considering the dynamics of the storage battery.

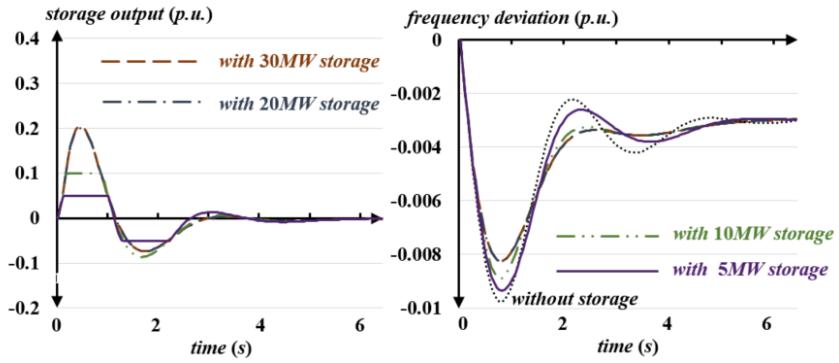

Figure 3. Dynamic simulation by considering the upward charge/discharge limit of storage and dynamics of the storage battery $H_s = 9s$.

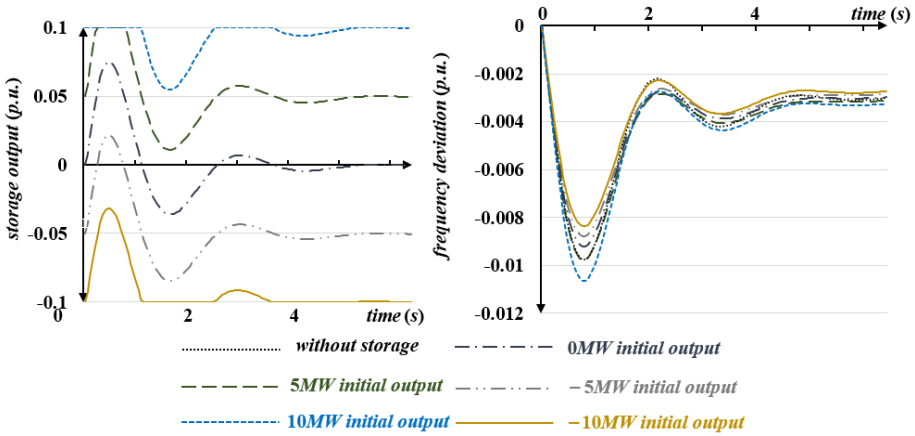

Figure 4. Dynamic simulation with variable initial output of the storage by considering the storage dynamics.

Figure 4 illustrates that the initial output values of the storage devices play a significant role in the behavior of the primary frequency response. The charging state of the storage devices helps to prevent the frequency drop, and the discharge state of the storage devices brings a worse situation in terms of the frequency nadir compared to the state without the use of the storage device. It should also be noted that the storage units with an initial output of -10 MW contribute to the inertial response exactly after the event, but the storage units with an initial output of 10 MW do this only after the frequency drops. These results seem reasonable. Storage devices usually have less free capacity to respond to frequency reduction.

2.2. The problem of minimization of ESS's planning cost

Usually, the generation planning of the power plant is done in 24-hour intervals, and economic load dispatch is carried out every 15 minutes. In fact, after the implementation of the economic load dispatch program every 15 minutes, the necessary measures will be determined to provide transient stability in the next period. To ensure that the frequency or the post-event rate of change occurs within the allowed range, the problem of economic load dispatch is solved.

The purpose of this method is to find the lowest contribution cost of ESS. Under-frequency events are discussed in this paper and the constraints related to the lowest and highest rate of change of frequency are considered in the problem.

2.2.1. Formulation of the storage planning problem

The vector $x = [x_1, x_2, \dots, x_N]^T$ represents the non-negative virtual inertia provided by the storage (decision variables of the optimization problem). The upper and lower limits of these variables are denoted by mathematical symbols $\bar{\bar{H}} = \left[\bar{\bar{H}}_1, \bar{\bar{H}}_2, \dots, \bar{\bar{H}}_N\right]^T$ and $\underline{H} = \left[\underline{H}_1, \underline{H}_2, \dots, \underline{H}_N\right]^T$. The problem of economic planning of storage is formulated as Equations (4 - 7):

$$\min_x : c^T x \tag{4}$$

$$s.t: f_{b,e}^{min_b} \tag{5}$$

$$r_{b,e}^{max_b} \tag{6}$$

$$x_n \in \{0, [\underline{H}_n, \bar{H}_n]\}, for \forall n \in N \tag{7}$$

In these equations, $N = \{1,2,\dots,N\}$ shows the set of storage units, c is the cost of virtual inertia, $f_{b,e}^{min_x}$ is the minimum frequency, and $r_{b,e}^{max_x}$ expresses the rate of change of frequency of each bus $b \in B$ during any given $e \in \varepsilon$ event.

2.3. Iterative solution to problem-solving

Searching in the solution space requires simulating the transient stability of the problem. It seems impractical to provide a comprehensive method for the final results in the real world. To reduce the computational burden, an algorithm for the planning problem is presented in this section. As shown in Figures 5 and 6, linearization can be used to approximate the role of virtual inertia of the storage devices at the minimum frequency of each bus and the highest rate of change of its frequency. The accuracy of the proposed method is optimal. Based on these linearizations, the mixed-integer linear problem is presented and an iterative method will be presented to solve it.

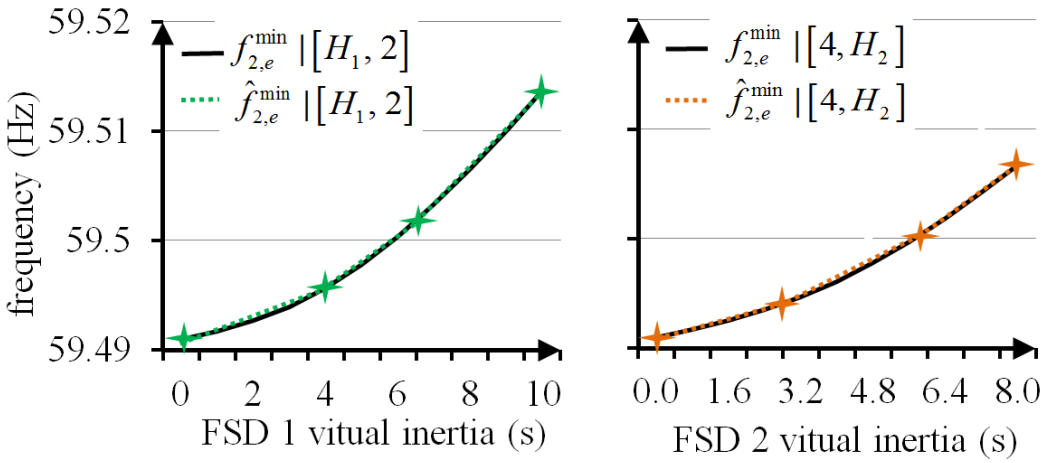

Figure 5. Minimum frequency linearization in a network with two storage devices.

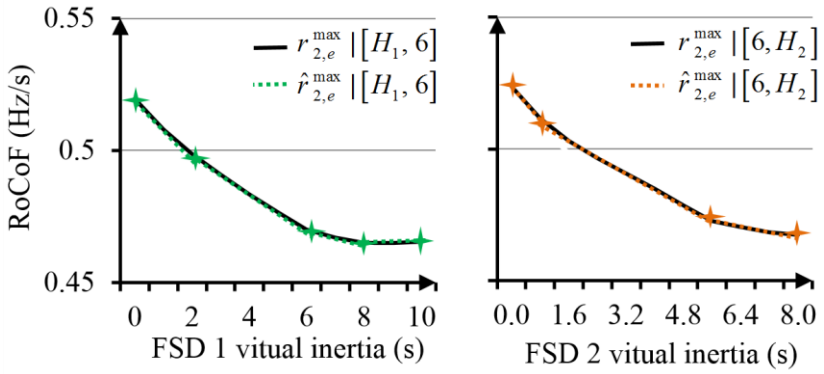

Figure 6. Linearization of the RoCoF in a network with two storage devices.

2.3.1. Formulation of the linearized planning problem

Considering that $\underline{H} \le x \le \bar{H}$, each of the solution zones $\{x_n : \underline{H}_n \le x_n \le \bar{H}_n\}$ can be divided into $\tilde{Z}_n$ sections. The favorable virtual inertia of the nth storage is shown by a vector $(\tilde{Z}_n + 1) \times 1$, named $h_n = [h_{n,0} = \underline{H}_n, h_{n,1}, \dots, h_{n,\tilde{Z}_n} = \bar{H}_n]^T$. The present settings of the virtual inertia are represented by $H = [h_1, h_2, \dots, h_N]^T$. The only difference between vectors $\grave{H}_{n,z} = [\dots, h_{n,2}, \dots]^T$ and $H = [\dots, h_n, \dots]$ is in the virtual inertia settings of the nth storage. Moreover, a vector $\grave{H}_{n,-1} = [\dots, h_{n,-1}, 0, h_{n+1}, \dots]^T$ with $h_{n,1} = 0$ and $Z_n = \{0,1, \dots, \tilde{Z}_n\}$ is defined. The metrics under study and their limits are provided as $m \in M = \{f^{\min}, (-r)^{\max}\}$, and $M_b \in \{\mathcal{E}_b, -\tilde{r}_b\}$, respectively. Therefore, the marginal gain of the zth part of virtual inertia's contribution to the nth storage is given as Equation (8). Also, the equivalent index of the rate of change of frequency or the minimum frequency is represented as Equation (9). With a planning

scheme, the value is defined as Equation (10), which shows the value of participated inertia, H, in the range $[h_{n,-1}, h_{n,2}]$. Figure 7 illustrates the definition of parameters.

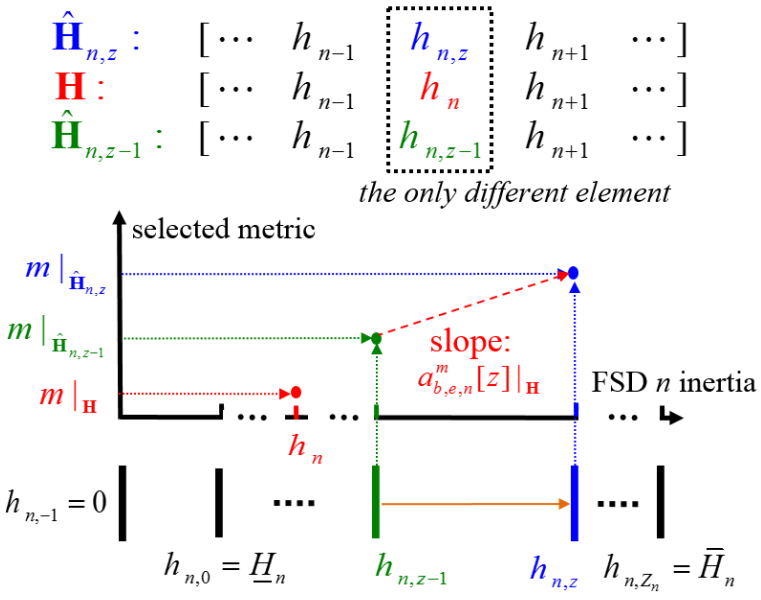

Figure 7. Demonstration of parameters adjustment.

$$\alpha_{b,e,n}^{m}[z]|_H = \frac{m_{b,e}|_{\bar{H}_{n,z-1}}}{h_{n,z} - h_{n,z-1}}, for\ \ z \in Z_n \quad (8)$$

$$v_{b,e}^{m}|_H = M_b - m_{b,e}|_H \quad (9)$$

$$\Delta h_{n,z} = \begin{cases} h_{n,z} - h_{n,z-1}, if\ \ h_{n,z} \le h_n \\ 0, if\ \ h_n \le h_{n,z-1} \\ h_n - h_{n,z-1}; otherwise \end{cases} \quad (10)$$

The objective function in Equation (11) deals with minimizing the overall cost of the contribution of storage devices. In the constraints of Equation (12), the parameter $\alpha_{b,e,n}^{m}[z]\big|_H d_{n,z}$ or $\Delta h_{n,z}$ is linearized in the form of z-segment virtual inertia related to the nth storage named $d_{n,z}$ or $\alpha_{b,n}^{m}[z]_H d_{n,z}$. Hence, $\sum_{n\in\epsilon, z\in\varepsilon_e} a_{p,n}^{m}[z]_H\left(d_{n,z} - \Delta h_{n,z}\right)$ is the linear improvement of the considered indices, and $v_{b,e}^{m}\big|_H$ is the minimum improvement necessary for each index to observe its limits. Equation (13) represents the upper limit of the virtual inertia $d_{n,2}$ related to the z th part. Equations (14) and (15) state that none of the storage devices can produce virtual inertia between zero and $\underline{H_n}$. The $(z+1)$ th part can establish

inertia only when the zth part proposes the whole inertia between $h_{n,z} - h_{n,z-1}$, and these constraints are given in Equations (16) and (17).

$$min_{d,u}: c^T d \quad (11)$$

$$s.t:\ for \forall b \in B, e \in \varepsilon, m \in M \quad (12)$$

$$\sum_{n\in N, z\in Z_n} a_{b,e,n}^{m}[z]|_H\left(d_{n,z} - \Delta h_{n,z}\right) \ge v_{b,e}^{m}|_H \quad for \forall b \in B, e \in \varepsilon, z \in Zn, n \in N \quad (13)$$

$$u_{n,z} \in \{0,1\} \quad (14)$$

$$d_{n,z} \le u_{n,z}\left(h_{n,z} - h_{n,z-1}\right) \quad (15)$$

$$u_{n,0} h_{n,0} \le d_{n,0} \quad (16)$$

$$u_{n,z+1}\left(h_{n,z} - h_{n,z-1}\right) \le d_{n,z}, z \ne \bar{Z}_n \quad (17)$$

The linearized problem of the contribution of power plants has made it possible to implement iterative algorithms. Here, a two-step method to solve the problem is introduced. This method has two loops. The outer loop, denoted by *s*, updates the solution space and divides the solution space. The inner loop, denoted by *k*, will improve the required criteria when there is a violation in the RoCoF or the frequency nadir from the allowed limit. Equation (18) gives the relationship related to updating the outer loop.

$$v_{b,e}^{m(s,k)} = v_{b,e}^{m(s,k-1)} + \beta_{b,e}^{m(s,k)}\left(M_b - m_{b,e}|d^{*(s,k-1)}\right) \quad (18)$$

At the end of each outer loop *s*, the algorithm updates the center of the solution space of the problem $H^{(s+1)}$ using the obtained optimal solution $d^*|_{H(s,K_s)} = d^{*(s,K_s)}$. To guarantee the convergence of the proposed method, the coefficient $\alpha_n^{(s)} \in [0,1]$ is used to break the solution space. Again, the virtual inertial space of each storage device is divided into a new space. Therefore, the marginal profit and its related restrictions are as follows.

In other words, it can be said that in the planning stage, based on the base load, the on and off status of the power plants and their working point is determined from the previous day, taking into account the energy reserve, and based on that, a contract with the gas

supply company is drawn. Then, any difference that occurs on the current day will be determined by operation. In fact, in operation, on/off status is not an issue anymore, and the only goal is to change the generation capacity of power plants. Therefore, there is a possibility of some difference in the operating point of the power plants, their gas consumption, or measures such as load shedding, so that the load can be fully met and the security restrictions of the network are respected.

$$h_{n,0}^{(s+1)} = max\left\{\underline{H}_n, d_n^{*(s,K_s)} - \frac{\alpha_n^{(s)}}{2}\left(h_{n,\bar{Z}_n}^{(s)} - h_{n,0}^{(s)}\right)\right\} \tag{19}$$

$$h_{n,Z_n}^{(s+1)} = min\left\{\bar{H}_n, d_n^{*(s,K_s)} + \frac{\alpha_n^{(s)}}{2}\left(h_{n,\bar{Z}_n}^{(s)} - h_{n,0}^{(s)}\right)\right\} \tag{20}$$

2.3.2. Sensitivity analysis of the problem

On the left side of Figure 8, the value in terms of related to bus 4 is shown for times $t =$ 1,2, and 3 s. According to the obtained results, the changes in the frequency nadir have an almost linear relationship with the injected power ΔP. Hence, the sensitivity of the frequency nadir to the injected power at other points can be found from $\frac{\partial \Delta f_{b,e}^{\min}}{\partial \Delta p} = \frac{\partial \Delta f_{b,e}^{\min}}{\partial p}$. These changes are provided on the right side of Figure 8, where the nonlinear behavior of $\frac{\partial \Delta f_{b,e}^{\min}}{\partial p}$ at any moment is clearly observed. Similar results to Figure 8 are provided in Figure 9, which shows the RoCoF with respect to injected power. In this case, bus 1 (two nods away from bus 69), bus 4 (two nodes away from bus 69), bus 43 (eleven nodes away from bus 69), and bus 17 (eleven nodes away from bus 69) are considered.

Figure 10 depicts the time-dependent changes of indices for bus 1 due to the injection of reactive power into bus 4.

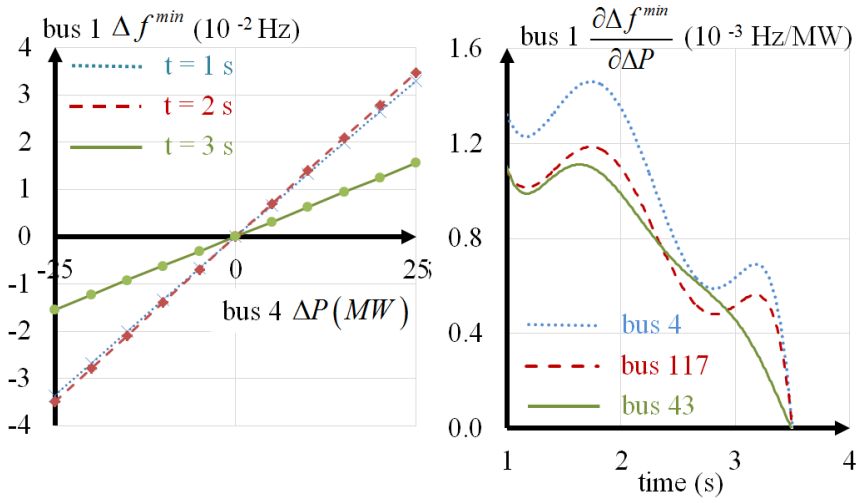

Figure 8. The minimum changes of frequency with respect to injected power.

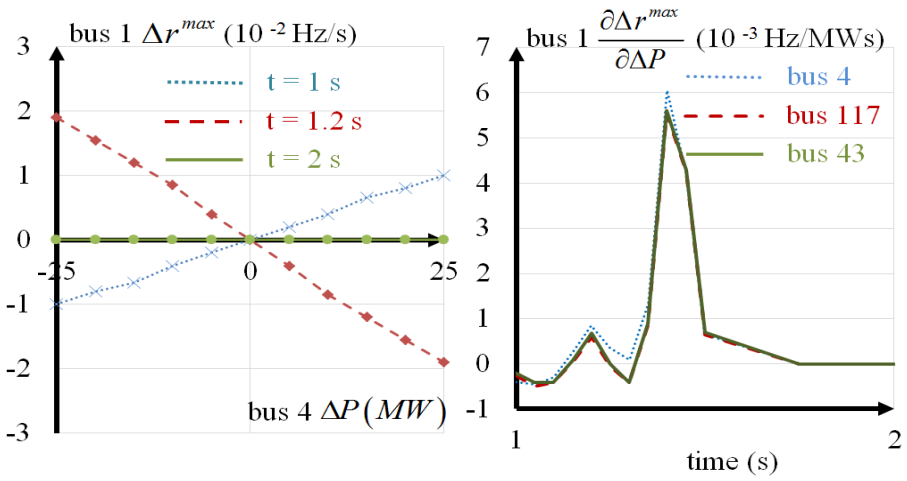

Figure 9. RoCoF in terms of injected active power.

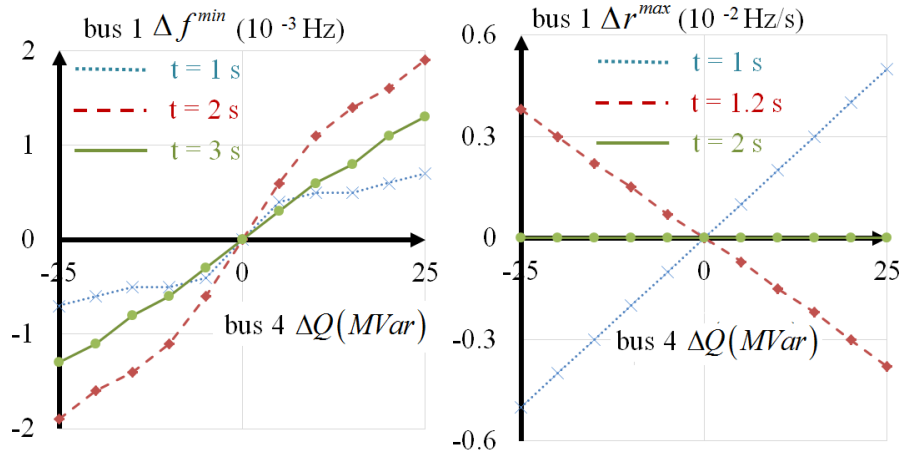

Figure 10. The change of time-dependent indices of bus 4 due to power injection into bus 4.

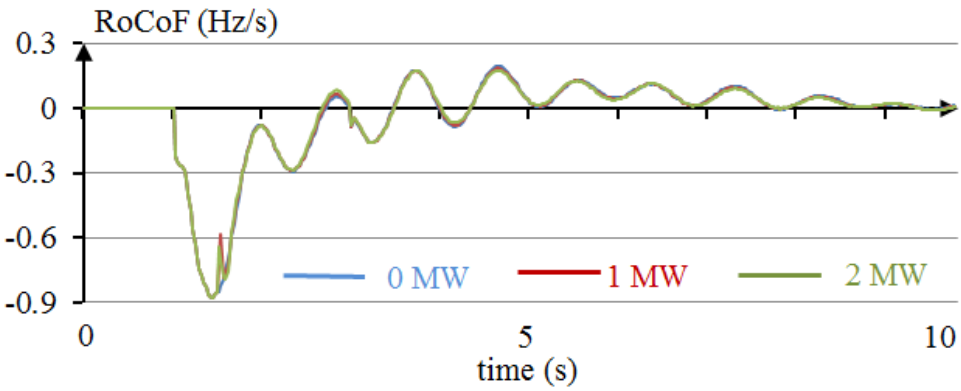

Figure 11. The RoCoF in bus 1 due to active power injection into bus 4.

The change of active power injected to bus 4 in time steps of 1.5 s with 0, 1, and 2 MW changes in the power value was analyzed. The graphs related to these changes are also shown in Figure 11. The results show that the output power of the storage devices has a small effect on the network frequency. Therefore, the estimation of each part can be estimated by reconstructing the frequency measurements in each bus.

3. Simulations and results analysis

In this paper, two networks have been examined. A three-bus network, which includes 4 generation units, 2 fast storage units, and 3 network load units. In this network, events usually occur in generation unit No. 4. The other network is the modified IEEE 118-bus network, which includes 8 fast storage units. The capacity of all storage units is considered equal to 15 MW. Also, the costs related to the energy supply of storage devices are different from each other. The energy storage capacity is also assumed to have no limit. There is a possibility of an event in four points of the network, where the generators located in bus 80 (the 389 MW unit), bus 100 (the 415 MW unit), bus 61 (the 386 MW unit), and bus 59 (the 433 MW unit), are among these cases. The permissible value of the frequency nadir and the maximum RoCoF are assumed to be 59.5 Hz and 0.5 Hz, respectively.

3.1. Case studies

In this paper, various study cases have been considered, each of which can represent a different aspect of simulation. These study cases are:

Case I: First, the effect of each technical parameter on the frequency response of the sample power system is investigated. A network with 10 traditional 120 MW units (1.2 p.u.) and variable inertia between 2.5 to 3.5 s (with steps of 0.1 s) and time constants $T_{i,1} = 0.5s$ $T_{i,2} = 2.5s$, $T_{i,3} = 5.5s$ has been considered. An event is assumed in which the load suddenly increases by 1 p.u. from the basic value of 10 p.u. and the amount of energy stored in the storage device is equal to zero. For all storage devices, we have $T_{fP} = 0.1s$ and$T_{sP} = 0.5s$. The purpose of this case is to somehow analyze the sensitivity of the model to the technical parameters of the problem.

Case II: In this case, the planning of the 3-bus network is carried out in such a way that it is necessary to solve the differential equations of the frequency swing in each case.

3.2. Simulation results

3.2.1. Case I

3.2.2.1. Impact of inertia of storage on frequency response

Figure 12 shows the effect of changing the inertia of energy storage on the frequency response of the power system. The output power of the storage device, the output power of the traditional power plants, and the frequency deviation in different values of the virtual inertia of the storage devices are shown. The higher the virtual inertia, the better the frequency response of the system. The frequency deviations or the distance between the frequency nadir and the nominal frequency are reduced and the intensity of the maximum RoCoF is also reduced. The deviation of the power balance of the network is answered with the simultaneous contribution of traditional power plants and energy storage. The more the inertia of grid storage devices increases, the contribution of storage devices to the power supply increases, and the share of traditional power plants

decreases. Therefore, higher values of virtual inertia require higher charging and discharging capacity of ESS.

3.2.1.2. Impact of the rated power of storage on frequency response

Figure 13 depicts the effect of rated power of energy storage on the frequency response of power systems. As can be seen, with the increase in charging and discharging capacity, the frequency response of the power system shows more improvement. Also, the contribution of ESS will increase.

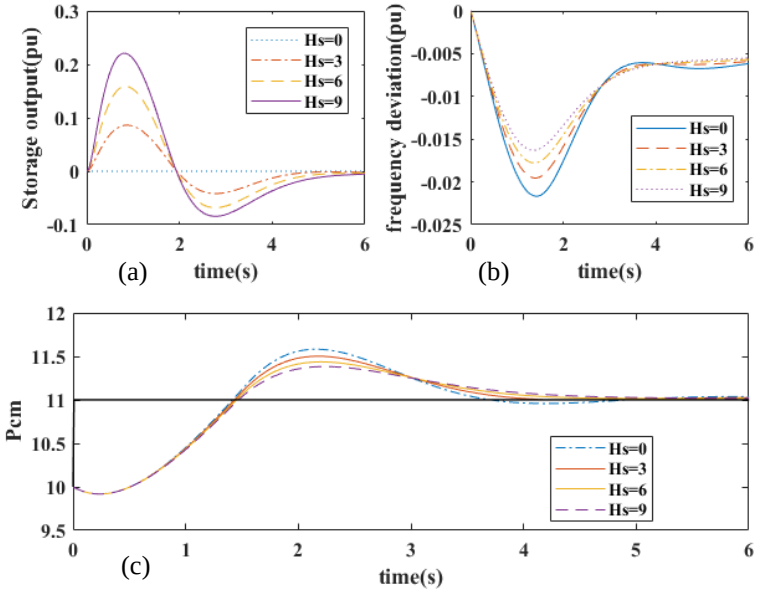

Figure 12. The effect of virtual inertia on the frequency response of the power system by considering the dynamics of the storage battery. (a) Frequency response (upper right), (b) storage output power (upper left), and (c) output power of traditional generators (bottom).

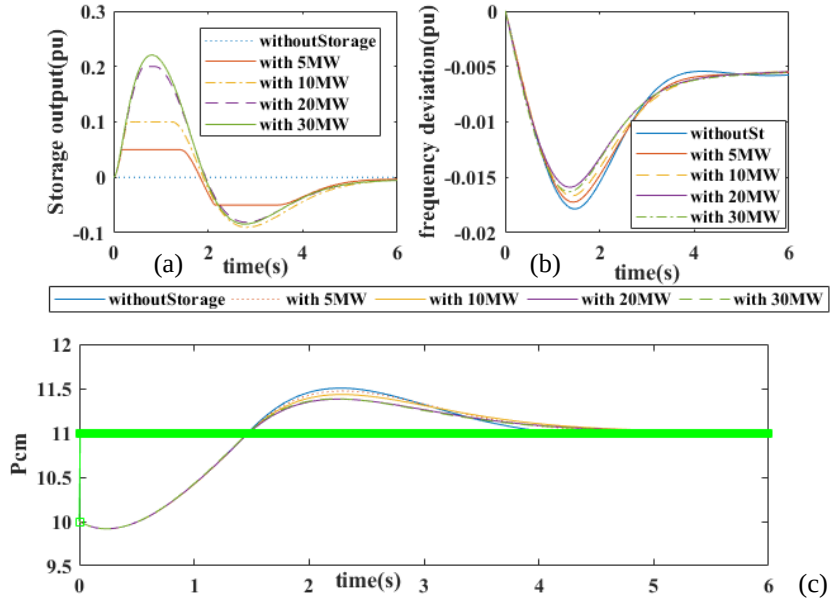

Figure 13. The effect of the rated power of the storage device on the frequency response of the network for $H_s = 9s$. (a) Frequency response (upper right), (b) storage output power (upper left), and (c) output power of traditional generators (bottom).

3.2.1.3. Impact of the rated power of storage on frequency response

Figure 14 shows the effect of the initial charge of the storage device on the frequency response. As it is known, the initial output values of the storage devices play a significant role in the behavior of the primary frequency response. The charging state of the storage devices helps to prevent the frequency drop and the discharging state of the storage devices brings a worse situation in terms of the frequency nadir compared to the state without the storage device. It should also be noted that the storage units with an initial output of −10 MW contribute to the inertial response exactly after the event, but the storage units with an initial output of 10 MW do this only after the frequency drops. These results seem reasonable. Storage devices usually have less free capacity to respond to frequency reduction.

3.2.2. Case II

Figure 15 shows the maximum RoCoF and the minimum frequency nadir of the network in the inertial space of storage batteries, which is divided into two categories: the possible space and the impossible (unacceptable) space. This space shows the importance of virtual inertial services and the non-linear relationship between selected parameters (such as the frequency nadir and RoCoF) with the virtual inertia of the network. To simultaneously meet the requirements of the RoCoF and the frequency nadir, it is necessary to find the intersection of the acceptable space of the two regions.

Table 1 lists some boundary points related to RoCoF and frequency nadir. As it is known, some of the solutions have provided only the constraint related to the frequency nadir, while others have provided that of the RoCoF, and some have met both constraints. The solution with the lowest allowed cost by observing both conditions is selected as the best solution to the optimization problem. In Table 1, red values are unacceptable while green ones are acceptable. The best solution obtained, which has the lowest cost among the allowed solutions, is marked with blue color.

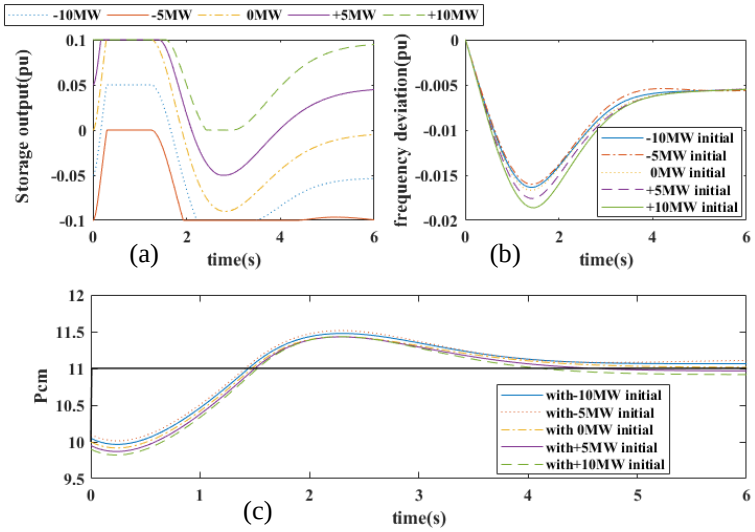

Figure 14. Investigating the effect of the initial charge level of the storage on the frequency response of the network for $H_s = 9s$. (a) Frequency response (upper right), (b) storage output power (upper left), and (c) output power of traditional generators (bottom).

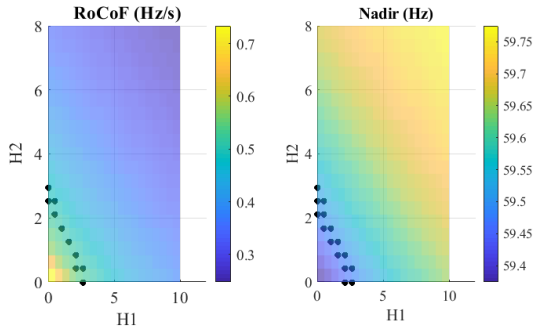

Figure 15. Maximum RoCoF (left) and frequency nadir (right) in different inertias of test network storages.

Table 1. Boundary points of constraints on frequency nadir and RoCoF.

H_1	H_2	RoCof	Frequency nadir	Cost ($)
0	**2.1053**	**0.5246**	**59.4823**	**421.0526**
0	**2.5263**	**0.5090**	**59.4997**	**505.2632**
0	**2.9474**	**0.4943**	**59.5159**	**589.4737**
0.5263	**1.6842**	**0.5206**	**59.4868**	**442.1053**
0.5263	**2.1053**	**0.5052**	**59.5038**	**526.3158**
0.5263	**2.5263**	**0.4907**	**59.5198**	**610.5263**
1.0526	**1.2632**	**0.5167**	**59.4911**	**463.1579**
1.0526	**1.6842**	**0.5015**	**59.5079**	**547.3684**
1.5789	**0.8421**	**0.5128**	**59.4954**	**484.2105**
1.5789	**1.2632**	**0.4979**	**59.5120**	**567.4211**
2.1053	**0**	**0.5246**	**59.4823**	**421.0526**
2.1053	**0.4211**	**0.5090**	**59.5159**	**589.4737**
2.1053	**0.8421**	**0.4943**	**59.5159**	**589.4737**
2.6316	**0**	**0.5052**	**59.5038**	**526.3158**
2.6316	**2.4211**	**0.4907**	**59.5198**	**610.5263**

4. Conclusions

The formation of virtual inertia is one of the different methods of controlling ESS. By using power electronic converters connected to these sources, it is possible to contribute to the primary frequency response or inertial response if an event is detected. Since storage devices are highly capable of quickly increasing their power from the lowest value to the highest value, they can provide a significant improvement in the frequency response. In this paper, the storage parameters effective in the improvement of the frequency response of the network were investigated and the sensitivity analysis of the contribution of ESS to providing inertia for the initial frequency response was discussed. The effect of power capacity and energy storage, the amount of virtual inertia designed for it, etc. on the improvement of frequency response parameters such as RoCoF and frequency nadir were analyzed and investigated. Also, an optimization-based method for the optimal management of ESS was presented, which determined the best necessary inertia for each of the storages. These inertias were chosen in such a way that in addition to providing the boundary constraints of the problem, the amount of operating costs of the storage devices was minimized.

References

[1] M. Sadeghi, and M. Abasi, "Optimal Placement and Sizing of Hybrid Superconducting Fault Current Limiter for Protection Coordination Restoration of the Distribution Networks in the Presence of Simultaneous Distributed Generation," *Electric Power Systems Research*, vol. 201, 107541, 2021.

[2] Y. Yang, S. Bremner, C. Menictas, and M. Kay, "Battery Energy Storage System Size Determination in Renewable Energy Systems: A Review," *Renewable and Sustainable Energy Reviews*, vol. 91, pp. 109-125, 2018.

[3] K. C. Divya, and J. Østergaard, "Battery Energy Storage Technology for Power Systems—An Overview," *Electric Power Systems Research*, vol. 79, no. 1, pp. 511-520, 2009.

[4] S. Darvish Kermani, V. Davatgaran, A. Beigzadeh, and M. Joorabian, "Power Equations for Non-Detection Zone of Islanding Detection in Renewable-Energy-based Microgrids with Multiple Connection Points to Micro-Grids," *Journal of Green Energy Research and Innovation*, vol. 1, no. 1, pp. 55-65, 2024.

[5] P. Du, "Design of New Primary Frequency Control Market for Hosting Frequency Response Reserve Offers from Both Generators and Loads," *Renewable Energy Integration for Bulk Power Systems: ERCOT and the Texas Interconnection*, pp. 137-175, 2023.

[6] N. Riaz, L. Peltonen, et al., "Enhancing Primary Frequency Control in Microgrids through Self-Smoothing Photovoltaic Systems," *25th European Conference on Power Electronics and Applications (EPE'23 ECCE Europe)*, pp. 1-10, 2023.

[7] X. Wei, Z. Jin, and G. Li, "Parameter Optimization for Temporary Primary Frequency Control of Wind Turbines Based on Analytical Derivation," 4*th International Conference on Mechanical Instrumentation and Automation*, 2023.

[8] A. H. Besheer, X. Liu, et al., "Overview on Fast Primary Frequency Adjustment Technology for Wind Power Future Low Inertia Systems," *Alexandria Engineering Journal,* vol. 78, no. 1, pp. 318-338, 2023.

[9] T. Liu, P. Wang, et al., "Operation-Area-Constrained Adaptive Primary Frequency Support Strategy for Electric Vehicle Clusters," *Journal of Modern Power Systems and Clean Energy*, vol. 11, no. 6, pp. 1982-1994, 2023.

[10] J. Li, R. Xiong, et al., "Design/Test of A Hybrid Energy Storage System for Primary Frequency Control using a Dynamic Droop Method in an Isolated Microgrid Power System," *Applied Energy*, vol. 201, no. 1, pp. 257-269, 2017.

[11] T. R. Oliveira, W. W. A. G. Silva, and P. F. Donoso-Garcia, "Distributed Secondary Level Control for Energy Storage Management in DC Microgrids," *IEEE Transactions on Smart Grid*, vol. 8, no. 6, pp. 2597-2607, 2017.

[12] Y. Wang, Y. Xu, et al., "Aggregated Energy Storage for Power System Frequency Control: A Finite-Time Consensus Approach," *IEEE Transactions on Power Systems,* vol. 10, no. 4, pp. 3675-3686, 2019.

[13] J. Ebrahimi, and M. Abasi, "Design of a Power Management Strategy in Smart Distribution Networks with Wind Turbines and EV Charging Stations to Reduce Loss, Improve Voltage Profile, and Increase Hosting Capacity of the Network," *Journal of Green Energy Research and Innovation*, vol. 1, no. 1, pp. 1-15, 2024.

[14] S. Sharma, S. H. Huang, and N. D. R. Sarma, "System Inertia Frequency Response Estimation and Impact of Renewable Resources in ERCOT Interconnection," *IEEE Power and Energy Society General Meeting,* pp.1–6, 2011.

[15] L. Sigrist, "A UFLS Scheme for Small Isolated Power Systems Using Rate-Of-Change of Frequency," *IEEE Transactions on Power Systems*, vol. 30, no. 4, pp. 2192-2193, 2015.

[16] Y. Wen, W. Li, G. Huang, and X. Liu, "Frequency Dynamics Constrained Unit Commitment with Battery Energy Storage," *IEEE Transactions on Power Systems*, vol. 31, no. 6, pp. 5115-5125, 2016.

[17] A. Ahmadi, A. E. Nezhad, and B. Hredzak, "Security-Constrained Unit Commitment in Presence of Lithium-Ion Battery Storage Units using Information-Gap Decision Theory," *IEEE Transactions on Industrial Informatics,* vol. 15, no. 1, pp. 148-157, 2019.

[18] M. Carrion, Y. Dvorkin, and H. Pandzic, "Primary Frequency Response in Capacity Expansion with Energy Storage," *IEEE Transactions on Power Systems*, vol. 33, no. 2, pp. 1824-1835, 2018.
[19] T. Xu, W. Jang, and T. Overbye, "Commitment of Fast-Responding Storage Devices to Mimic Inertia for the Enhancement of Primary Frequency Response," *IEEE Transactions on Power Systems*, vol. 33, no. 2, 1219-1230, 2018.
[20] T. Chakraborty, D. Watson, and M. Rodgers, "Automatic Generation Control Using an Energy Storage System in a Wind Park," *IEEE Transactions on Power Systems,* vol. 33, no. 1, pp. 198-205, 2018.
[21] G. C. Gissey, P. E. Dodds, and J. Radcliffe, "Market and Regulatory Barriers to Electrical Energy Storage Innovation," *Renewable and Sustainable Energy Reviews,* vol. 82, pp. 781-790, 2018.
[22] J. Cao, D. Wenjuan, W. Haifeng, and M. McCulloch, "Optimal Sizing and Control Strategies for Hybrid Storage System as Limited by Grid Frequency Deviations," *IEEE Transactions on Power Systems,* vol. 33, no. 5, pp. 5486-5495, 2018.
[23] Y. Wen, W. Li, G. Huang, and X. Liu, "Frequency Dynamics Constrained Unit Commitment with Battery Energy Storage," *IEEE Transactions on Power Systems*, vol. 31, no. 6, pp. 5115-5125, 2016.
[24] M. Ramirez, R. Castellanos, G. Calderon, and O. Malik, "Placement and Sizing of Battery Energy Storage for Primary Frequency Control in an Isolated Section of the Mexican Power System," *Electric Power Systems Research,* vol. 160, pp. 142-150, 2018.
[25] B. Lian, A. Sims, D. Yu, C. Wang, and R. W. Dunn, "Optimizing Lifepo4 Battery Energy Storage Systems for Frequency Response in the UK System," *IEEE Transactions on Sustainable Energy*, vol. 8, no. 1, pp. 385-394, 2016.
[26] S. Pulendran, and J. E. Tate, "Energy Storage System Control for Prevention of Transient Under-Frequency Load Shedding," *IEEE Transactions on Smart Grid,* vol. 8, no. 2, pp. 927-936, 2017.
[27] G. He, Q. Chen, C. Kang, Q. Xia, and K. Poolla, "Cooperation of Wind Power and Battery Storage to Provide Frequency Regulation in Power Markets," *IEEE Transactions on Power Systems*, vol. 32, no. 5, pp. 3559-3568, 2017.
[28] M. Abasi, M. Joorabian, A. Saffarian, and S. G. Seifossadat, "A Comprehensive Review of Various Fault Location Methods for Transmission Lines Compensated by FACTS devices and Series Capacitors," *Journal of Operation and Automation in Power Engineering*, vol. 9, no. 3, pp. 213-225, 2021.
[29] M. F. Arani, and Y. A. R. I. Mohamed, "Cooperative Control of Wind Power Generator and Electric Vehicles for Microgrid Primary Frequency Regulation," *IEEE Transactions on Smart Grid*, vol. 9, no. 6, pp. 5677-5686, 2018.
[30] S. Izadkhast, P. Garcia-Gonzalez, P. Frias, and P. Bauer, "Design of Plug-In Electric Vehicle's Frequency-Droop Controller for Primary Frequency Control and Performance Assessment," *IEEE Transactions on Power Systems*, vol. 32, no. 6, pp. 4241-4254, 2017.
[31] M. Abasi, M. F. Nezhadaneini, M. Karimi, and N. Yousefi, "A Novel Metaheuristic Approach to Solve Unit Commitment Problem in the Presence of Wind Farms," *Rev Roumaine des Sciences Techniques-Series Electrotechnique et Energetique*, vol. 60, no. 3, pp. 253-262, 2015.

Declaration of Competing Interest

The authors declare that they have no known competing financial interests or personal relationships that could have appeared to influence the work reported in this paper. The ethical issues, including plagiarism, informed consent, misconduct, data fabrication and/or falsification, double publication and/or submission, redundancy, have been completely observed by the authors.

Credit Authorship Contribution Statement

Moaiad Mohseni: Conceptualization, Data curation, Formal analysis, Methodology, Validation, Roles/Writing-original draft. **Alireza Niknam Kumle:** Conceptualization, Data curation, Formal analysis, Methodology, Software, Validation. **Rezvan Keshavarzpour:** Methodology, Software, Validation.

Bibliography

Moaiad Mohseni was born in Kwait. He received his B.SC Degree in Electrical Engineering, Kazeroon Branch, Islamic Azad University, Kazeroon, Iran in 2001, and his M.S. and Ph.D. degrees in Electrical Engineering from Dezful Branch, Islamic Azad University, Dezful, Iran, in 2011 and 2021, respectively. His Research Include Power Market and Smart Grid and renewable energy systems.

Alireza Niknam Kumle born in Iran in 1989, obtained a Ph.D. in Electrical Power Engineering from Shahid Chamran University of Ahvaz in 2021. With over 60 published papers and 10 authored books, he has completed 11 industrial research projects and holds a power systems patent. Recognized as the top researcher in Khuzestan province in 2021, he received four titles from the National Elite Foundation from 2021 to 2023. Currently an Assistant Professor at Arak University's Electrical Engineering Department, Kumle focuses on fault analysis, reactive power control, power quality improvement, and FACTS devices in HVAC and HVDC transmission lines.

Rezvan Keshavarzpour was born in Iran in 1990. She received her bachelor's and master's degrees in Electronics Engineering and Electrical Engineering (Power Systems) from Islamic Azad Universities of Shooshtar and Ahvaz branches, Iran, in 2014 and 2019, respectively. She is now employed at National Iranian South Oil Company (NISOC), Ahvaz, Iran. Her specialized interests include evaluation and improvement of power quality of power systems, operation of power systems, and protection of power systems.

Journal of Green Energy Research and Innovation

Voltage Sag Reduction by ANFIS in Wind Turbine Generation Units

Saman Darvish Kermani, Ali Morsagh Dezfuli, Abdolreza Behvandi, Mehrdad Kankanan

Highlight

- Adoption of a modified d-q converted three-phase voltage regulator
- Operation using an NN, FL, ANFIS, or PI controller instead of a three-phase regulator
- Rectifying voltage irregularities by promptly restoring the voltage to the nominal magnitude

Graphical Abstract

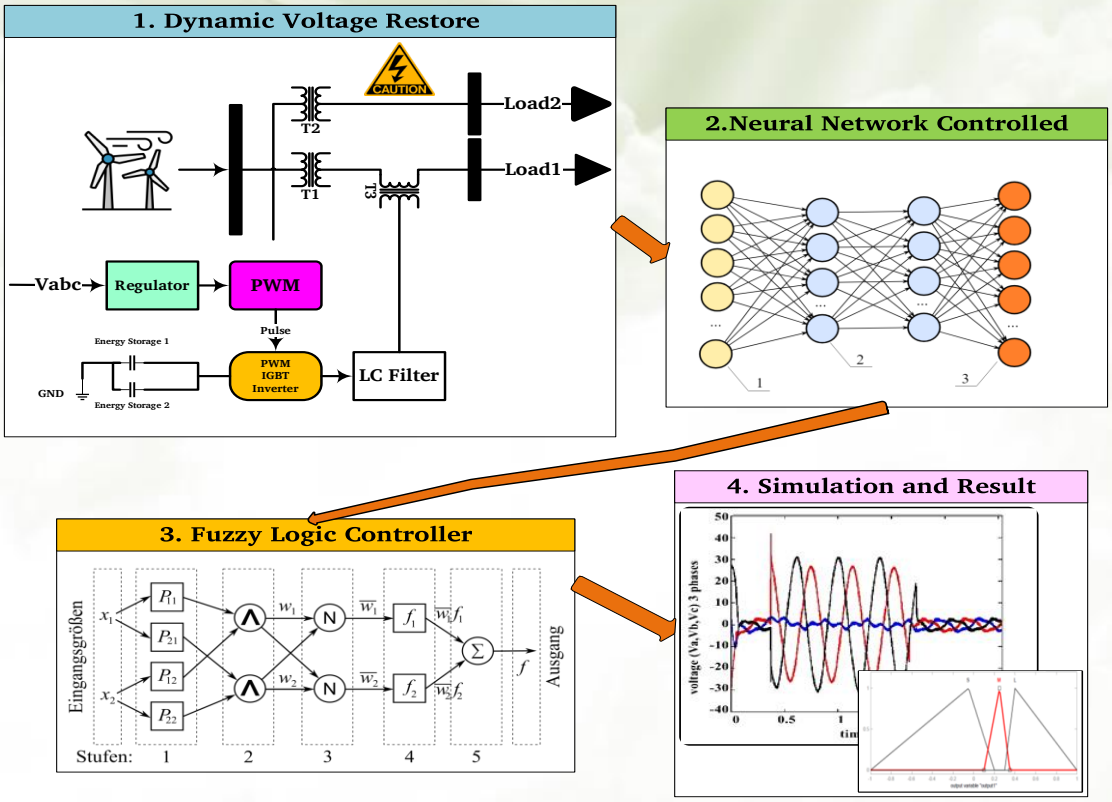

Use your device to scan and read the article online

Citation

S. D. Kermani, A. Morsagh Dezfuli, A. Behvandi, and M. Kankanan," Voltage Sag Reduction by ANFIS in Wind Turbine Generation Units," *Journal of Green Energy Research and Innovation*, vol. 1, no. 3, pp. 49-76, 2024.

https://doi.org/10.61186/jgeri.1.3.49

Online ISSN: 3041-9018

Journal of Green Energy Research and Innovation

Journal Homepage: www.jgeri.araku.ac.ir

Voltage Sag Reduction by ANFIS in Wind Turbine Generation Units

Saman Darvish Kermani [1], Ali Morsagh Dezfuli [2*], Abdolreza Behvandi [3], Mehrdad Kankanan [3]

[1] *GHD Advisory, Melbourne VIC 3000, Australia.*
[2] *Department of Electrical Engineering, Faculty of Engineering, Shahid Chamran University of Ahvaz, Ahvaz 61357-85311, Iran.*
[3] *Department of Electrical Engineering, Ramhormoz Branch, Islamic Azad University, Ramhormoz, Iran.*

* ***Corresponding Author:*** *a-morsaghdezfuli@stu.scu.ac.ir*

ARTICLE INFO

Keywords:
Dynamic voltage restorer,
Power quality,
Neural network,
Fuzzy logic,
Adaptive neuro-fuzzy inference system,
Voltage sags,
Voltage swells.

Article history:
Received: 01 January 2024;
Revised: 15 February 2024;
Accepted: 17 February 2024;

Article type:
Research Article

ABSTRACT

The Power Quality (PQ) issue refers to the occurrence of irregular voltage, current, or frequency that leads to failure or incorrect functioning of equipment used by end users. The PQ meter is utilized to monitor a diverse range of power supply characteristics, all of which possess the capacity to impact the effectiveness of both operational procedures and machinery. The dynamic voltage restorer (DVR) performs the role of a specialized power device employed to mitigate the voltage drop experienced at the terminal of a sensitive load. DVR can be controlled by various control designs. This work conducts a comparative analysis on a normally managed voltage system and a medium-power DVR controlled by a neural network (NN), fuzzy logic (FL), or adaptive neuro-fuzzy inference system (ANFIS) by utilizing an output voltage regulator. The identification and rapid compensation of voltage perturbations, such as voltage sag, are essential elements in monitoring and controlling DVRs. The conventional PI controller is commonly employed in regulating DVRs. While the traditional controller possesses certain merits, it is not free of limitations. One such downside pertains to its utilization of constant gains, which can impede its capability to provide optimal control performance in instances where system parameters undergo fluctuations. Possible solutions have been proposed to effectively tackle this issue, such as the use of NNs, FL, or ANFIS controllers. Furthermore, to attain both rapid dynamic response and robustness, a modified d-q converted three-phase voltage regulator was adopted. Instead of employing a conventional three-phase regulator, this particular regulator is operated by means of an NN, FL, ANFIS, or PI controller. The suggested voltage regulator offers a prompt solution for rectifying voltage irregularities, such as voltage sag, by promptly restoring the voltage to the nominal magnitude. The primary source of power adopted in this study is a wind turbine unit.

1. Introduction

In a review of previous articles and research, it can be seen that the increasing prevalence of extremely responsive end-user devices has garnered the interest of both end consumers and providers concerning power quality [1]. The observed phenomenon

can be attributed to the growing prevalence of a wide array of advanced electrical and electronic devices, including but not limited to computers, programmable logic controllers, and variable-speed drives. Today, the demand for electricity is so high that it is almost impossible to even imagine human life without it. This has imposed a lot of strain on governments to meet the huge demands for electricity. Therefore, the provision of quality energy has turned into one of the basic foundations of any country's macro-policies [2]. Voltage fluctuations can occur throughout or across a substantial segment of the system due to issues arising at either the transmission or distribution level.

Furthermore, under heavy load conditions, the system may experience a significant voltage drop. Voltage sags can occur at any given point in time, with magnitudes ranging from 10 to 90 percent and durations spanning from half a cycle to one minute [3]. Moreover, the nature of faults might vary, resulting in either balanced or unbalanced conditions, with magnitudes that may deviate from anticipated values. These magnitudes are impacted by factors such as the proximity to the fault and the interconnections among transformers.

In contrast, voltage swell is a sudden rise in the supplied voltage, measuring between 110% and 180% of the root-mean-square (RMS) voltage at the fundamental frequency of the network. This phenomenon persists for a duration spanning from 0.5 cycles to 60 seconds [3]. The relative infrequency of voltage swells in distribution networks diminishes their significance in comparison to voltage sags.

Several potential approaches to preventing voltage sag have been discussed in [4], including previous research in the field. The equipment and approaches that had been utilized were all taken into consideration with regard to voltage sags in radial and mesh grids. Within the scope of these investigations, the publications about issues that are associated with voltage sag have been categorized according to a set of predetermined criteria. Among these aspects is the evaluation of the unpredictability of the demand for electricity or the availability of renewable sources. A presentation has been made regarding the recommendations that pertain to the voltage sag research. The incorporation of the uncertainties associated with renewable energy sources and the usage of electricity serve as the foundation for these proposals. Reference [5] makes a contribution to creating a mitigation mechanism that is both cost-effective and efficient for voltage sag situations, both with and without the presence of distributed generation (DG) and renewable energy resources (RES). In [6], the optimal placement of DG units is determined in a network with unbalanced loads. To address this, parametric and cost functions have been developed to formulate the problem. A novel approach is employed to solve the unbalanced load flow problem, specifically utilizing the group search optimizer algorithm, which is a newly modified swarm intelligence algorithm discussed in this paper. The technique that has been provided in [7] is capable of evaluating the performance of voltage sag at wind turbine connection sites in a manner that is both efficient and precise. Furthermore, it offers a reliable long-term performance evaluation of the tendency and degree of voltage sag occurrence anticipated to generate wind turbine disconnection. The reduction and control of voltage sag in wind turbines, which is quite intriguing, have been the subject of articles published [8]. The primary objective of [9] is

to investigate the impact that a voltage drop has on a wind turbine system equipped with a double-fed induction generator. Wind power converting systems can be modeled by space vector technology. Several different grid voltage disturbances are taken into consideration in this paper, and the performance of the system is analyzed.

The identification of voltage disturbances, such as voltage sag, and the prompt adjustment to mitigate these disturbances are two essential elements of DVR control. In a given scenario, it is commonly observed that a single-phase ground fault is responsible for inducing the most significant voltage drop. It can be inferred from this observation that the equilibrium of the voltage's typical waveforms is disrupted as the voltage decreases. When the d-q transformation is used for the three balanced power line voltages, the resulting value will be equivalent to the DC value that is directly related to the peak input voltage. This will enable accurate detection of voltage disturbances. In this instance, it is sufficient to compare the DC peak with the reference value [10] so that the voltage disturbance is accurately identified. Conversely, if the three input voltages are not in a state of balance, the result of the d-q transformation will encompass both the component of current ripple and the component of direct current. In the given situation, the inclusion of a low-pass filter (LPF) is important to effectively attenuate the alternating current (AC) component and accurately discern the precise occurrence of the voltage perturbation. Although the LPF may effectively attenuate the AC ripple, it is incapable of bypassing the inherent time delay necessary for accurately detecting the precise occurrence of a voltage disturbance. Furthermore, due to the prevalence of unbalanced line voltages during normal sag voltage scenarios, it becomes imperative to provide a zero-sequence voltage into the line. To facilitate the provision of a zero-phase sequence voltage, the system necessitates the incorporation of three single-phase inverters, along with either a five-leg transformer or three single-phase transformers. In the given case, it is unfeasible to use the commonly used three-phase d-q transformed voltage control method [11-12] to regulate the output voltage. To rectify the asymmetrical voltage disruption, it is important to employ a voltage regulation mechanism for the inverter.

Currently, there is a notable increase in public interest in many techniques encompassed under artificial intelligence (AI), including NNs, FL, and genetic algorithms (GA). A novel method for detecting voltage disturbances is formulated and suggested, employing NNs, FL, or ANFIS control, in this research as its novelty and main contributions.

The identification of voltage disturbances can be achieved even in scenarios characterized by very imbalanced voltage conditions. The reason for this is that these methodologies enable the measurement of the magnitude of the three-phase voltage. An alternative approach to attaining a rapid dynamic response involves the utilization of a modified d-q transformed voltage regulator in the context of an inverter. The control of the regulator for the three voltage phases in this approach is achieved by the utilization of various control mechanisms, such as NNs, FL, ANFIS, or PI controllers. The application of voltage regulators enables the quick adjustment of voltage perturbations, such as voltage sag, thereby restoring the voltage level to its nominal value promptly.

The employment of a DVR is commonly acknowledged as a highly economical strategy for addressing voltage sags and swells, notwithstanding the existence of various alternative

options. The incorporation of a PI controller in a DVR result in a design that is both uncomplicated and capable of delivering satisfactory performance in a wide range of operational scenarios. The fundamental concern that necessitates attention in the context of conventional controllers pertains to the tuning of controller gains. There is a potential for the controller to exhibit inadequate control performance using fixed gains when changes occur in the quantities of the system and operation status and one of the motivations and the necessity of this research is to solve this problem.

The use of NNs, FL, or ANFIS methodologies can be employed to effectively address a diverse set of operational scenarios. Nevertheless, a challenge occurs concerning the parameters linked to the number of neurons in the NN approach or membership functions in the fuzzy method, along with the rules, which heavily rely on the expertise of the professionals. In the case that it becomes necessary to modify the settings, the sole method available is a process of experimentation and refinement. The ANFIS method is employed to effectively tackle the previously mentioned problem and improve the controller's adaptability. The ANFIS approach involves the generation of a fuzzy inference system by employing a chosen set of input and output data. In contrast, the outcomes of the simulation revealed that both an NN and a simplistic FL controller exhibit a satisfactory disposition. This implies that the utilization of an ANFIS controller structure may not be essential for achieving improved outcomes. However, it would also indicate that building an ANFIS controller is comparatively less complex than alternative methodologies. This paper presents an analysis of the DVR and its underlying functioning concept. Furthermore, the present study examines the suggested controller, which encompasses potential options, such as an NN, FL, or ANFIS controller. Subsequently, the outcomes of the simulations conducted using the MATLAB/Simulink platform provide a comparative analysis of the suggested solutions regarding their performance in voltage sag and swell, respectively. After conducting a comparative analysis of the injection voltages employed in different methodologies, the findings are presented in this article along with detailed explanations and a concluding statement.

The paper is organized as follows. Section 2 explains the DVR. Then, Section 3 discusses its operating principles. Section 4 presents the DVR scheme. Section 5 presents the neural network-controlled disturbance detector. Voltage regulator by adopting a modified d-q transformation method is discussed in Section 6. The neural network method is implemented in Section 7. Section 8 is dedicated to the fuzzy logic control of the DVR. Section 9 is related to the design of the DVR with an ANFIS controller, and Sections 10-12 present the simulation results and suggestions for future research.

2. Dynamic Voltage Restorer (DVR)

The DVR is connected in series to provide voltage to the system so that load voltage is properly regulated. The DVR was developed around three decades ago [13]. The customary placement site for this component is within a distribution system, more precisely positioned between the power source and the feeder responsible for the

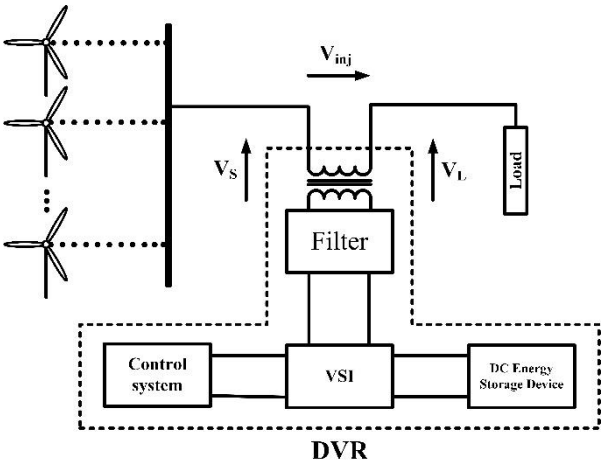

Figure 1. A schematic of a DVR.

important load. If a disturbance occurs, its primary objective is to promptly raise the load voltage to avert any power interruptions to the load mentioned [14]. Various control algorithms and circuit topologies can be employed to develop a DVR [15-16].

In addition to its core function of voltage oscillation compensation, a DVR may be enhanced with supplementary features, including the adjustment of voltage harmonics, the mitigation of voltage transients, and the restriction of fault currents [17]. The full design of a DVR consists of several key components, namely a voltage injection transformer, an output filter, energy storage equipment, a voltage source inverter (VSI), and a control platform. Figure 1 shows the ultimate arrangement of the DVR.

2.1. Voltage Injection Transformer

By utilizing the high-voltage windings, this transformer facilitates the establishment of a connection between the DVR and the distribution network. Moreover, it is capable of effectively integrating the injected compensating voltages produced by the VSCs with the supply voltage. This transformer's design holds significant relevance due to its susceptibility to saturation, overrating, overheating, cost, and performance. It is conceivable that the injected voltage may encompass fundamental harmonics, switching harmonics, and potential components of the DC voltage [18]. When the transformer design is not acceptable, the injected voltage could possibly cause saturation in the transformer. This saturation could result in the DVR not operating effectively [19].

2.2. Output Filter

The major function of the output filter is to mitigate the presence of high-frequency switching harmonics. This filter is tasked with regulating the harmonic voltage content generated by the VSI, ensuring its compliance with relevant standards. The rating of the load VA is approximately 2% [20], which is a low value.

2.3. Voltage Source Inverter

A VSI is a power electronic system comprising switching devices such as IGCTs, IGBTs, and GTOs. It can generate a sinusoidal voltage with adjustable frequency, magnitude, and phase angle as required. The utilization of the VSI in the DVR application serves the

purpose of either temporarily substituting the supply voltage or creating the missing portion of the supply voltage [21].

2.4. DC Energy Storage Device

The DC energy storage device is responsible for providing the DVR with the necessary power during the compensatory procedure. Various alternative storage methods have been suggested, including flywheel energy storage [22], superconducting magnetic energy storage (SMES) [23], and supercapacitors [24-25]. These possess the advantage of exhibiting a rapid response time. The utilization of a lead-acid battery represents an alternate option [21-22]. The time-consuming process of extracting energy from batteries has led to the perception that batteries have limited suitability for usage in DVR applications [16]. Finally, conventional capacitors are an alternative that can be employed [26-27].

2.5. Control system

The primary goal of the control system is to preserve a consistent voltage at the load connection point, even in the presence of disturbances within the system. The inclusion of a voltage correction mechanism is a common practice in the control system of the general design. The function is responsible for ascertaining the appropriate reference voltage to be injected by the DVR. Moreover, the VSI control, as elucidated in this study, consists of a Pulse Width Modulation (PWM) controller integrated with a PI controller. The controller input is a type of error signal that is obtained by comparing the reference voltage with the injected voltage value, as depicted in Figure 2. Once a PI controller processes the error, the resulting output is fed into a PWM signal generator. This generator is responsible for regulating the operation of the DVR inverter, ensuring the appropriate injected voltage is provided.

3. Operating Principle of DVR

One of the principal roles of the DVR is to dynamically regulate the bus voltage by injecting a voltage, denoted by Vinj. This is achieved by employing a voltage injection transformer. The management of the momentary magnitudes of the three injected phase voltages is designed to mitigate or prevent any adverse effects that may arise from a bus malfunction on the load voltage VL. This suggests that any variations in voltage resulting from disruptions in the alternating current feeder will be counterbalanced by a corresponding voltage. There is no discernible association between the nature of a malfunction or any event that transpires within the system and the operational capacity

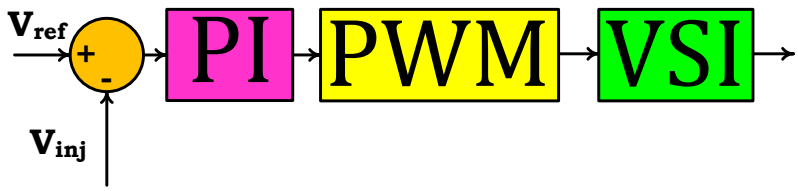

Figure 2. A classical PI controller.

of the DVR. Due to the infinite impedance of the step-down transformer for the zero-sequence component, it is possible to achieve a more economic configuration by solely addressing the positive and negative sequence components of the voltage disturbance observed at the input of the DVR. This argument holds true for the majority of practical instances.

The DVR offers two operational modes: standby mode and turbo mode. During the standby state (V_{inj} =0) of the voltage injection transformer, the low voltage winding is found to be short through the converter. The absence of semiconductor switching is a characteristic of this operational mode, as the triggering of individual inverter legs is designed to create a short-circuit path for the transformer connection. The DVR will mostly utilize this mode for the majority of its operational duration. During the boost mode, characterized by a positive V_{inj}, the DVR encounters a disruption in its supply voltage. Consequently, it responds by introducing a compensatory voltage via the voltage injection transformer.

4. DVR scheme

The conventional power circuit of a DVR comprises several components as depicted in Figure 3. Switches S1, S2, and S3 are employed for maintenance. Both the charging transformer (TR1) and the rectifier (REC) possess a power rating that is significantly inadequate. In the standby state of operation, the sole requirement is to charge the capacitor responsible for energy storage. During the standby state, it is observed that all switches in the inverter are in the off mode. Additionally, the secondary winding of the series transformer (TR2) is found to be short-circuited by bypass thyristors (BS).

In standby settings, the series transformer must possess a low leakage reactance to minimize the undesired voltage drop across the transformer. In the event of a voltage distribution breakdown, the bypass switches (BS) are deactivated by means of control over the inverter. The process involves introducing the regulated voltage into the series transformer, thereby transferring the energy held in the DC capacitor. After deactivating all bypass switches, the inverter is regulated to rectify the voltage disturbance. The control block diagram of the DVR consists of three main components, namely the voltage regulator component, the phase tracking component (PLL), and the voltage magnitude tracking control component, as depicted in Figure 4.

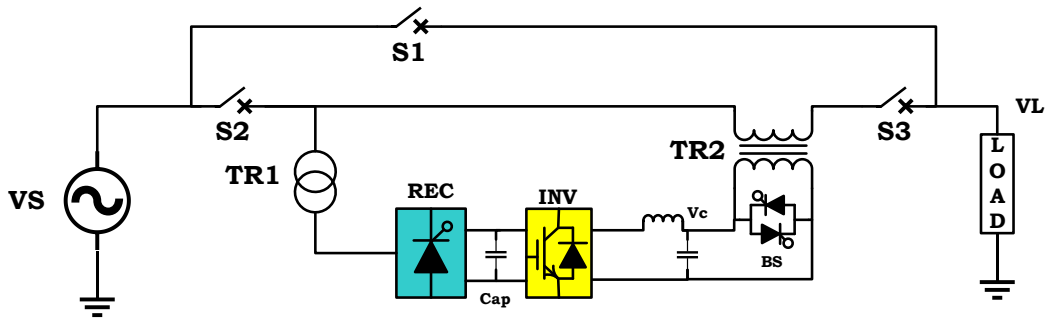

Figure 3. The configuration of the DVR.

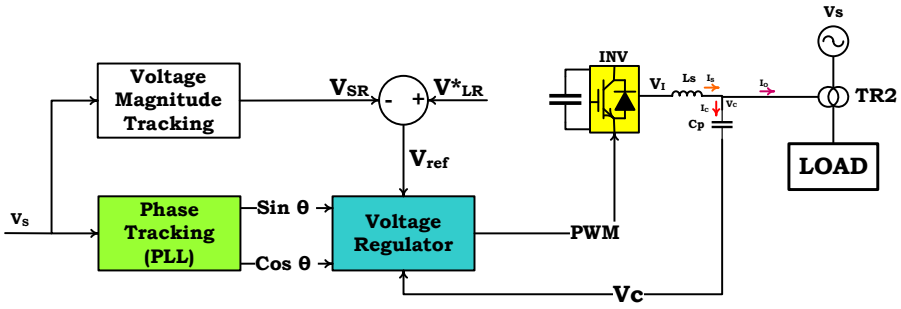

Figure 4. The control configuration of the DVR.

The initial stage involves the utilization of NN, FL, or ANFIS control methods by the magnitude tracking component to ascertain the magnitude of the input voltage Vs(t). The aforementioned methodologies possess the capability to expeditiously monitor the magnitude of the input voltage, particularly in instances where voltage perturbations, such as voltage sag, are present.

Additionally, the phase tracking component is tasked with ascertaining the phase angle of the input voltage Vs(t) during the system's standby state. Conversely, in the event of a phase leap and voltage sag occurring in the input voltage waveform, the phase tracking component generates a reference waveform that remains unaffected by the fluctuations in the input voltage waveform. The phase-locked loop (PLL) module is tasked with the responsibility of accurately monitoring and adjusting the phase of the input voltage signal. Its primary objective is to produce a sinusoidal reference waveform in-phase with the input signal. This synchronized reference waveform is then utilized for control objectives. The voltage regulator assumes the responsibility of regulating the single-phase inverter to rectify any disruptions in the input voltage. The achievement of this objective is facilitated by employing the outcomes of the phase tracking module and the voltage magnitude tracking module.

The voltage regulator block generates a signal known as PWM. Figure 4 illustrates that the voltage regulator acquires phase information from the phase tracking component and magnitude information from the magnitude tracking portion. These components will be further elaborated upon in the following sections. The load voltage reference V_{LR}^* is generated by monitoring the magnitude of the input voltage. When the input voltage level is within acceptable limits, the value of V_{LR}^* will be equivalent to the magnitude (V_{SR}) of the input voltage. Conversely, when the input voltage exceeds the voltage tolerance threshold, the magnitude of V_{LR}^* will assume a fixed value equivalent to the reference voltage. In the context of a single-phase inverter, the voltage regulator's voltage reference is established based on the disparity between the input voltage's magnitude and the magnitude of the reference voltage.

5. Neural Network Controlled Disturbance Detector

Previous studies have shown evidence that NNs possess the capability to undergo training processes that enable them to perform intricate tasks across several fields of application. These tasks encompass but are not limited to pattern recognition, identification, classification, speech processing, visual analysis, and control systems.

The artificial neural network (ANN) control system is classified as a non-linear control method. The system possesses the capability to adapt and arrange itself. ANN enables the monitoring of nonlinear interactions by utilizing input and output data, hence eliminating the requirement for a comprehensive mathematical model [28]. The categorization of ANN control can be based on the network's architecture, which often falls into four distinct categories: feedforward neural networks, feedback NNs, local approximation NNs, and fuzzy NNs.

Considering the input voltage as $v = V_m \sin(\omega t + \theta)$, it can be rewritten as Equation (1) by adopting the trigonometric formula.

$$v = V_m \cos(\theta) \sin(\omega t) + V_m \sin(\theta) \cos(\omega t) \quad (1)$$

Equation (1) reveals that the equation consists of sinusoidal terms, including $\sin(\omega t)$ and $\cos(\omega t)$, along with magnitude terms that are contingent upon θ.

Equation (2) can be derived from Equation (1) by applying the delta rule of the NN, as stated in reference [28].

$$Y = WX \quad (2)$$

Where Y denotes the estimated value by the delta rule. Also, W and X are calculated by Equation (3) as follows:

$$\begin{matrix} W = [V_m \cos(\theta) & V_m \sin(\theta)] \\ X = [\sin(\omega t) & \rightleftarrows\rightleftarrows \cos(\omega t)]^T \end{matrix} \quad (3)$$

Figure 5 depicts an instance of the adaptive linear combiner that is controlled by an NN and employs the delta rule. In the given context, the output of this specific instance is determined by a linear combination of its two inputs, denoted by $\sin(\omega t)$ and $\cos(\omega t)$.

The weight vector W is utilized to assign weights to the components of the input vector, thereby forming several coefficients. Subsequently, the weighted inputs are calculated, leading to the generation of a linear output known as the inner product Y. X might consist of either continuous analog values or binary data. Both types of values are potentially attainable. This implies that the weights undergo continuous fluctuations and can assume values that are either positive or negative.

During the training phase, the linear combiner is provided with input patterns and their corresponding desired replies. The adaptation method automatically sets the weights to ensure that the output responses to the input patterns closely approximate the desired responses for each pattern. A potential formulation of the equation that characterizes the adaptation process can be denoted as Equation (4).

$$W(k+1) = W(k) + \mu X(k) e(k) \quad (4)$$

Where μ is the training rate.

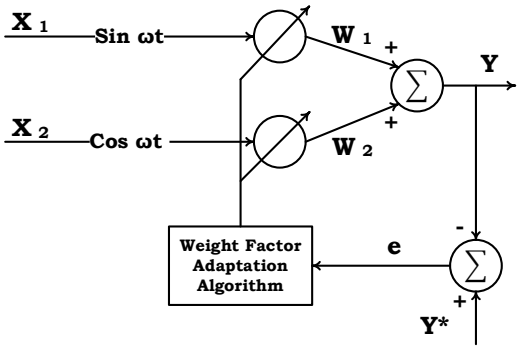

Figure 5. An NN-controlled adaptive linear combiner.

The weighting factor, represented by W, will attain its maximum value of Y if the training operation is successful. By monitoring W, it was feasible to obtain the maximum value of the input voltage instantaneously without any temporal delay.

Additionally, the utilization of an NN-driven approach enables the independent tracking of the peak phase voltages, hence presenting another advantageous aspect of this methodology. If a disturbance affects solely one- or two-phase voltages, it becomes feasible to exclusively regulate the phase voltages associated with those specific disturbances. In the context of the synchronous reference frame approach, however, the task of independently identifying and regulating corresponding phases poses significant challenges.

6. Voltage regulator by adopting a modified d-q transformation method

Figure 6 displays the control design of a voltage regulator for a single-phase inverter. The utilization of a standard voltage regulator with three-phase d-q transformation in [29-30] was rendered impracticable due to the discrepancy between the controlled inverter system, which is a single-phase inverter, and the required three-phase inverter. Alternatively, if it is feasible to find the q-axis component (V_{qs}) in Figure 6, despite the anticipated voltage of the inverter capacitor being the d-axis component (V_{ds}), the commonly used three-phase d-q transform can be employed. The utilization of the phase shift filter is a technique that can be employed to obtain the q-axis variable, commonly referred to as V_{qs}. Nevertheless, this approach exhibits a high degree of sensitivity towards variations in the frequency of the voltage employed as the input. Furthermore, the performance of a phase shift filter is notably suboptimal when utilized for voltage transients, such as instances of voltage sag. In the context of this article, it is assumed that the energy storage remains constant, while the voltage regulator is tasked with initiating PWM. The normal three-phase voltage regulator is modified to function as a single-phase voltage regulator, as seen in Figure 6.

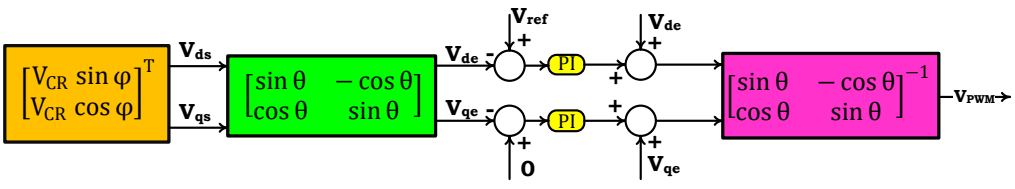

Figure 6. The control block diagram of the voltage regulator for single-phase inverter.

The q-axis variable can be defined with the assumption that the voltage of the inverter filter capacitor is a d-axis variable.

$$V_{ds} = V_c(t) = V_{CR} \sin \varphi \quad (5)$$

$$V_{qs} = V_{CR} \cos \varphi \quad (6)$$

in which ϕ denotes the phase shift between the voltage of the capacitor and the voltage of the utility input, $V_s(t)$. By utilizing the control block configuration depicted in Figure 6, it becomes feasible to attain Equations (7-8).

$$V_{de} = V_{CR} \sin \varphi \sin \theta + V_{CR} \cos \varphi \cos \theta \quad (7)$$

$$V_{qe} = V_{CR} \cos \varphi \sin \theta - V_{CR} \sin \varphi \cos \theta \quad (8)$$

Assuming that the inverter capacitor voltage is properly regulated, we have $V_{CR} = V_{ref}$ and $\phi = \theta$. Thereby, Equations (9-10) will be expressed noting Equations (7-8) as follows:

$$V_{de} = V_{ref} \quad (9)$$

$$V_{qe} = 0 \quad (10)$$

Considering the q-axis variable, we have

$$V_{qs} = V_{ref} \cos \theta \quad (11)$$

$$V_{ref} = V_{SR} - V_{LR}^* \quad (12)$$

However, Equations (9-10) can only be effectively used in ideal circumstances. In reality, it becomes imperative to account for other factors, such as compensating for the time delay caused by the inverter LC filter and the adverse impacts of dead time on the inverter switches. To mitigate the suboptimal effects, a PI controller and a feed-forward control scheme incorporating V_{de} and V_{qe} components have been employed. The magnitude (V_{qe}) is effectively regulated to a value of zero, resulting in the utilization of the d-axis controller's output for the generation of the PWM signal. It is crucial to consider that the q-axis variable (V_{qs}) can solely be obtained from Equation (11) by the utilization of the voltage reference (V_{ref}) and phase tracking information $(\cos \theta)$ as mentioned in references [31-32].

7. Implementation of Neural network method

The utilization of the synchronous reference frame (SRF) approach is based on the instantaneous values of the source voltage (v_{sa}, v_{sb}, v_{sc}). This approach is employed to generate the reference voltages $(V_{ca}^*, V_{cb}^*, V_{cc}^*)$ necessary for implementing the neural network method [33]. The adoption of reference voltages is necessary for the implementation of the NN approach. Abnormal situations and deviations in supply voltage can be identified by examining the disparity between the d-voltage of the supply and the d-reference value. This action is undertaken in the event of an occurrence that deviates from the usual, commonly known as an abnormal state. The control methodology generates a reference voltage that accurately represents the three phases. The reference voltage is transmitted via a controller, subsequently generating a switching signal to

facilitate the activation of the power switching components within the VSI. This guarantees that the DVR will effectively provide the necessary reference voltage as demanded by the system. Lastly, it is imperative to guarantee that the load voltage remains consistent with its designated reference standard.

This method has the potential to be employed for the mitigation of other forms of voltage oscillations, such as voltage sag/swell, voltage unbalance, and harmonic voltage. However, the focus of this study is solely on investigating voltage sag/swell as a form of voltage disturbance. The load-rated voltage is produced by applying the voltage difference between the reference voltage and the injected voltage to the voltage source, resulting in the generation of the load-rated voltage, as illustrated in Figure 7. The DVR operates in a state of low power consumption throughout its normal functioning, hence avoiding any instances of voltage sag or swell. The DVR is considered to be in a state of constant equilibrium during its operation under these specified conditions.

The Multilayer Feed Forward Neural Network (MLFFN) is a widely adopted topology in contemporary applications [34-35]. This specific network is comprised of several output neurons and some intermediate neurons, also called hidden layers. Initially, the transmission of data across the network is facilitated by the input layer. Subsequently, the information propagates through the concealed levels and ultimately emerges via the output layer. Figure 8 illustrates a block diagram of a three-layer MLFFN interconnected by weight matrices W and bias vectors b. These weight matrices and bias vectors serve as the free parameters inside the network.

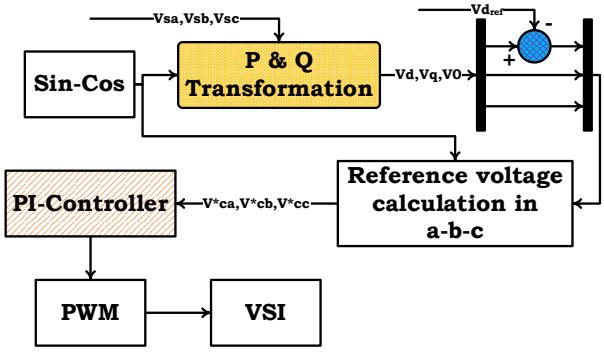

Figure 7. The control of the injected voltage by adopting the traditional PI controller (CPI).

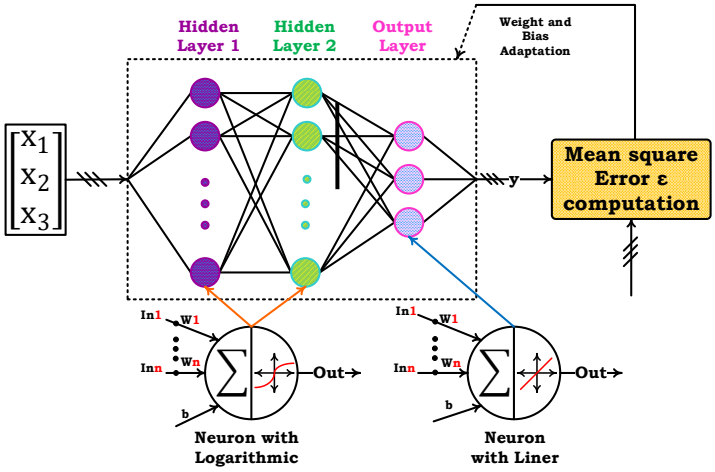

Figure 8. An NN for modeling.

The ANN utilizes training to modify the weight matrix (W) and bias vector (b). The ANN is designed to approximate its function to that of the system in a manner that is executed. Furthermore, the ANN aims to reduce the discrepancy between the observed output y and the reference function, given by ε. Each of the inputs in the input column vector x is allocated with a suitable weight, represented by W. The transfer function f receives an input that consists of the sum of the weighted inputs, in addition to the bias term. The activation vector, denoted as a, is calculated by Equation (13):

$$a = \sum(w.x + b) \tag{13}$$

In the context of generating their output, neurons possess the capability to utilize a wide range of differentiable transfer functions. The tan-sigmoid transfer function, commonly referred to as the tansig function, is employed in both the input layer and the hidden layer in this specific case.

$$tan\,sig(a) = \frac{2}{1+e^{-2a}} - 1 \tag{14}$$

In contrast, the output layer employs the linear transfer function known as *purelin*.

$$purelin(a) = a \tag{15}$$

The present study used the least mean square error (LMS) approach for training supervision. During this procedure, the learning rule is applied based on a predetermined set of desired network behaviors, encompassing the subsequent aspects:

$$\{x_1, y_1\}, \{x_2, y_2\}, \ldots \{x_n, y_n\} \tag{16}$$

in which the variable x denotes an input provided to the network, while the variable y indicates the related output that aligns with the target. After each input is applied to the network, the network's output is assessed in relation to the target. A distinction exists between the goal output and the network output, and this distinction is utilized to ascertain the inaccuracy. The average of the sum of the errors is calculated as follows:

$$\varepsilon = \frac{1}{n}\sum_{k=1}^{n} e(k)^2 \tag{17}$$

$$\varepsilon = \frac{1}{n}\sum_{k=1}^{n} \left(y(k) - y'(k)\right)^2 \tag{18}$$

The potential output of the network is y', whereas the output of the target can be denoted by y. The primary objective of the LMS method is to iteratively modify the weights and biases of the linear network to find the minimum mean square error to the greatest extent possible [36].

8. Fuzzy Logic Control of DVR

Due to the increasing adoption of power semiconductor switches in bespoke power devices, the system exhibits non-linear characteristics, rendering it challenging to conceptually characterize and intricate in nature. The fuzzy logic system is an exceptional and robust approach that exhibits the ability to concurrently employ quantitative information and experiential knowledge [37]. FL is an approach applied in the control system method and can be incorporated in various systems, spanning from compact,

embedded microcontrollers to extensive, networked, multi-channel PC or workstation-based data gathering and control systems [38-39]. It is a computational approach that can be employed for problem-solving in the domain of control systems.

In recent years, there has been an increasing demand for FL-controlled applications because of the advancing complexity of contemporary technology. In several cases pertaining to the control process, the absence of a mathematical model or the excessive computational demands in relation to available computer processing power and memory may impede its implementation. In these particular cases, a system that relies on empirical criteria may demonstrate more efficacy. Furthermore, FL proves to be a highly suitable option for cost-effective applications that rely on affordable sensors, low-resolution analog-to-digital converters, and single-chip microcontroller processors with a capacity of either four bits or eight bits. The enhancement of system performance can be achieved by the incorporation of additional rules, while the integration of new features facilitates seamless system upgrades. The integration of an additional layer of intelligence into the preexisting control mechanism represents one of the various methods by which fuzzy control can be employed to augment the efficacy of conventional controller systems that are currently operational.

An additional approach to exert control is through the utilization of FL control in the context of voltage injection within a DVR. This design philosophy deviates from previous approaches by incorporating the expertise of controller design specialists. The concept originates from the fuzzy set theory. There exist scenarios where it is not feasible to establish accurate mathematical formulations, thus making FL controllers an attractive substitute. One benefit of utilizing this controller is its ability to mitigate the inaccuracy and transient overshoot associated with PWM.

The conventional PI controller is substituted with the fuzzy logic controller (FLC) to attain the intended outcomes. The voltages produced by the three-phase source undergo a conversion process into the d and q coordinates, as described in reference [38]. A comparison is conducted between the reference values for V_d and V_q and the altered values, resulting in the acquisition of voltage errors. The processing of these problems is carried out by a pair of FL controllers. In order to generate PWM inverter signals, the outputs produced are subsequently converted back into the three-phase domain and subsequently compared with a carrier signal.

Contrary to conventional controllers, the application of a mathematical model of the regulated system process is not a prerequisite for the implementation of a fuzzy logic controller. Therefore, it is necessary to possess a comprehensive understanding of the system's operational procedures and the associated control prerequisites. The designer of the fuzzy controller must establish the control input variable, control strategy and decision, and solution output variable to determine the information data that enters the system, how they are processed, and the information data that exit the system. The FLC comprises three main components that serve as its building blocks. The user's text does not contain any information to be rewritten. The three components are the fuzzifier, inference engine, and defuzzifier.

8.1. Fuzzifer

To guarantee the effective functioning of the FLC, it is imperative that all control and solution variables, which play a crucial role in creating the control surface, are formulated using fuzzy set notations accompanied by linguistic labels. The process of decomposing each system variable into fuzzy regions is achieved by employing a set of three distinct classes of linguistic labels, which are described by their respective membership grades. This is undertaken to streamline the procedure. One method for quantifying the extent to which a variable is linked to a certain category or label is to employ the concept of membership grade. The term "fuzzification" refers to the procedure of converting input/output variables into linguistic labels. When the program is executed, it utilizes reference fuzzy sets for the inputs d and q, as depicted in Figures 9 and 10. The fuzzy sets are subsequently employed to establish a fuzzy set that expresses the notion corresponding to the label in a semantic manner. To ensure a seamless and solid control surface, it is important to establish an overlap between successive labels. The design of the overlap should be such that the cumulative vertical points of the overlap do not exceed a value of one.

The membership function of input-d and input-q is constructed using a direct method, as depicted in Figures 9 and 10. The use of an error rate signal, such as the discrepancy between the actual signal and its converted version, is a prudent choice. However, the input signals themselves are employed in this study to simplify and expedite the response time for the FL approach.

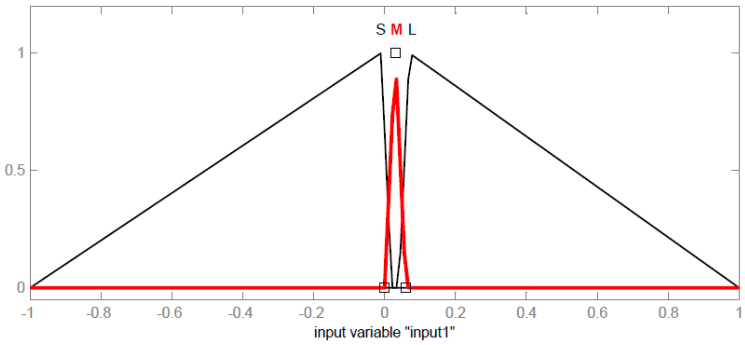

Figure 9. Membership function input-d.

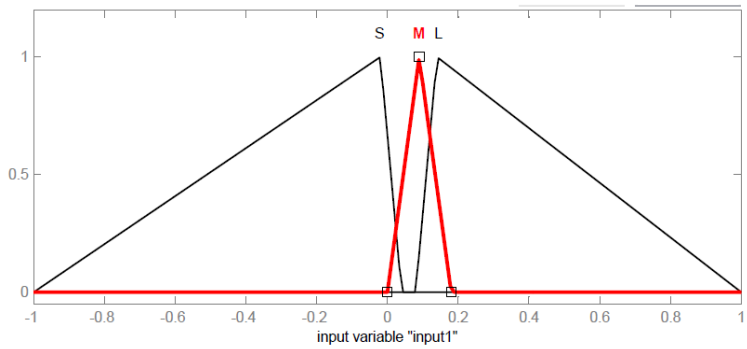

Figure 10. Membership function input-q.

8.2. Inference Engine

The control surface is subject to a set of regulations that dictate its functioning, specifically in terms of establishing a connection between the input variables of the system and the corresponding output variables. The proposition (fuzzy proposition) implies (fuzzy proposition), exemplifying a frequently employed rule. The set of rules for the fuzzy controller is obtained from the MacVicar-Whelan decision table, as shown in Table 1. The table shown in this context proposes a clear and specific course of action for a particular set of uncomplicated rules since it solely necessitates a single input. These principles are employed to ascertain the most appropriate course of action for control. Every rule that contains at least some level of truth (a value greater than zero for membership grade) in its premises is activated upon reading a set of input variables. This action facilitates the development of the control surface by its proper modification. In the case a given set of input variables is received, every rule is triggered. Once all the rules have been executed, the final control surface is characterized as a fuzzy set. This is achieved by utilizing linguistic labels defined by membership grades. The purpose of this representation is to symbolically reflect the output of the controller.

8.3. Defuzzifier

For the system to function efficiently, it is necessary to transform the fuzzy set that represents the controller output in linguistic labels into a crisp solution variable for which a defuzzifier is utilized. There are several different defuzzification strategies from which one might choose. When it comes to estimation, the two methods that are utilized the most frequently are the Mean of Maxima (MOM) and the Center of Area (COA). It is typical practice to implement this method in the majority of control applications. This method delivers a result that is very responsive to all of the rules that are being executed, and it does so by calculating the centroid of the ultimate fuzzy region, which is also widely referred to as the control surface. As a consequence, the results tend to transmit without interruption throughout the control surface. It is executed using reference fuzzy sets shown in Figures 11 and 12 for outputs d and q.

Table 1. The fuzzy control rules.

No.	Rule
1	If input 1 is S, then output 1 is S.
2	If input 1 is M, then output 1 is M.
3	If input 1 is L, then output 1 is L.

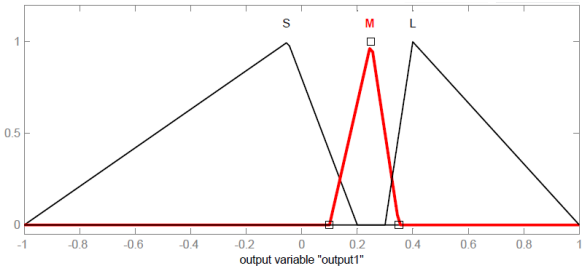

Figure 11. The membership function output-d.

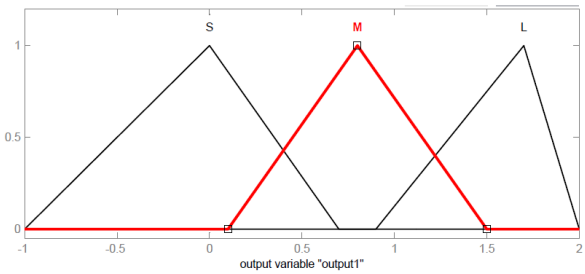

Figure 12. The membership function output-q.

9. Design of DVR with ANFIS Controller

The Adaptive-Neuro-based Fuzzy Inference System (ANFIS) is a variant of the Fuzzy Inference System (FIS) that may be integrated into adaptive networks. The ANFIS serves as a fundamental framework for developing a collection of fuzzy rule bases, which incorporate the necessary membership functions to establish the desired input and output pairings as defined. The produced Fuzzy Inference System (FIS) transfers the qualities of the input to the membership functions of the input, thus influencing the rule base. A correspondence exists between the established rules and a collection of output attributes, whereby the output attributes are converted into the output membership function to generate a singular, definitive result.

9.1. Creating Neuro-Fuzzy Inference System

The proposed ANFIS controller is trained using the generated FIS by mapping the calculated input-output data. A hybrid learning algorithm is used to train the proposed ANFIS controller during 45 epochs. Figure 13 shows the structure of the generated FIS with two inputs and a single output, each having two membership functions. Here, unlike the FL, which is described later, there are two inputs for each structure, one of which is the actual signal (*Vp* or *Vq*) and an error rate signal between this actual signal, and the transformed actual signal is another input.

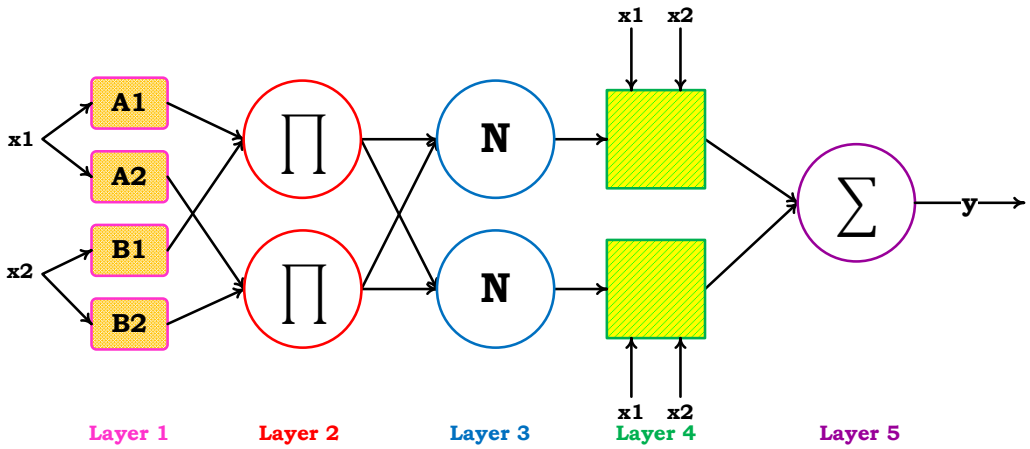

Figure 13. The structure of the generated neuro-fuzzy inference system.

Table 2. System and DVR parameters and constants.

Voltage source	22.5 kV, 50 Hz	
Basic load	2000 kVA	
Load	2500 kVA	
Tr. basic load	2.5kV, 20000,380	
Tr. load	2.5kV, 20000,380	
DVR	DC link voltage	100V
	PWM frequency	10 kHz
	Filter L	6 mH, 0.2 Ohm
	Filter C	20 uF, 0.2 Ohm
	Injection Tr.	1.5kV,100,1000

10. Simulation

The performance enhancement of the DVR in mitigating voltage sag and swell is demonstrated by the simulation of a simplified distribution system in MATLAB/SIMULINK, using the suggested controller. Table 2 presents a summary of the system's parameters and the constant value. It is assumed that the load bus voltage remains constant at 1 per unit (p.u.) during voltage sags and swells. Several figures depict the simulation findings that were deemed to be the most noteworthy.

The phrase "line voltage notch" pertains to a decrease in the supplied voltage that manifests as a dip in the waveform of the line voltage. This phenomenon is observed when the electrical current transitions between the phases. During the notching interval, a transient short circuit occurs between the two commutating phases, leading to a decrease in the line voltage. The supply impedance is the primary determinant of the extent to which voltage reduction is limited.

The use utilization of the conventional PI controller is a widespread practice in the regulation of DVRs. Nonetheless, this traditional controller relies on constant gains, which may result in inadequate control performance in the presence of parameter fluctuations within the system. Throughout this inquiry, a comprehensive analysis has been conducted to compare the performance of the DVR under two distinct scenarios: one utilizing the standard PI controller, and the other employing advanced control techniques such as NN, FL, or ANFIS controllers. In the initial situation, the DVR is tasked with showcasing the smoothness and appropriateness of the signal shape of the injected voltage. In the second scenario, the waveform of the load voltage signal is susceptible to either being accepted or rejected. Implementation of the NN, FL, ANFIS, and PI controller for three phases is shown in Figure 14.

The main structure of all four methods is the same and only the voltage regulator design differs from each other. For example, the voltage regulator design of NN, FL, and PI methods are demonstrated in Figures (15-17), respectively.

DVR system has some structure inside, e.g., the LC filter of DVR shown in Figure 18.

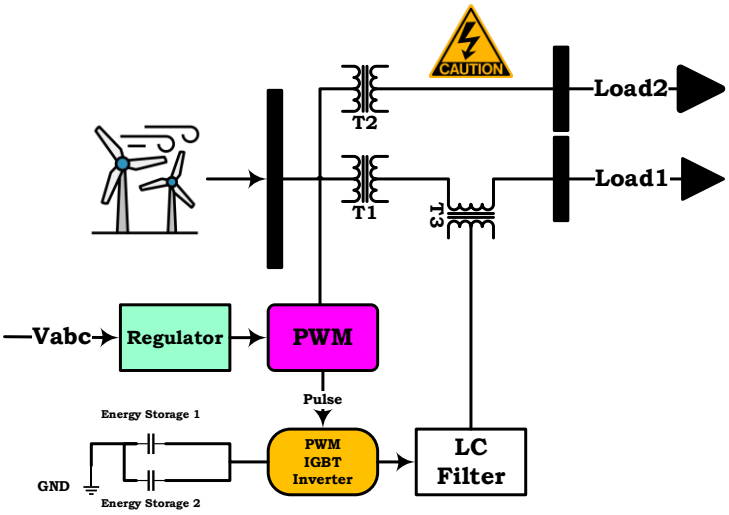

Figure 14. A schematic of DVR implementation by MATLAB/SIMULINK software.

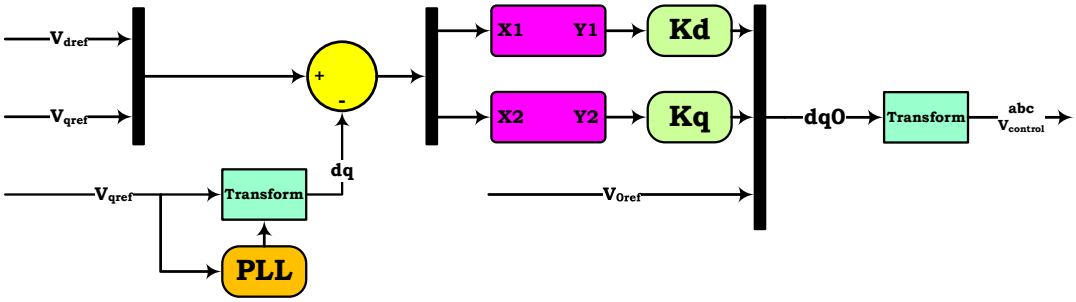

Figure 15. The regulator structure of DVR for NN.

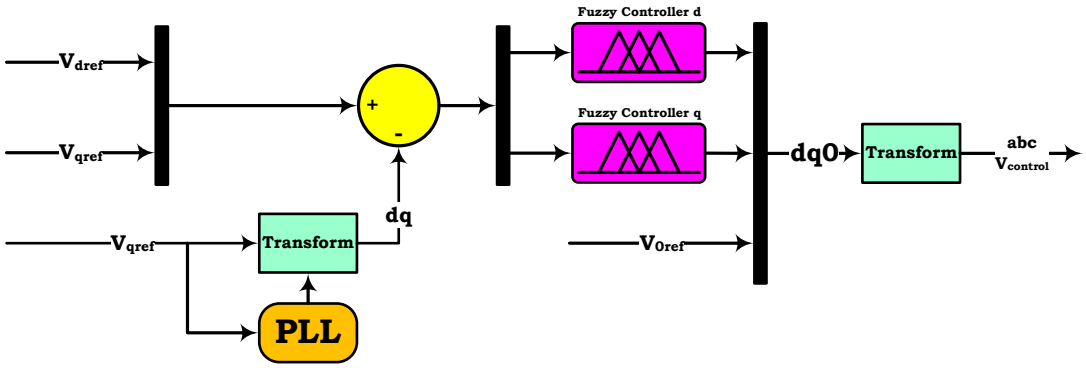

Figure 16. The voltage regulator structure of DVR for FL.

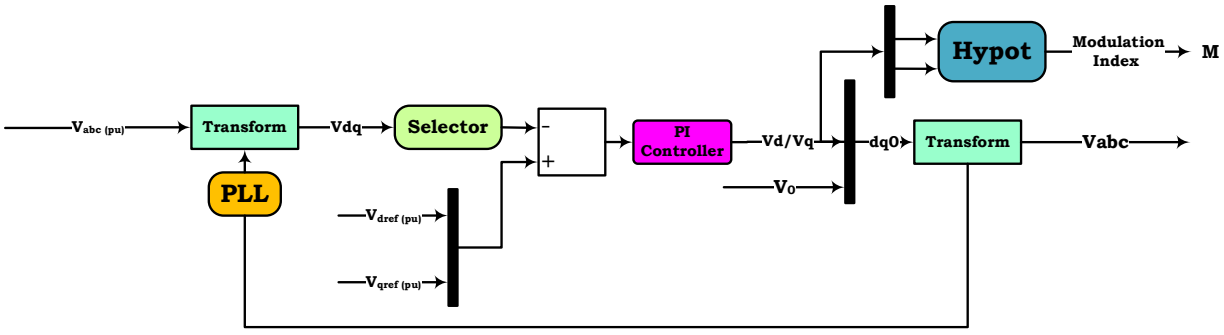

Figure 17. The voltage regulator structure of DVR for PI controller.

Figures 19 and 20 show a three-phase voltage sag simulated for PI and NN methods, respectively. The simulation started with a supply voltage of 100% and a phase (B)-to-ground fault with 1.8 Ohm fault resistance occurs from 0.019 sec to 0.085 sec, resulting in

sagging as per Figures 19(a-e) and 20(a-e) for the PI and NN methods, respectively. Furthermore, Figures 19(c) and 20(c) illustrate the voltage injected by the DVR, along with the related load voltage after correction. The load voltage is sustained at a value of 1 p.u. due to the presence of the DVR. The comparison of these two signals in Figures 19(c) and 20(c) demonstrates the better injection of voltage by the NN method. The load voltages of the two methods are acceptable but, the se of the NN method results in more balanced and better shape of voltage. Figure 21 is a comparison between the sSource voltage and the critical load voltage in NN, showing that an acceptable compensation is done.

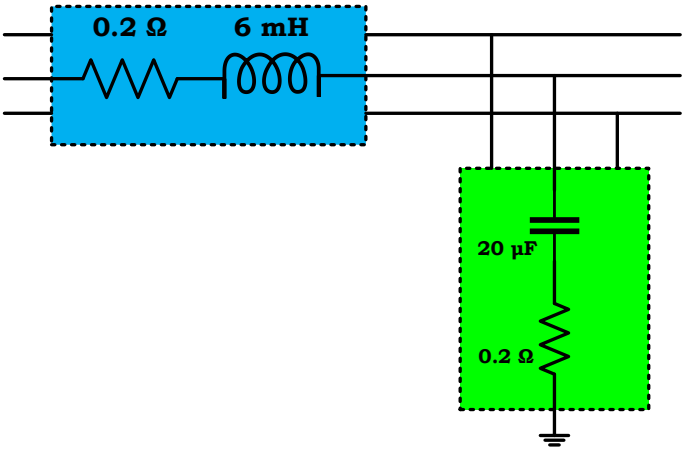

Figure 18. The LC filter structure of DVR.

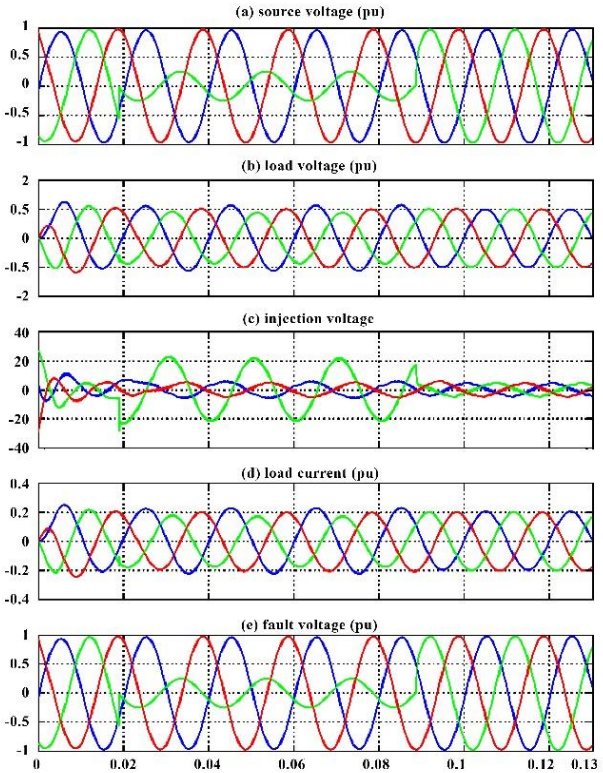

Figure 19. The PI controller signals 1 Phase (B) to ground fault, (a) Source Voltage [pu], (b) Load Voltage [pu], (c) Injection Voltage, (d) Load Current [pu], (e) Fault Voltage [pu].

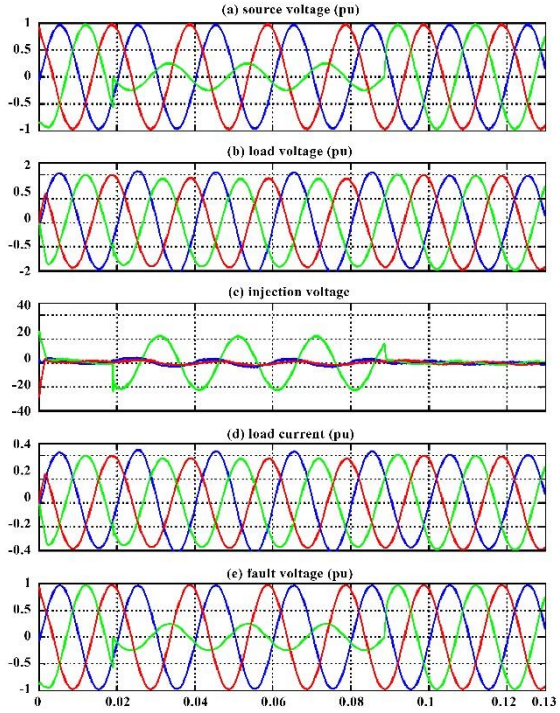

Figure 20. NN controller signals1 Phase (B)-to-ground fault, (a) source voltage [pu], (b) load voltage [pu], (c) injection voltage, (d) load current [pu], and (e) fault voltage [pu].

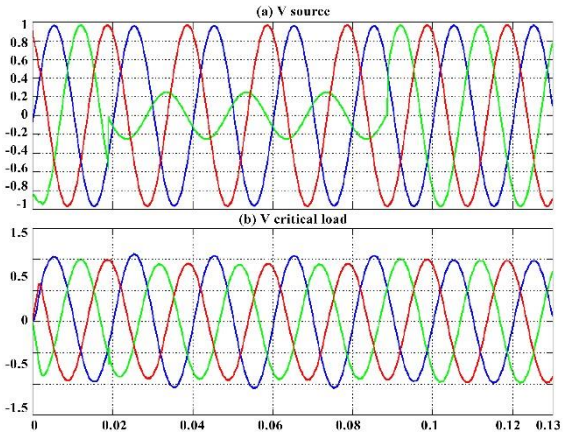

Figure 21. NN controller signals1 Phase (B)-to-ground fault, (a) V source, and (b) V critical load.

Figure 22 shows the three-phase voltage sag simulated for the FL method. The simulation started with a supply voltage of 100% and two phases (B and C)-to-ground faults with 0.1 Ohm fault resistance, each phase occurring from 0.019sec to 0.085sec and causing sagging as shown in Figure 22(a-e) for the FL method. Furthermore, Figure 22(c) illustrates the voltage injected by the DVR and the corresponding load voltage with correction. The load voltage is sustained at a value of 1 p.u. due to the presence of the DVR. The load voltage of this method is acceptable. Figure 23 is a comparison between the source voltage and critical load voltage in FL, reflecting an acceptable compensation. The ANFIS method is modeled as shown in Figure 24. Values of *d* and *q* assumptions as actual signals and an error rate signal between the actual signal and transformed actual signal make two inputs.

Here, the ANFIS method could be designed like the FL method, but as there is no need to define a membership function in this method and it itself does that, this method is more comfortable and somehow more accurate than the FL method. For example, Figure 25 shows the membership function of input1-q that is designed by the ANFIS method. To check the accuracy of the ANFIS work, there is a training data check and test shown in Figure 26.

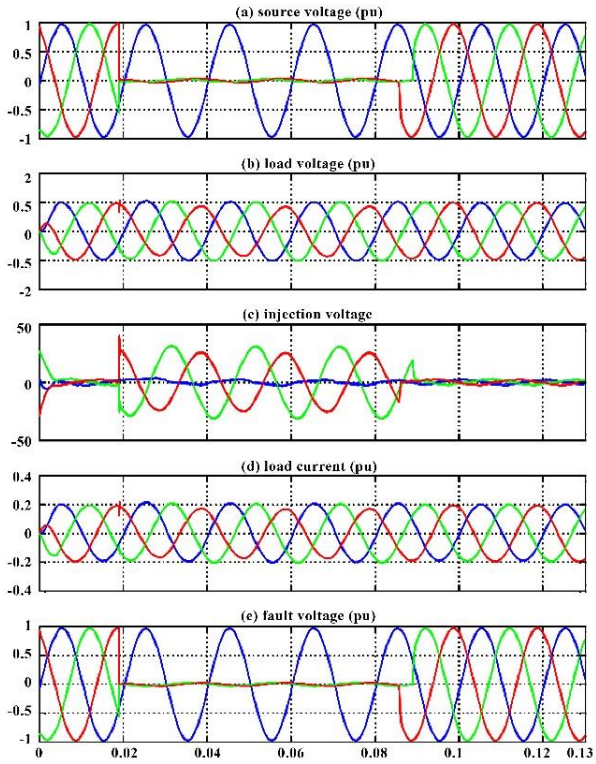

Figure 22. FLC signals 2 Phases- (B and C)-to-ground faults, (a) source voltage [pu], (b) load voltage [pu], (c) injection voltage, (d) load current [pu], and (e) fault voltage [pu].

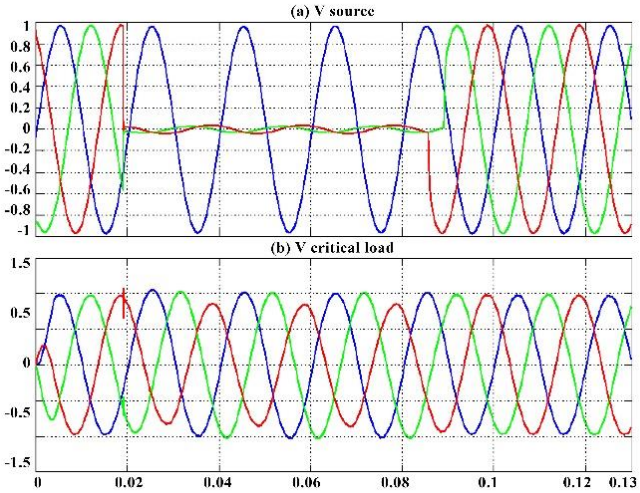

Figure 23. FLC signals 2 phases (B and C)-to-ground faults, (a) V source, and (b) V critical load.

Figure 27 shows a three-phase voltage sag simulated for the ANFIS method. The simulation started with a supply voltage of 100% and two phase (B and C)-to-ground faults with 0.1 Ohm fault resistance, each occurring from 0.019sec to 0.085sec and causing sagging as shown in Figure 27(a-e) for the ANFIS method.

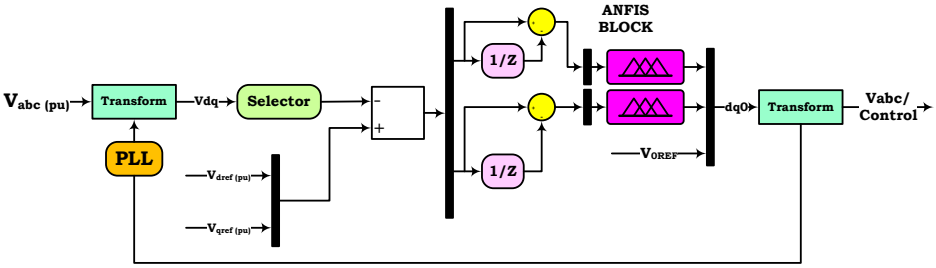

Figure 24. The voltage regulator structure of DVR for FL.

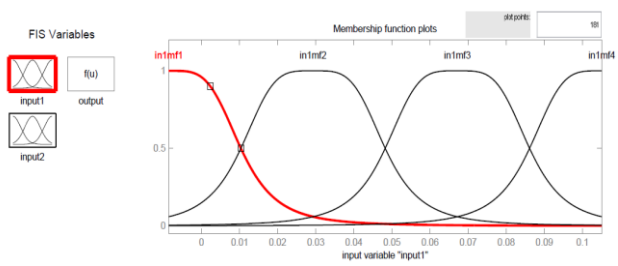

Figure 25. The membership function input1-q.

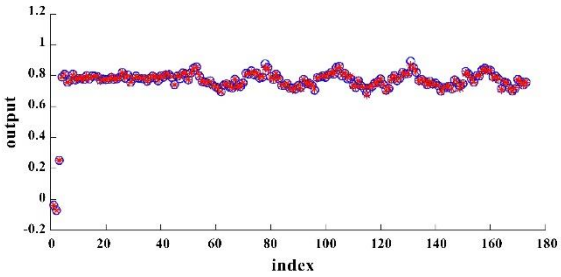

Figure 26. The ANFIS training data test.

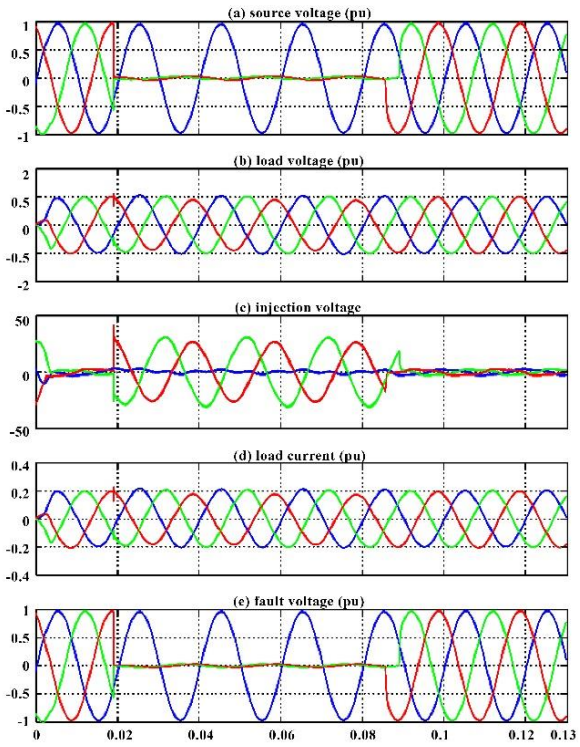

Figure 27. ANFIS controller signals two phases (B and C)-to-ground faults, (a) source voltage [pu], (b) load voltage [pu], (c) injection voltage, (d) load current [pu], and (e) fault voltage [pu].

11. Comparing Injection Voltages of The Methods

Three injection voltages of the controllers of various methods in the same conditions (fault in B & C phases with R_f=0.1 Ohm) are shown in Figures 28-31. There aren't any special parameters that show which method can possibly better measure Total Harmonic Distortion (THD) in various DVRs so their comparison may turn out to be a good practice. However, it seems that all methods are acceptable, but as shown in these figures, the PI controller doesn't perform as accurately as the other methods. Finally, the ANFIS method is a good choice because of its simpler design.

12. Conclusion

A DVR is a highly efficient device designed to mitigate the voltage drop experienced in distribution networks. This article discussed the control strategies that can be employed to mitigate voltage sag by utilizing the DVR technology. The recommended controller was constructed by utilizing the usual PI controller, NN, FL, and ANFIS training methodologies. The controller was subsequently trained using the input and output data that were provided. The efficiency of the recommended DVR with NN, FL, and ANFIS controller was

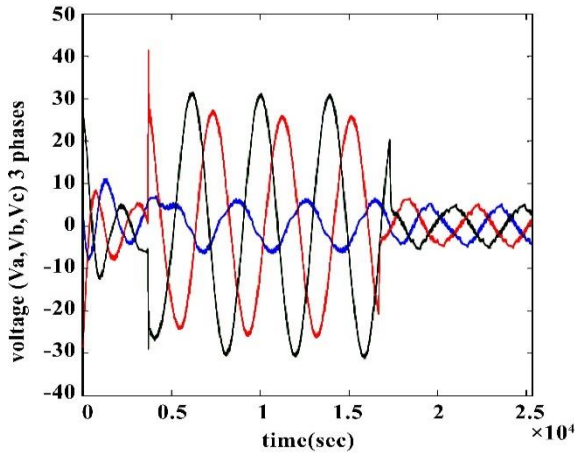

Figure 28. The PI controller injection voltages.

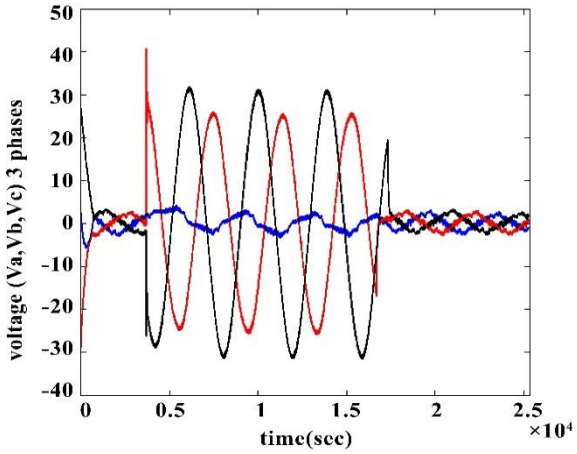

Figure 29. The FLC injection voltages.

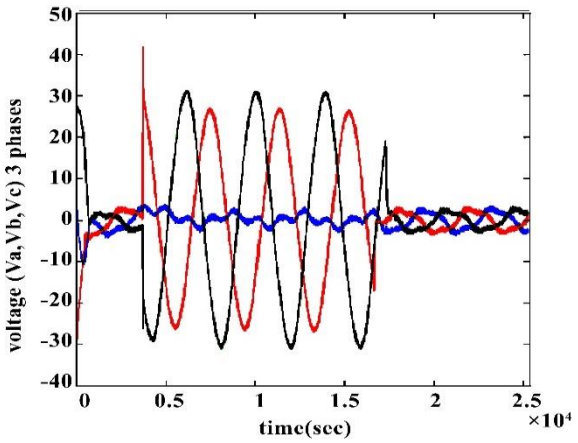

Figure 30. The ANFIS controller injection voltages.

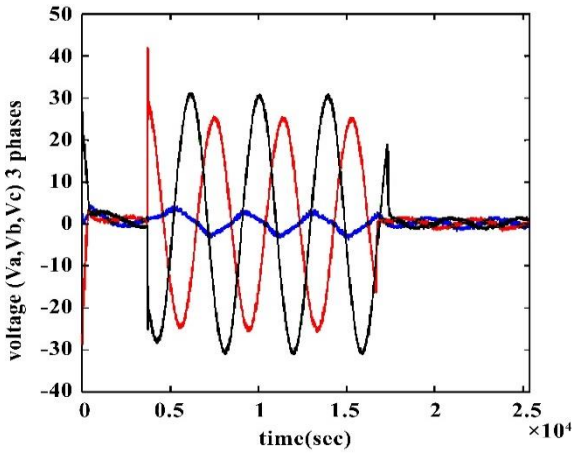

Figure 31. The NN controller injection voltages.

superior to that of the traditional PI controller in mitigating the voltage sag on the test system under investigation. This scenario pertained to the evaluation of the application of a one or two-phase to ground fault.

This study demonstrated the application of MATLAB/Simulink for modeling and simulating a DVR. A control system was developed by the d-q-o approach. The control mechanism in question utilized a scaled error between the source side of the DVR and its reference in order to correct for sags and swells. The simulation findings demonstrated that the performance of various DVRs across four distinct approaches was satisfactory in mitigating voltage sags and swells. The accuracy of the PI controller was comparatively lower than that of the alternative methodologies. Upon careful consideration, it can be argued that the ANFIS technique was a prudent selection due to its relative ease of construction.

Furthermore, the results of the simulation indicated that the DVR exhibited commendable voltage control capabilities and effectively mitigated voltage sags and swells. The DVR exhibited the ability to effectively manage both balanced and unbalanced conditions with ease. Additionally, it introduced the requisite voltage component to promptly rectify any deviation in the input voltage, hence facilitating the preservation of the output voltage at a consistent level and guaranteeing its equilibrium. The final achievements of this research were as follows:

- Constructing a controller by utilizing the usual PI controller, NN, FL, and ANFIS training methodologies and using the input and output data
- Improving the efficiency of the recommended DVR with NN, FL, and ANFIS controller versus the traditional PI controller in mitigating the voltage sag on the test system under investigation
- Using a scaled error between the source side of the DVR and its reference to correct for sags and swells
- The ability to effectively manage both balanced and unbalanced conditions with ease

In future research, other methods can be used instead of the ANFIS method. Also, the evaluation indices of the proposed method can be considered stricter to help improve the quality of the network voltage.

References

[1] M. Abasi, A. Saffarian, M. Joorabian, and S. G. Seifossadat, "Location of Double-Circuit Grounded Cross-Country Faults in GUPFC-Compensated Transmission Lines Based on Current and Voltage Phasors Analysis," *Electric Power Systems Research*, vol. 195, 107124, 2021.

[2] M. Abasi, M. Joorabian, A. Saffarian, and S. G. Seifossadat, "A Comprehensive Review of Various Fault Location Methods for Transmission Lines Compensated by FACTS Devices and Series Capacitors," *Journal of Operation and Automation in Power Engineering*, vol. 9, no. 3, pp. 213-225, 2021.

[3] IEEE Std. 1159 – 1995, "Recommended Practice for Monitoring Electric Power Quality," 1995.

[4] I. C. Barutçu, and A.Erduman. "Review on Voltage Sag Studies for Distribution Grid Including Renewable Energy Sources," *Mugla Journal of Science and Technology*, vol. 9, no. 1, pp. 16-23.

[5] M. Hasan, "Detection, Analysis, and Mitigation of Voltage Sag in Renewable Energy-Rich Power Grids," *University of Wollongong*, 2020.

[6] M. F. Nezhadnaeini, M. Hajivand, M. Abasi, and S. Mohajerami "Optimal Allocation of Distributed Generation Units Based on Different Objectives by a Novel Version Group Search

Optimizer Algorithm in Unbalance Load System," *Revue Roumaine Des Sciences Techniques Série Électrotechnique Et Énergétique*. vol. 61, no. 4, pp. 338–342, 2016.

[7] S. Shakeri, S. Esmaeili, and M. H. R. Koochi, "Determining Accurate Area of Vulnerability for Reliable Voltage Sag Assessment Considering Wind Turbine Ride-Through Capability," *International Journal of Electrical Power & Energy Systems*, vol. 119, 105875, 2020.

[8] A. Chakraborty, and T. Maity, "Integrated Control Algorithm for Fast and Accurate Detection of the Voltage Sag with Low Voltage Ride-Through (LVRT) Enhancement for Doubly-Fed Induction Generator (DFIG) Based Wind Turbines," *Control Engineering Practice*, vol. 131, 105393, 2023.

[9] C. K. Shiva, V. Vigya, et al., "Analysis of Voltage Sag in DFIG Based Wind Power System," *AIP Conference Proceedings*, vol. 2418, no. 1, 2022.

[10] C. Fitzer, M. Barnes, and P. Green, "Voltage Sag Detection Technique for a Dynamic Voltage Restorer," *IEEE Transactions on Industry Applications*, vol. 40, no. 1, pp. 203-212, 2004.

[11] P. T. Cheng, C. C. Huang, C. C. Pan, and S. Bhattacharya, "Design and Implementation of Series Voltage Sag Compensator Under Practical Utility Conditions," *IEEE Transactions on Industry Applications*, vol. 39, no. 3, pp. 844-853, 2003.

[12] J. Li, Y. Yang, et al., "A Voltage Sag Detection Method Based on Modified S Transform with Digital Prolate Spheroidal Window," IEEE *Transactions on Power Delivery*, vol. 36, no. 2, pp. 997-1006, 2020.

[13] B. H. Li, S. S. Choi, and D. M. Vilathgamuwa, "Design Considerations on the Line-Side Filter Used in the Dynamic Voltage Restorer," *IEE Proceedings - Generation, Transmission, and Distribution*, vol. 148, no. 1, pp. 1-7, 2001.

[14] E. K. K. Sng, S. S. Choi, and D. M. Vilathgamuwa, "Analysis of Series Compensation and DC-Link Voltage Controls of a Transformerless Self- Charging Dynamic Voltage Restorer," *IEEE Transactions on Power Delivery*, vol. 19, no. 3, pp. 1511-1518, 2004.

[15] W. Jing, X. Aliqin, and S. Yueyue, "A Survey on Control Strategies of Dynamic Voltage Restorer," *13th International Conference on Harmonics and Quality of Power,* pp. 1-5, 2008.

[16] J. G. Nielsen, and F. Blaabjerg, "A Detailed Comparison of System Topologies for Dynamic Voltage Restorers," *IEEE transactions on industry applications*, vol. 41, no. 5, pp. 1272-1280, 2005.

[17] Y. H. Cho, and S. K. Sul, "Controller Design for Dynamic Voltage Restorer with Harmonics Compensation Function," *Conference Record of the 2004 IEEE Industry Applications Conference, 2004. 39th IAS Annual Meeting,* vol. 3, pp. 1452-1457, 2004.

[18] S. Sanati, and Y. Alinejad-Beromi, "Fast and Complete Mitigation of Residual Flux in Current Transformers Suitable for Auto-Reclosing Schemes Using Jiles-Atherton Modeling," *IEEE Transactions on Power Delivery*, vol. 37, no. 2, pp. 765-774, 2022.

[19] S. Sasitharan, M. K. Mishra, B. K. Kumar, and V. Jayashankar, "Rating and Design Issues of DVR Injection Transformer," *International Journal of Power Electronics*, vol. 2, no. 2, pp. 143-163, 2010.

[20] H. Kim, J. H. Kim, and S. K. Sul, "A Design Consideration of Output Filters for Dynamic Voltage Restorers," *IEEE 35th Annual Power Electronics Specialists Conference*, vol. 6, pp. 4268-4272, 2004.

[21] M. H. J. Bollen, "Understanding Power Quality Problems," *New York: IEEE Press*, 2000.

[22] B. Wang, and G. Venkataramanan, "Dynamic Voltage Restorer Utilizing a Matrix Converter and Flywheel Energy Storage," *IEEE transactions on industry applications*, vol. 45, no. 1, pp. 222-231, 2009.

[23] C. Zhan, V. K. Ramachandaramurthy, et al., "Dynamic Voltage Restorer Based on Voltage Space Vector PWM Control," *IEEE Transactions on Industry Applications*, vol. 37, no. 6, pp.1855-1863, 2001.

[24] J. H. Han, J. G. Shon, I. D. Seo, and H. j. jeon, "Development of On-Line Type Dynamic Voltage Compensation System using Super Capacitor," *7th International Conference on Power Electronics*, pp. 455-460, 2007.

[25] Y. Li, Y. L. Wang, B. H. Zhang, and C. X. Mao, "Modeling and Simulation of Dynamic Voltage Restorer Based on Super Capacitor Energy Storage," *International Conference on Electrical Machines and Systems*, pp. 2064-2066, 2008.
[26] T. Jimichi, H. Fujita, and H. Akagi, "Design and Experimentation of a Dynamic Voltage Restorer Capable of Significantly Reducing an Energy-Storage Element," *IEEE transactions on industry applications*, vol. 44, no. 3, pp. 817-825, 2008.
[27] A. Ghosh, A. K. Jindal, and A. Joshi, "Design of a Capacitor- Supported Dynamic Voltage Restorer (DVR) for Unbalanced and Distorted Loads," *IEEE Transactions on Power Delivery*, vol. 19, no. 1, pp. 405-413, 2004.
[28] J. Ebrahimi, and M. Abasi, "Design of a Power Management Strategy in Smart Distribution Networks with Wind Turbines and EV Charging Stations to Reduce Loss, Improve Voltage Profile, and Increase Hosting Capacity of the Network," *Journal of Green Energy Research and Innovation*, vol. 1, no. 1, pp. 1-15, 2024.
[29] P. T. Cheng, C. C. Huang, C. C. Pan, and S. Bhattacharya, "Design and Implementation of Series Voltage Sag Compensator under Practical Utility Conditions," *IEEE Transactions on Industry Applications*, vol. 39, no. 3, pp. 844-853, 2003.
[30] J. G. Nielsen, M. Newman, H. Nielsen, and F. Blaabjerg, "Control and Testing of a Dynamic Voltage Restorer (DVR) at Medium Voltage Level," *IEEE Transactions on Power Electronics,* vol. 19, no. 3, pp. 806-813, 2004.
[31] Y. H. Chung, H. J. Kim, et al., "Neural Network Controlled Voltage Disturbance Detector and Output Voltage Regulator for Dynamic Voltage Restorer," *2007 European Conference on Power Electronics and Applications,* pp. 1-9, 2007.
[32] Y. H. Chung, G. Kwon, et al., "Medium Voltage Dynamic Voltage Restorer with Neural Network Controlled Voltage Disturbance Detector," *International Conference on Power System Technology, Chongqing, China*, pp. 1-7, 2006.
[33] C. Benachaiba, and B. Ferdi, "Voltage Quality Improvement Using DVR," *Electrical Power Quality and Utilisatio*n, vol. 14, no. 1, pp. 39-46, 2008.
[34] B. Arandian, "Utilizing Hybrid Sine Cosine Shuffled Frog Leaping Algorithm for Optimal Energy Management in the Residential building with Renewable Energy Resources and Corresponding Uncertainties," *Journal of Green Energy Research and Innovatio*n, vol. 1, no. 1, pp. 66-79, 2024.
[35] M. V. Rajesh, R. Archana, A. Unnikrishnan, R. Gopikakumari, and J. Jacob. "Evaluation of the ANN Based Nonlinear System Models in the MSE and CRLB Senses," *World Academy of Science, Engineering and Technology*, vol. 48, no. 34, pp. 211-215, 2008.
[36] R. Dehini, A. Bassou, and B. Chellali, "Generation of Voltage References Using Multilayer Feed Forward Neural Network," *Przeglad Elektrotechniczny*, 2012.
[37] M. Abasi, A. T. Farsani, A. Rohani, and M. A. Shiran, "Improving Differential Relay Performance During Cross-Country Fault Using A Fuzzy Logic-Based Control Algorithm," *5th Conference on Knowledge-Based Engineering and Innovation,* pp. 193-199, 2019.
[38] A. Elmitwally, M. S. Kandil, and M. Elkateb, "A Fuzzy-Controlled Versatile System for Harmonics, Unbalance and Voltage Sag Compensation," *IEEE Power Engineering Society Summer Meeting*, vol. 3, pp. 1439-1444, 2000.
[39] F. Juardo, M. Valverde, and J. Carpio, "Voltage Sag Correction by Dynamic Voltage Controller Based on Fuzzy Logic Controller," *CCECE 2003-Canadian Conference on Electrical and Computer Engineering. Toward a Caring and Humane Technology,* vol. 1, pp. 421-424, 2003.

Declaration of Competing Interest

The authors declare that they have no known competing financial interests or personal relationships that could have appeared to influence the work reported in this paper. The ethical issues, including plagiarism, informed consent, misconduct, data fabrication and/or falsification, double publication and/or submission, redundancy, have been completely observed by the authors.

Credit Authorship Contribution Statement

Saman Darvish Kermani: Conceptualization, Formal analysis, Investigation, Methodology, Resources, Roles/Writing - original draft. **Ali Morsagh Dezfuli:** Methodology, Resources, Roles/Writing - original draft. **Abdolreza Behvandi:** Conceptualization, Methodology, Supervision, Roles/Writing - original draft. **Mehrdad Kankanan:** Resources, Validation, Visualization, Roles/Writing - original draft.

Bibliography

Saman Darvish Kermani received his PhD degree in 2016 from Shahid Chamran University of Ahvaz, Ahvaz, Iran in the field of electrical engineering. He is currently working at GHD Advisory Melbourne VIC 3000 Australia in the field of renewable energy. His main research interests include optimization, nature-inspired metaheuristic algorithms, islanding, microgrid, smart grid, power quality, modeling of electrical networks, and distributed renewable resources.

Ali Morsagh Dezfuli was born in Dezful, Iran in 1992. He received the B.Sc. degree from the Jundi-Shapur University of Technology of Dezful, Dezful, Iran in 2015, the M.Sc. degree from the Shahid Rajaee Teacher Training University of Tehran, Tehran, Iran in 2017 and he is a PhD candidate at Shahid Chamran University of Ahvaz, Ahvaz, Iran all in Power Electrical Engineering. His research interests are: Voltage and Frequency Control of Microgrid, Power Electronics, FACTs Devices and Power System Protection.

Abdolreza Behvandi was born in 1987 in Iran. He received his B.Sc., M.Sc., and Ph.D. degrees all in Electrical Engineering (Power Systems) in 2010, 2012, and 2019 from Isfahan University of Technology, Isfahan University, and Shahid Chamran University of Ahvaz, respectively. Currently, he is an Assistant Professor at Department of Electrical Engineering, Ramhormoz Branch, Islamic Azad University, Ramhormoz, Iran. His special interests are power system studies, power system protection, renewable energy, and microgrids.

Mehrdad Kankanan, born on June 25, 1986, is an accomplished author and researcher in the field of Electrical Engineering. He holds an MSc (2011) and a Ph.D. (2018) in Electrical Engineering from Shahid Chamran University of Ahvaz, Iran. As an Assistant Professor in the Electrical Engineering Department at Islamic Azad University of Ramhormouz, Mehrdad Kankanan focuses his expertise on Semiconductor Devices, with a special emphasis on Solar Cells, Digital Circuits, and Power Electronics.

Journal of Green Energy Research and Innovation

Scenario-Based Planning of Participation of Virtual Power Plants in Storage and Energy Markets in Terms of Load Response and Market Price Uncertainty

Hamidreza Hanif, Mohammad Zand, Morteza Azimi Nasab, Seyyed Mohammad Sadegh Ghiasi, Sanjeevikumar Padmanaban

Highlight

- Providing an inertial response for ESS with fast response capability
- Investigating the effect of inertial response in establishing frequency response and network behavior after sudden events
- Considering the new model of the problem and applying the novel algorithm for this problem

Graphical Abstract

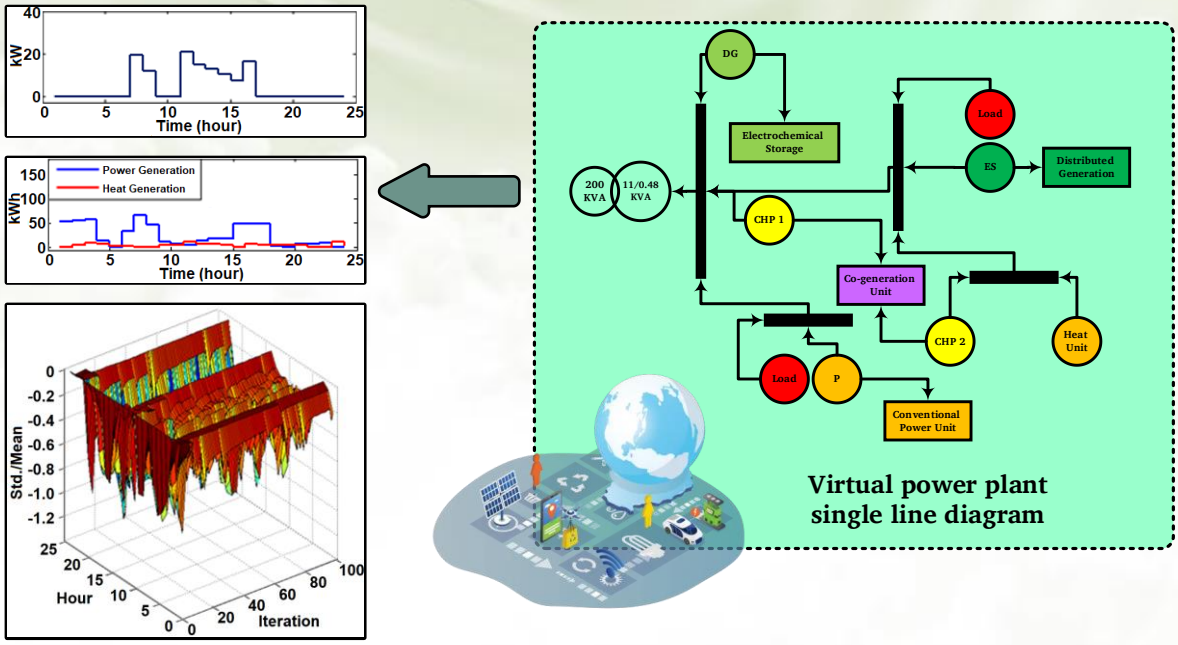

Optimum Result

Use your device to scan and read the article online

Citation

H. Hanif, M. Zand, M. Azimi Nasab, S. M. S. Ghiasi, and S. Padmanaban,"Scenario-Based Planning of Participation of Virtual Power Plants in Storage and Energy Markets in Terms of Load Response and Market Price Uncertainty," *Journal of Green Energy Research and Innovation*, vol. 1, no. 3, pp. 77-95, 2024.

https://doi.org/10.61186/jgeri.1.3.77

JGERI Journal of Green Energy Research and Innovation

Online ISSN: 3041-9018

Journal of Green Energy Research and Innovation

Journal Homepage: www.jgeri.araku.ac.ir

Scenario-Based Planning of Participation of Virtual Power Plants in Storage and Energy Markets in Terms of Load Response and Market Price Uncertainty

Hamidreza Hanif [1], Mohammad Zand [2]*, Morteza Azimi Nasab [3], Seyyed Mohammad Sadegh Ghiasi [4], Sanjeevikumar Padmanaban [5]

[1] *Iran University of Science and Technology (IUST), Tehran, Iran.*
[2] *Young Researcher and Elite Club, Hamedan Branch, Islamic Azad University, Hamedan, Iran.*
[3] *Young Researcher and Elite Club, Borujerd Branch, Islamic Azad University, Borujerd, Iran.*
[4] *Department of Electrical Engineering, Ahvaz Branch, Islamic Azad University, Ahvaz, Iran.*
[5] *Department of Electrical Engineering, IT and Cybernetic, University of South-Eastern Norway, 3918 Porsgrunn, Norway.*

* ***Corresponding Author:*** *dr.zand.mohammad@gmail.com*

ARTICLE INFO

Keywords:
Virtual power plants,
Storage and energy markets,
Combined heat and power,
Price uncertainty.

Article history:
Received: 29 December 2023;
Revised: 06 February 2024;
Accepted: 26 February 2024;

Article type:
Research Article

ABSTRACT

Environmental concerns, advancements in the new energy industry, and rising power generation and transmission costs are driving the electricity industry towards innovation. This has led to the installation of distributed energy resources (DERs) in many regions. Virtual power plants (VPPs), which manage decentralized energy systems by aggregating the capacity of various distributed generations (DGs), storage devices, and distributable loads, are used for trading energy and services. The research focuses on the planning of price-based unit commitment (PBUC) managed by VPPs over a 24-hour period. Simulation results demonstrate that the proposed framework effectively develops strategies for VPP market production and consumer interaction, especially with load-shedding capabilities. A key aspect of the study is examining the impact of uncertainties on VPP strategies. Probability density functions and the Monte Carlo method are used to model and assess these uncertainties. Simulations without energy price and demand uncertainties indicate that the model is suitable for strategizing VPP market production and consumer interaction. However, simulations that include market price uncertainties and predicted VPP loads show that VPP profits are influenced by market volatility. Increased price and demand fluctuations significantly affect VPP strategies, sometimes resulting in losses during certain periods.

1. Introduction

Due to the gradual exhaustion of fossil fuel-based energy sources and widespread concern about environmental protection, renewable energy sources (RES) and demand response (DR) technology are deployed in the power system [1-3]. However, insufficient management as well as the bottleneck of technology are the main obstacles to their further development.

1.1. Literature review

The use of distributed algorithms in the multi-player strategy optimization problem accelerates the convergence of the bidding method, which confirms the usability and effectiveness of the proposed models [4]. The problem of planning DERs has been investigated from aspects of various models including modeling techniques, solution methods, reliability, diffusion, uncertainty, stability, DR, and multi-objective perspectives in the framework of microprocessors and VPPs. This allows researchers with different perspectives to look for possible applications in microgrid planning and VPP [5]. Reference [6] outlines the unique operational requirements of DC distribution systems and highlights the challenges and opportunities they create for the market. The DC distribution systems have been introduced to the market, including tradable services, design objectives, market participants, design options, and performance metrics. A minimal cost estimation model was presented to determine the optimal DG picker portfolio. The proposed scheduling framework for the IEEE Reliability Testing System has been tested in relation to the IEEE 69-bus distribution network [7]. Literature [8] presents a new VPP model that presents all available full-scale distributed renewable technologies. The proposed VPP operates as a single plant in the wholesale electricity market to maximize profits from its performance to meet demand. In the electricity market, three common mediums to long-term electricity decomposition methods are built on average tracking times and point prices, where the latter is predicted by the ARIMA model, while the relationship between point prices and costs is also predicted. The margin of the VPP is obtained. The marginal cost can also be adjusted based on the ARIMA model. Based on the aforementioned factors concerning investment and complementary benefits, a VPP measurement model has been developed [9-10]. The proposed optimal decision model maximizes the use of clean energy to achieve higher economic benefits while reaching rational control of performance risks [11-12]. The proposed method is also easy to track for VPP operators because of less computation. Finally, power curves are obtained per hour, which the operator takes advantage of to increase or decrease the market price. Also, comparative results of deterministic and uncertainty cases are presented. The results show that the profit margin at the maximum strength is reduced by 25.91% and the VPP is resisting the uncertainty of the day's market price [13]. In Reference [14], the effect of combining distributed energy generation technologies on major electricity price changes in different EU energy markets is investigated using a maximum entropy econometric approach. Knowing how much each unit of electricity produced by each technology can change the price of electricity can be very useful for formulating optimal strategies in a decision on a portfolio of electricity technologies. In this study, the VPP model uses renewable energy sources such as wind power plants (WPP), solar power plants (SPP), biogas power plants (BPP), and pumped-hydro storage power plants (PHSP) as energy storage system (ESS). The purpose of VPP is to maximize daily net profit over 24 hours. The proposed mixed-integer linear programming (MILP) is modeled in GAMS software and solved using CPLEX [15]. This paper examines the VPP bidding strategy in

the energy services and regulatory market. The performance of distributed energy sources (DER) and battery energy storage within a VPP is analyzed. The VPP bidding strategy includes the spin reserve contract and the bid/bid contract of the day. A robust two-step optimization model is proposed to determine the VPP buying/selling power of each contract to maximize the profit of VPP [16]. With the rapid development of renewable energy, VPP technology has gradually become a key technology for solving large-scale renewable energy development. The optimization of gas-VPP's stochastic dispatching is discussed [17]. The effects of resource utilization techniques, for example, processing time (PT), response time (RT), computational cost, and energy consumed by resources have also been analyzed [18]. The authors in [19] examine two different sources of uncertainty: the stochastic, applied approach to market price uncertainty, and the information gap decision theory (IGDT), incorporated in the model of counting for uncertainty in wind power generation. Uncertainty is involved in the problem through random electricity prices as well as uncertain wind power generation. The bidding problem for a working day is set as a Markov Decision Process (MDP) that is solved using a kind of stochastic dual programming algorithm [20-21]. The Stack Berg two-stage game model is linearized and solved with the Column Generation and Constraint (CC&G) algorithm. In addition, the thermal unit operating in automatic generation control (AGC) mode guarantees optimal real-time scheduling of total actuators for the entire dispatch cycle [22]. Experimental results show that the proposed DRL-based algorithm can successfully learn the characteristics of DGs and industrial user demands. It can be learning to choose measures to minimize the cost of VPPs [23-24]. Reference [25] investigates the real-time multi-stage random power management strategy of a VPP using a three-tiered language protocol based on the computer programmer's compiler, which utilizes the possibility of storing the battery in a VPP.

The problem addressed [26] is the participation planning of price-based unit commitment (PBUC) that is resolved by the VPP over a fixed period (24 hours). Price and demand have uncertainty in this problem and normal logarithmic and normal probability functions have been used to model these uncertainties. The Monte Carlo method is used to investigate the impact of the possible variables mentioned on how the VPP strategy is implemented. The study network consists of 2 samples. In the first case, the presence of CHP units in the network is neglected. The objective function is to maximize the profit of VPPs for the market taking into account its constraints. In reference [27], a model for developing a strategy for proposing VPP production to the electricity wholesale market is presented, in which the desired optimization problem is a Price-based Unit Commitment (PBUC) participation planning problem, while Supply and demand balance constraints and VPP security constraints are also considered in the problem. It is worth mentioning that in the mentioned model, the market prices in the studied period are available as input Information without error in forecasting. In other words, VPP strategies are formulated in the absence of uncertainty in price and predicted demand. Also, in reference [28], it was mentioned how to set the price of the power plant taking into account the uncertainty of the price. To model the uncertainty, the probability density function has been used. In this

method, it is necessary to examine the pricing in such a way that the market is considered daily and the producers and consumers present their offer curves hourly, in blocks of energy and price.

1.2. Main contributions

The hypotheses made in the article are:

The target problem in this research is the participation planning of PBUC, which is solved by VPP in a certain period (24 hours).

I. Probability density functions are used to model uncertainty.
II. The Monte Carlo method is used for the effect of these uncertainties on the indicators of the problem.
III. Among the highlights of this research is the investigation of the effects of uncertainty on the strategy of the virtual power plant.

1.3. Structure of the paper

In the following, the structure of the article is described. In the second part, we examine the objective function and constraints of the problem (taking into account CHP units). In the third section, the network under study and assumptions together with simulation scenarios are introduced. In the fourth part, the review, simulation, and analysis of results for VPP 1 considering the energy market are discussed, and finally, in the fifth part, conclusions and suggestions are provided.

2. Objective function and constraints of the problem (taking into account CHP units)

One of the most important issues addressed in research today is the replacement of traditional generation units with other units. Alternative power plants, renewable energy sources, and CHP units are among the problems faced by dispersed power plants, which are defective in their control. The VPP needs to be adjustable at any time. One of the reasons for accepting the replacement of traditional units with VPPs is the production of electricity at a price close to the traditional ones. It is important to note that cogeneration units typically require more investment than conventional energy conversion systems. However, their energy consumption is much lower; in other words, the average cost of converting one unit of energy into CHP units is lower than other methods [28].

The objective function of the problem of economic distribution of cogeneration is given in Equation (1) [26]:

$$min\, f_{cost} = \sum_{i=1}^{N_p} C_i(P_i) + \sum_{j=1}^{N_C} C_j(O_j, H_j) + \sum_{k=1}^{N_h} C_k(T_k) \quad (1)$$

Equality constraints include Equations (2)-(3):

$$\sum_{i=1}^{N_p} P_i + \sum_{j=1}^{N_C} O_j = P_d \quad (2)$$

$$\sum_{j=1}^{N_C} H_j + \sum_{k=1}^{N_h} T_k = H_d \quad (3)$$

Inequality constraints are provided in Equations (4)-(10):

$$P_i^{min_{i_i}^{max_p}} \quad (4)$$

$$O_i^{min_{j_{i_i}}^{max_c}} \quad (5)$$

$$H_j^{min_{j_{j_j}}^{max_c}} \quad (6)$$

$$T_k^{min_k{}_k^{max_h}} \quad (7)$$

$$C_i(P_i) = a_i + b_i P_i + C_i P_i^2 \quad (8)$$

$$C_j(O_j, H_j) = a_j + b_j O_j + c_j O_j^2 + d_j H_j + e_j H_j^2 + f_j O_j H_j \quad (9)$$

$$C_k(T_k) = a_k + b_k T_k + c_k T_k^2 \quad (10)$$

here, the minimum fuel cost is f_{cost}, and production costs of traditional power plants, cogeneration, and thermal units are c_i, c_j, c_k, a_i, b_i, c_i. Also, a_j, b_j, c_j, d_j, e_j, f_j are the fuel cost coefficients of cogeneration unit j, a_k, b_k, c_k are the fuel cost coefficients of the thermal unit k. The output power of the traditional and cogeneration units is given by P_i and O_j. The heat generated in the cogeneration unit and heat in the thermal unit are shown as H_j and T_k. Heat demand and power demand are denoted by H_d and P_d. Also, N_p, N_c, and N_h indicate the number of traditional power units, cogeneration, and heat. P_i^{min} and P_i^{max} are the minimum and maximum power output of traditional units, O_j^{min} and O_j^{max} express the minimum and maximum power output of cogeneration units, H_j^{min} and H_j^{max} are the minimum and maximum heat production of cogeneration units, and minimum and maximum heat production of thermal units are denoted by T_k^{min} and T_k^{max}. Also, in this study, binary coding methods, sequential selection, and two-point combinations are used. The coded variables include U_t with string length 1, P_{dg}, $P_{capacity}$, and P_{curt} with string length 8. The initial population size is 200, the probability of a cut is 0.95, and the probability of a mutation is 0.05. The number of iterations for the Monte Carlo simulation is 100 iterations. The single-line diagram of the first virtual power plant is shown in Figure 1. To ensure the accuracy of the results of the algorithm implementation, the simulation results are compared with the results of [27].

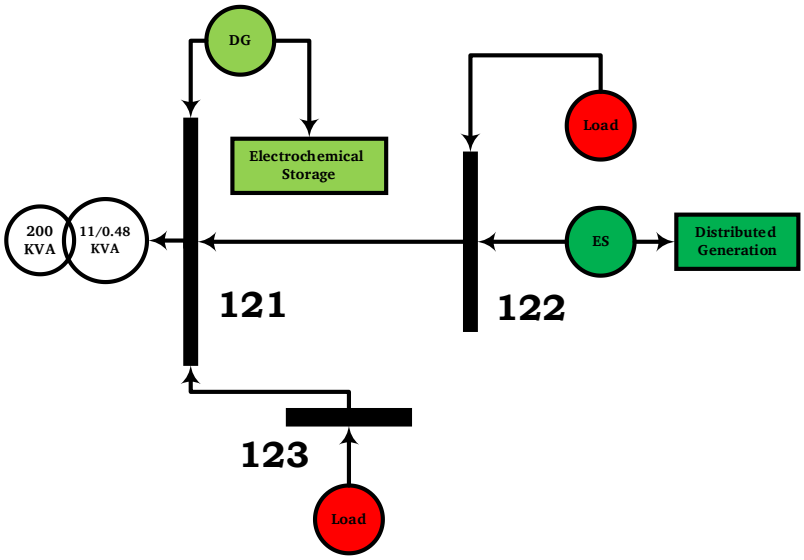

Figure 1. Single-line diagram of VPP 1.

2.1. Simulation and Analysis of Results for VPP 1 Considering Energy Market

Due to the disconnected loads in the system, it is possible to disconnect up to a maximum of 25 kW at 7-8 and 11-18 hours. Also, the cost of the load interruption to pay the consumer is obtained by the relationship $C(P) = 0.01P^2 + P$, where P is the power not supplied. The binary variable U_{DG} was used to indicate the switched on/off status of the DG. The DG production cost function is calculated according to $C(dg) = 0.01P_{dg}^2 + 8.5P_{dg}$. The maximum profit is 29227$. Table 1 provides the hourly input data including the amount of load, energy price, hourly retail, wholesale, and reservation amounts. Figure 2 provides the hourly deterministic baseline simulation considering the energy market. As mentioned earlier, the minimum battery life is 5 kWh.

Table 1. Hourly input data [27].

Hour	Load (kW)	Energy price ($/MWh)			Hour retail	Load (kW)	Energy price ($/MWh)		
		retail	Wholesale	Reservation			retail	Wholesale	Reservation
1	97	9	11.5	12.5	13	135	11	14.5	15
2	92	9	11.5	12.5	14	128	11	14.5	15
3	90	9	11.5	12.5	15	115	11	14.5	15
4	88	9	11.5	12.5	16	105	11	6.5	7
5	90	9	11.5	12.5	17	104	9	6.5	7
6	92	9	11.5	12.5	18	105	9	6.5	7
7	95	9	11.5	12.5	19	108	9	6.5	7
8	100	9	11.5	12.5	20	108	9	6.5	7
9	105	9	11.5	12.5	21	106	9	6.5	7
10	110	11	11.5	12.5	22	104	9	14	14.5
11	120	11	14.5	15	23	102	9	14	14.5
12	135	11	14.5	15	24	98	9	14	14.5

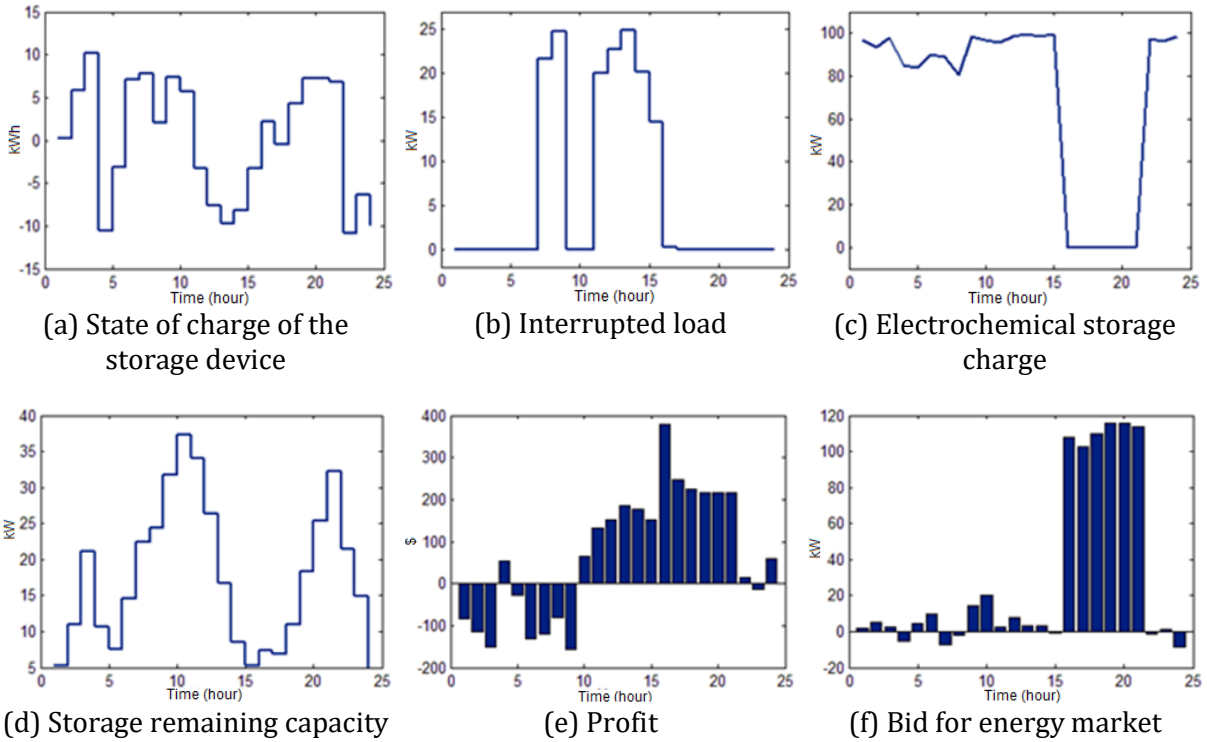

(a) State of charge of the storage device (b) Interrupted load (c) Electrochemical storage charge

(d) Storage remaining capacity (e) Profit (f) Bid for energy market

Figure 2. Hourly Deterministic Baseline simulation considering the energy market.

To study the effect of uncertainty on energy price forecasting and demand on the VPP strategy, various scenarios are defined as tabulated in Table 2. In these scenarios, the standard deviation rate has different values, indicating market price volatility [6].

In the first scenario, the results are similar to the base case and are only averaged over the results after 100 iterations. As a result, they do not differ significantly from the base case, so the results of this section are ignored. In the sixth scenario, by applying standard deviation S = 0., the product has high fluctuations (relative to standard deviation 0.02). As has been stated, production has changed to the standard deviation. Expected VPP profits in the energy market under price uncertainty are provided in Table 3, and bid for the energy market in different iterations is given in Figure 3.

Table 2. Scenarios.

Scenario number	Standard deviation	Price uncertainty	Demand Uncertainty
1	0.00	×	×
2	0.02	✓	×
3	0.05	✓	×
4	0.10	✓	×
5	0.15	✓	×
6	0.02	✓	✓
7	0.05	✓	✓
8	0.10	✓	✓
9	0.15	✓	✓

Table 3. Expected VPP profits in the energy market under price uncertainty.

Scenario number	1	2	3	4	5
Profit ($)	30012	28534	19856	5610.7	463.9693

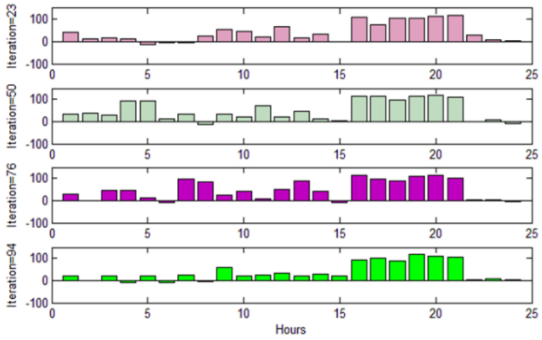

Figure 3. Bid for the energy market in different iterations (S = 0.05).

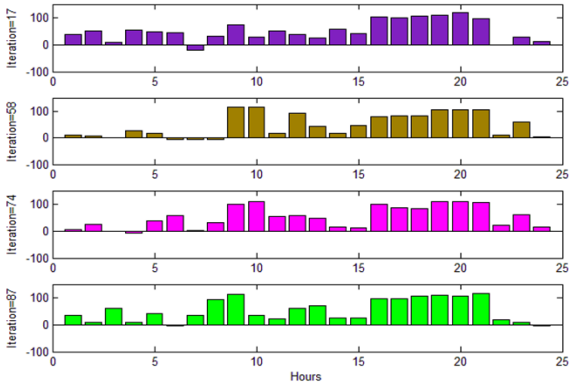

Figure 4. Bid for the energy market in different iterations (s = 0.10).

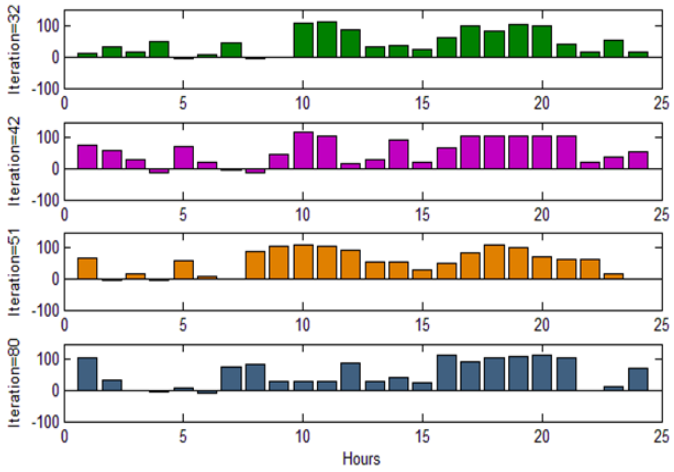

Figure 5. Bid for the energy market in different iterations (s = 0.15).

2.2. Sixth to Ninth Scenarios (In the Presence of Price and Demand Uncertainty)

In this case, in addition to the energy price, the load is also uncertain and the normal density function is used for modeling. It is seen from Figures 4-10 that despite the uncertainty of the load along with the uncertainty of the price, changing the production of DG, electrochemical storage device, bid and sell strategy, and profit of the plant is affected.

2.3. Simulation and Analysis of Results for VPP 1 in the Reserve Market

In this case, the problem is solved by considering the possibility of involving the VPP in the spinning reserve market. It is worth noting that DG and disconnected loads are spin reserve resources. The maximum capacity of the DG to supply the reservation is 30 kW as we can see in Figure 6(a).

Figure 6(b) shows the charge and discharge of the electrochemical device. During 1-8 hours, the amount of VPP load is low. Therefore, the device is charged. The device is then discharged at high load times. At hours 7-8 and 15-11, the retail price is lower than the energy price. So, in this case, the maximum profit will be generated by cutting off, as we can see in Figure 6(c).

In Figures 6(d)-(g), respectively, the amount of VPP bid for rotational energy and reserve and profit and the remaining storage capacity are shown. The VPP bid rate for and spinning reservation is zero when DG is not switched off. In Figure 6(d), the positive values represent the VPP purchase from the market and the negative values represent the VPP energy sold to the market. In this case, the maximum profit is 106 × 2.8651. Table 4 provides the VPP expected profit in the energy market under uncertainty of demand for scenarios 6-9. Table 5 presents the expected VPP profit in the reserve market under price uncertainty for scenarios 1-9.

Table 4. VPP expected profit in the energy market under uncertainty of demand.

Scenario number	6	7	8	9
Profit ($)	12625	6432.6	210.53	-12.8107

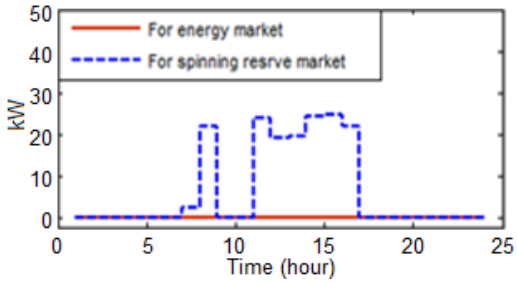

(a) DG production for the market /Interrupted load

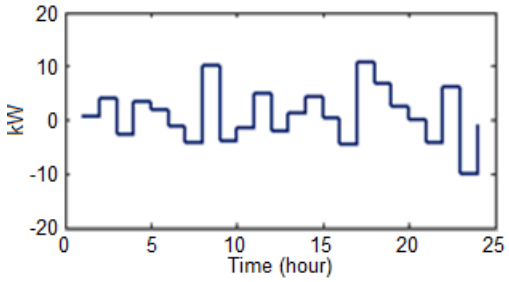

(b) Charging and discharging status of electrochemical storage

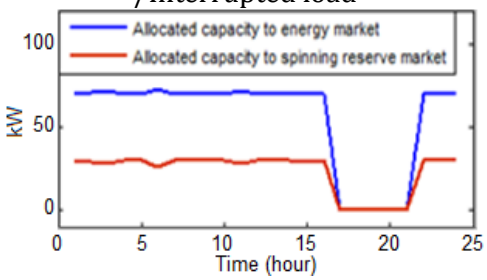

(c) Charged status at various times

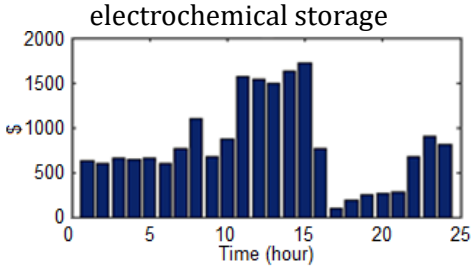

(d) Bidding for the energy market

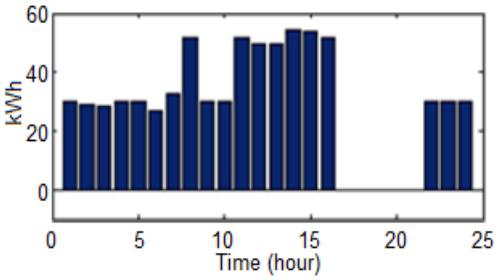

(e) Bidding for the reserve market

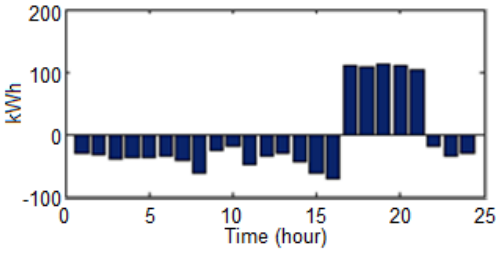

(f) Energy market benefit

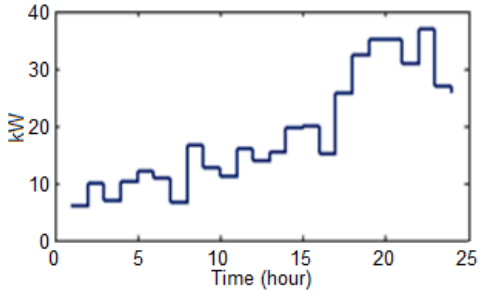

(g) Quantity of remaining storage capacity

Figure 6. Baseline simulation results with reservation market in mind**.**

Table 5. Expected VPP profit in the reserve market under price uncertainty.

Scenario number	1	2	3	4	5	6	7	8	9
Profit (1000$)	2993	1984.8	751.18	87.094	1.6253	1980.8	300.76	56.643	1.0093

2.4. Case Study II (VPP 2)

In this section, a new network is considered. This network is based on the previous network with the addition of 4 new units. These 4 units comprise one traditional power generation unit (P1), one heat generator unit (T1), and two CHP units (O1, H1, O2, H2) as shown in Figure 7.

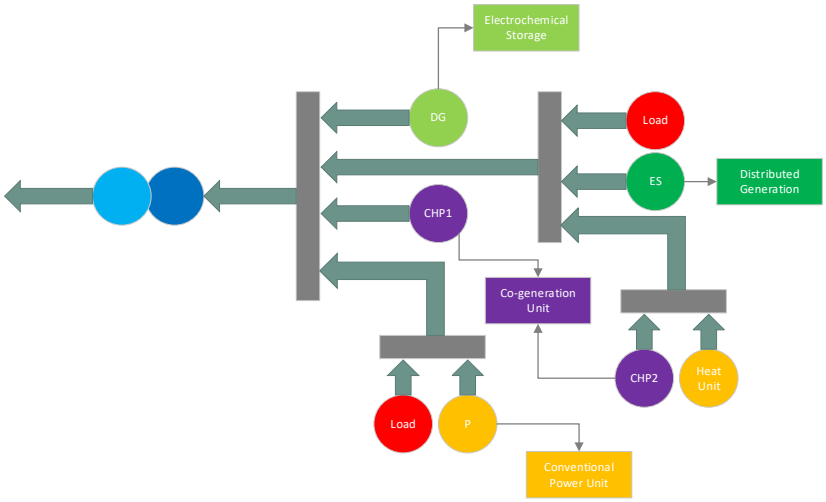

Figure 7. Virtual power plant single line diagram 2.

The objective function and constraints of the four units are given in Equations (11)-(23):

$$C_1(P_1) = 5 \times P_1 \quad (11)$$

$$C_1(O_1, H_1) = 650 + 4.5 \times O_1 + 0.0345 \times O_1^2 + 0.0042 \times H_1 + 0.0003 \times H_1^2 + 0.00031 \times O_1 \times H_1 \quad (12)$$

$$C_2(O_2, H_2) = 250 + 6 \times O_2 + 0.0435 \times O_2^2 + 0.0006 \times H_2 + 0.00027 \times H_2^2 + 0.00011 \times O_2 \times H_2 \quad (13)$$

$$C_1(T_1) = 3.4T_1 \quad (14)$$

$$f_{cost} = C_1(P_1) + C_1(O_1, H_1) + C_2(O_2, H_2) + C_1(T_1) \quad (15)$$

Constraints:

$$O_1 + O_2 + P_1 = 150 \quad (16)$$

$$H_1 + H_2 + T_1 = 15 \quad (17)$$

$$1.000000781914894 \times H_1 - O_1 - 105.7446809 \leq 0 \quad (18)$$

$$0.177777778 \times H_1 + O_1 - 247 \leq 0 \quad (19)$$

$$-0.169847328 \times H_1 - O_1 + 98.8 \leq 0 \quad (20)$$

$$1.158415842 \times H_2 - O_2 - 46.88118818 \leq 0 \quad (21)$$

$$0.151162791 \times H_2 + O_2 - 130.6976744 \leq 0 \quad (22)$$

$$0.067681895 \times H_2 - O_2 + 45.07614213 \leq 0 \quad (23)$$

Four binary variables are assigned to indicate the on and off status of the four units added to this section. Having a value of zero indicates that the unit is off. Simulation of this system has been done by genetic algorithm over 24 hours.

2.5. Simulation and Analysis of Results for VPP 2 Considering Energy Market

Figure 8(a) shows the production diagram of the dispersed generation unit during the period under study. As shown in this figure, the DG is switched on at hours 5-1, 11-11, and 24-22, because the maximum benefit is obtained by staying on the DG. Figure 8(b) shows the status of the load interruption at different times. As stated in the problem

assumptions, a definitive load is allowed between hours 7-8 and 18-11. However, since the DG is off at hours 16-18 and the retail price is high, there is no need for a definitive load. Figure 8(c) illustrates the amount of charge and discharge of the electrochemical storage device. Similar to the previous simulation, the positive values indicate the storage device charge and the power transfer to the grid (power injection to the grid) and the negative values denote the storage device discharge and power absorption from the grid.

Figure 8(g) shows the production rate (power and heat) for cogeneration unit 1. The power generating unit is switched off during the hours 4-8, 13-12, and 17-24, and power generation is done through other sources. Given the constraints in the problem, the second cogeneration unit and the first power-generating unit must produce a total of 150 kW. Referring to Figures 8(h) and (i), this is well evident. And, the total power of these three producers will be 150. It is also switched off during hours 6-8, 12-31 and 20-22. As explained above, the cogeneration unit and the first heat-generating unit compensate for this shortfall in aggregate and produce 15 kW of heat in total.

Units are switched on and off due to the use of a genetic algorithm, coding and applying binary variables (U1, U2, U3, U4), and applying the bit transfer method. The power plant biddings to the market are visible in Figure 8(d). It is observed that it always has negative values, which means selling energy to the market. The reason for this and the difference with the base grid is the application of the new power generation capacity to the equilibrium of energy production and consumption. Figures 8(d) and (e), respectively, show the results of the bid for the energy market and the amount of VPP profit during the study period. The maximum profit is 8.0864×10^3. With the increase in production units, there will be opportunities for more production and more profit for the plant.

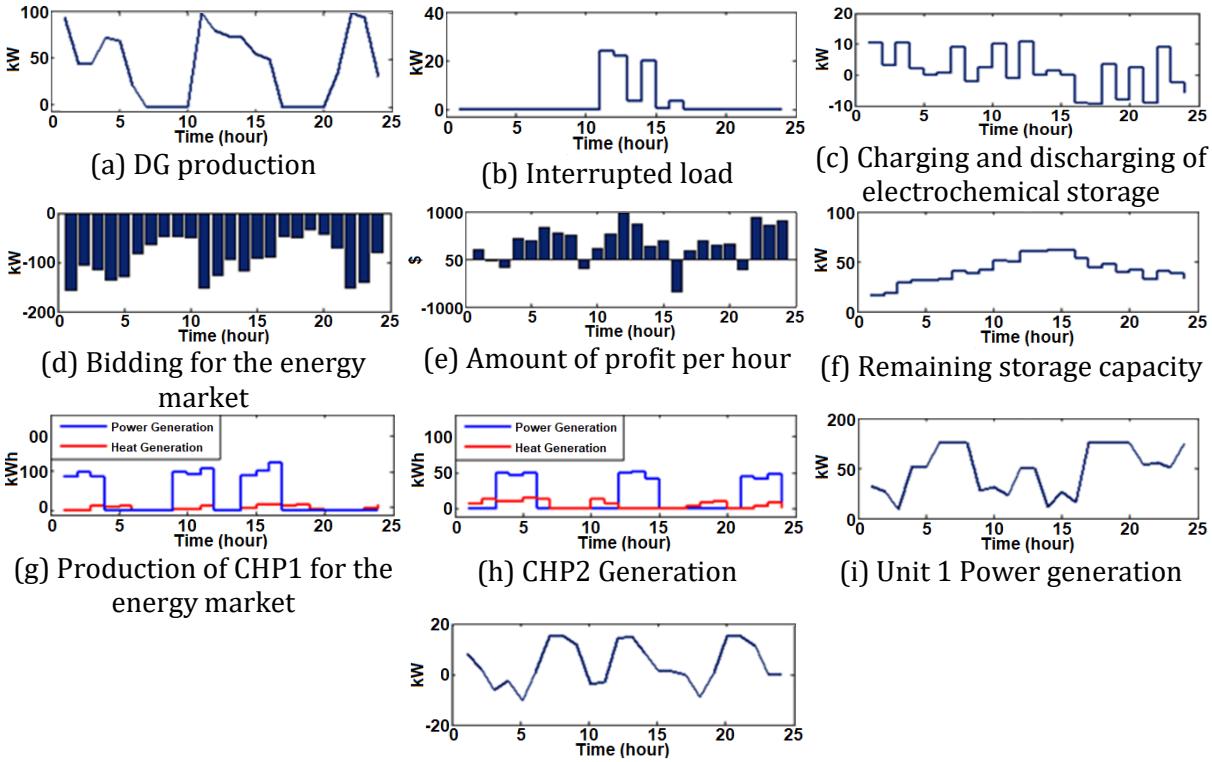

(a) DG production
(b) Interrupted load
(c) Charging and discharging of electrochemical storage
(d) Bidding for the energy market
(e) Amount of profit per hour
(f) Remaining storage capacity
(g) Production of CHP1 for the energy market
(h) CHP2 Generation
(i) Unit 1 Power generation
(j) Unit heat generation 2 for the energy market

Figure 8. Simulation results of the new grid considering the energy market.

Figure 8(f) shows the amount of remaining battery capacity per hour. As mentioned earlier, the minimum battery life is 5 kWh.

2.6. Second to fifth scenarios (in the presence of energy price uncertainty)

Similar to the first network simulation (VPP1), in this section, the results are simulated for uncertainty in the energy price, and the normal logarithmic function is used for modeling. Table 6 provides the expected VPP profit (including CHP units) in the energy market under price uncertainty for scenarios 1-5.

The results are compiled for different scenarios and are ignored because of their similarity to the first network. In Figures 9(g) and (h), the amount of output is reduced relative to the base case. This is in line with the description of the preceding sections.

2.7. Sixth-ninth scenarios (in the presence of uncertainty in price and demand)

In this section, the results are simulated for uncertainty in demand, and the normal function is used to model. Given the uncertainty of demand along with price uncertainty, the dispersion rate increases, and the results change (predominantly, decrease). Table 7 tabulates the expected VPP profit (including CHP units) in the energy market under price uncertainty for scenarios 6-9.

Table 6. Expected VPP profit (including CHP units) in the energy market under price uncertainty.

Scenario number	1	2	3	4	5
Profit ($)	7448.3	6957.7	947.48	613.69	987.834

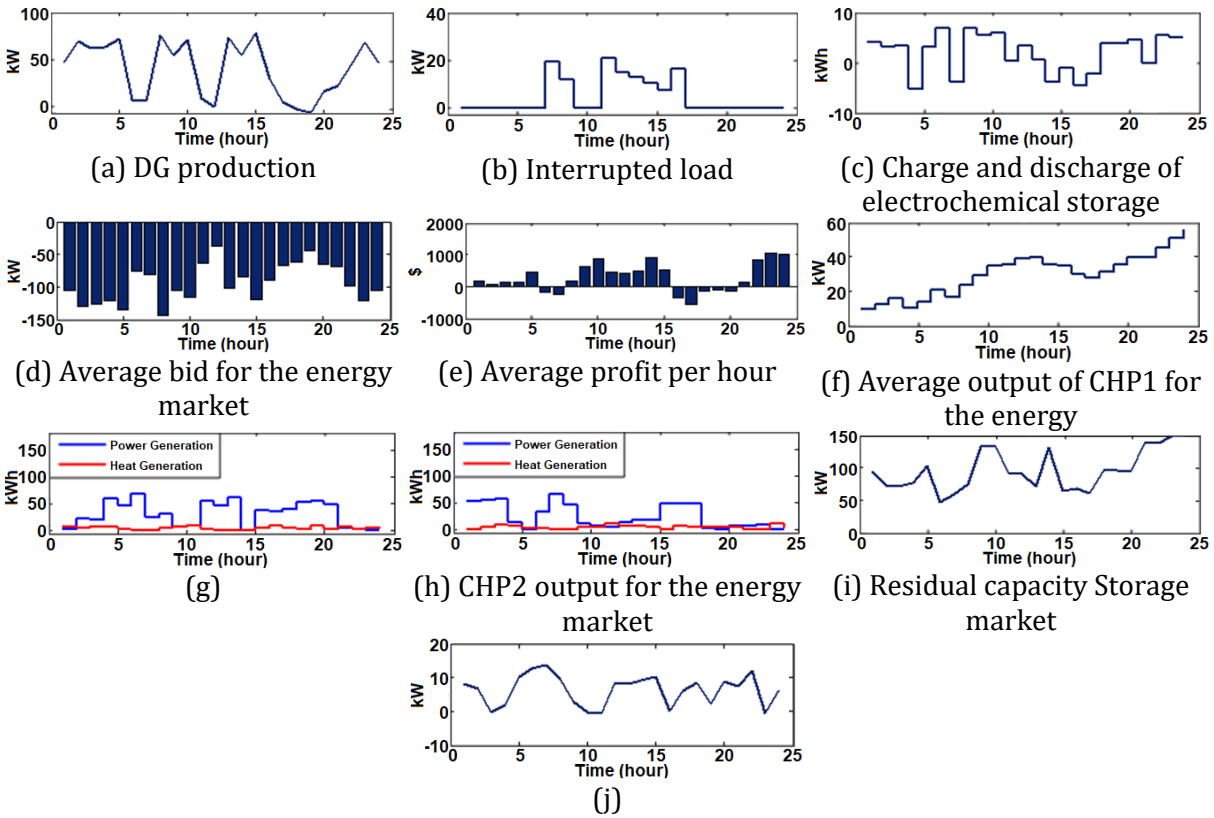

(a) DG production (b) Interrupted load (c) Charge and discharge of electrochemical storage

(d) Average bid for the energy market (e) Average profit per hour (f) Average output of CHP1 for the energy

(g) (h) CHP2 output for the energy market (i) Residual capacity Storage market

(j)

Figure 9. Simulation results of the new grid (in the presence of price uncertainty and S = 0.02) considering the energy market.

2.8. Second to fifth scenarios (in the presence of energy price uncertainty)

This section provides the results for scenarios 1 to 5, where the focus is on the Virtual Power Plant (VPP) profit in the reserve market under energy price uncertainty. Table 8 highlights the expected VPP profit (with CHP units) for each scenario, showing a range from $419.77 in scenario 5 to $24,565 in scenario 1.

2.9. Sixth-ninth scenarios (in the presence of uncertainty in price and demand)

In this section, the results are simulated for uncertainty in demand, and the normal function is used to model. Given the uncertainty of demand along with price uncertainty, the dispersion rate increases, and the results change (predominantly, decrease) as shown in Table 9. Simulation results of the new network (in the presence of price and demand uncertainty and S = 0.02) with respect to the reserve market are provided in Figure 10.

Table 7. VPP expected profit (including CHP units) in the energy market under uncertainty of demand.

Scenario number	6	7	8	9
Profit ($)	6577.8	712.02	489.76	643.780

Table 8. Expected VPP profit (with CHP units) in the reserve market under price uncertainty.

Scenario number	1	2	3	4	5
Profit ($)	24565	17680	8367.5	2230.3	419.77

Table 9. VPP expected profit (including CHP units) in the energy market under uncertainty of demand.

Scenario number	6	7	8	9
Profit ($)	6577.8	712.02	489.76	643.780

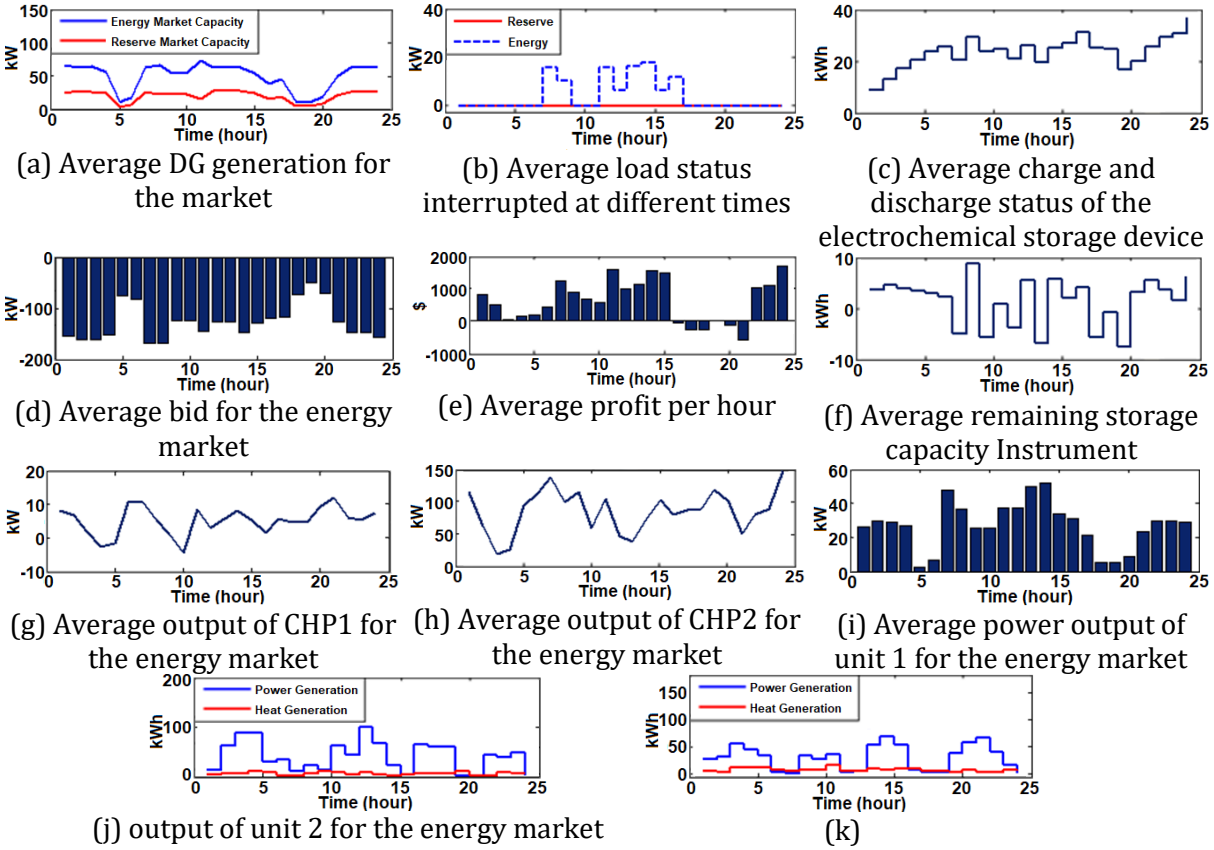

(a) Average DG generation for the market
(b) Average load status interrupted at different times
(c) Average charge and discharge status of the electrochemical storage device
(d) Average bid for the energy market
(e) Average profit per hour
(f) Average remaining storage capacity Instrument
(g) Average output of CHP1 for the energy market
(h) Average output of CHP2 for the energy market
(i) Average power output of unit 1 for the energy market
(j) output of unit 2 for the energy market
(k)

Figure 10. Simulation results of the new network with respect to the reserve market.

3. Simulation results of standard deviation to mean Monte Carlo stop

Standard deviation to average ratio (in the presence of price uncertainty and s = 0.02) given the reserve market is illustrated in Figure 11.

Figure 11(a) provides the standard deviation to average profit ratio at hour 17 taking into account price uncertainty per standard deviation 0.02, while Figure 11(b) depicts the standard deviation to average energy purchase and sale by applying price uncertainty per standard deviation 0.02, 24-hour time.

4. Conclusions

In this research, the introduction of two networks and the simulation and analysis of the results related to each of them were discussed. The reason for choosing CHP units as distributed generation units in this research is the energy production of these units with a cost close to the cost of traditional power plants.

Also, the uncertainty of price and demand was applied to affect different parameters of the problem along with different scenarios. To model these uncertainties, logarithmic and normal functions were used. Also, in this research, the binary coding method, sequential selection, and two-point combination were used. The coded variables include Ut with a string length of 1, Pdg, Pcapacity, and Pcurt with a string length of 8.

The size of the initial population is 200, the cut-off probability is 0.95 and the mutation probability is 0.05. The number of iterations in the Monte Carlo simulation is 100. From the results of the simulation, it can be pointed out the effect of different amounts of standard deviation on the production units in such a way that with increased standard deviation, the dispersion has increased and the nature of those products has undergone decreasing changes.

It can also be stated that the profit of the power plant increases due to different reasons such as the connection of the virtual power plant into the reservation market because of the high reservation price compared to other energy market rates and the addition of CHP units due to the increase in production opportunities. Also, the profit increase is 8.0864 x 103 compared to the base scenario.

Due to the addition of production units, the opportunity for production will increase and the power plant will earn more profit. From the study of different scenarios, it can be concluded that the use of the Monte Carlo method is a suitable tool to stop the simulation process because by increasing the number of iterations in this method, convergence is achieved and ideal results appear.

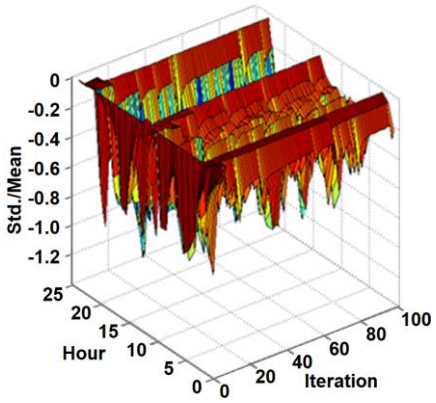

(a) Standard deviation to average profit ratio at hour 17 taking into account price uncertainty per standard deviation 0.02

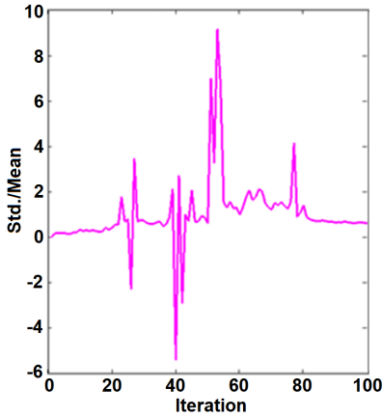

(b) Standard deviation to average energy purchase and sale by applying price uncertainty per standard deviation 0.02, 24-hour time

Figure 11. Standard deviation to average ratio (in the presence of price uncertainty and s = 0.02) given the reserve market.

Nomenclature

i, j	Bus indices
t	Time index
S_b	Setting of VPP branches
S_{dg}	Setting of DGs
$S_{hour,i}$	Settings of the allowed clock (time) that may be interrupted if load interruption is necessary.
S_{int}	Setting of interrupted loads
S_{str}	Setting of electrochemical storage
S_n	Setting of the VPP curve (node)
E_t	VPP's bid for the energy market (positive and negative values indicate the amount of buying from the energy market and selling to the energy market, respectively)
$I_{i,t}$	Binary values showing the state of participation of a DG
$J_{i.t}$	Binary values indicating the DG startup
$K_{i,t}$	Binary values indicating the DG shutdown
$Load_{E,t}$	VPP-supplied load if the bid for spinning reserve and market for generation is not called.
$Load_{ER,t}$	VPP-supplied load if the bid for spinning reserve and market for generation is called.
$Loos_{E,t}$	VPP's power loss if the spinning reserve for generation is not called.
$Loss_{ER,t}$	VPP's power loss if the spinning reserve for generation is called.
$P_{curt,i,t}$	Load not-supplied for trading in the electricity market
$P_{\mathrm{dg,i,t}}$	DG generation for the electricity market
$P_{g,i,t}$	Total real power generation at the node (pathway)
$P_{i,t}$	Real power injection to node i
$P_{str,i,t}$	The charge/discharge amount of the electrochemical storage in kWh (negative and positive values indicate the discharge and charge states, respectively)
$Q_{\mathrm{g,i,t}}$	Reactive power generated at node i
$Q_{i,t}$	Total reactive power injected to node i
$R_{curt,i,t}$	Load not-supplied to provide spinning reserve service
$R_{dg,i,t}$	DG generation for market spinning reserve
R_t	VPP bid for market spinning reserve
S_{ij}	Apparent power flow from node i to node j
$V_t(V_{1,t}, V_{2,t}, \ldots, V_{N_n,t})$	Voltage amplitude vector
$V_{i,t}$	Voltage magnitude at node i

$\theta_t(\theta_{1,t}, \theta_{2,t}, \dots, \theta_{N_n,t})$	Voltage angle vector
$\theta_{i,t}$	Voltage angle at node i
AR_k	Establishment of a proper reserve by VPP
E_{exch}^{max}	Refers to the heating rate of transformer capacity connection or contractual capacity for power exchange between VPP and the upstream network
$LOAD_t$	The total expected load of VPP.
MSR_i	Ability to increase DG reservation kW/min
MUT_i, MDT_i	Limitation on the minimum time of operation and DG shutdown per hour
N_n	Number of VPP nodes.
$P_{curt,i}^{max}$	Upper limit for breaking on interruptible load
$P_{d,i,t}$	Real power demand at node i
$P_{dg,i}^{min}, P_{dg,i}^{max}$	Upper and lower limits on DG generation
$P_{str,i}^{max}$	The installed capacity of the electrochemical storage in kWh
$Q_{d,i,t}$	Reactive power demand at node i.
$R_{dgu,i}, R_{dgd,i}$	Limits of increasing and decreasing DG in kWh
$R_{str-ch,i}, R_{str-dch,i}$	Maximum rate of charge and discharge of electrochemical storage in kW
S_{ij}^{max}	Capacity of the line between node i and node j
$T_{i,t}^{on}, T_{i,t}^{off}$	The number of hours DG units were on/off in t hours
V_i^{max}, V_i^{min}	Maximum and minimum voltage magnitude at node i
$\rho_{E,t}$	Price at energy market
$\rho_{R,t}$	Price at spinning reserve market
$\rho_{L,t}$	Retail energy rate of the VPP
$C_{dg,i,t}(P_{dg,i,t})$	The cost function of DG generation
$C_{int,i,t}(P_{curt,i,t})$	The consumer's fixed cost curve for interrupting its load
$C_{str}(P_{srt,i,t})$	Operating cost of electrochemical storage
$SC_{dg,i,t}, SHC_{dg,i,t}$	DG startup and shutdown costs

References

[1] C. M. S. Kumar, S. Singh, et al., "Solar Energy: a Promising Renewable Source for Meeting Energy Demand in Indian Agriculture Applications, "*Sustainable Energy Technologies and Assessments*, vol. *55*, pp. 102905, 2023.

[2] P. A. Østergaard, N. Duic, Y. Noorollahi, and S. Kalogirou, "Renewable Energy for Sustainable Development, "*Renewable Energy*, vol. 199, pp. 1145-1152, 2022.

[3] M. K. G. Deshmukh, M. Sameeroddin, D. Abdul, and M. A. Sattar, "Renewable Energy in the 21st Century: a Review, "*Materials Today: Proceedings*, vol. 80, pp.1756-1759, 2023.

[4] G. Zhang, C. Jiang, X. Wang, B. Li, and H. Zhu, "Bidding Strategy Analysis of Virtual Power Plant Considering Demand Response and Uncertainty of Renewable Energy," *IET Generation, Transmission & Distribution,* vol. 11, no. 13, pp. 3268-3277, 2017.

[5] S. M. Nosratabadi, R. Hooshmand, and E. Gholipour, "A Comprehensive Review on Microgrid and Virtual Power Plant Concepts Employed for Distributed Energy Resources Scheduling in Power Systems," *Renewable and Sustainable Energy Reviews,* vol. 67, pp. 341-363, 2017.

[6] L. Piao, M. De Weerd, and L. De Vries, "Electricity Market Design Requirements for DC Distribution Systems," *IEEE Second International Conference on DC Microgrids (ICDCM)*, pp. 95-101, 2017.

[7] D. Yang, S. He, Q. Chen, D. Li, and H. Pandzic, "Bidding Strategy of a Virtual Power Plant Considering Carbon-Electricity Trading," *CSEE Journal of Power and Energy Systems,* vol. 5, no. 3, pp. 306-314, 2019.

[8] N. Naval, R. Sánchez, and J. M. Yusta, "A Virtual Power Plant Optimal Dispatch Model with Large and Small-Scale Distributed Renewable Generation," *Renewable Energy*, vol. 151, pp. 57-69, 2020.

[9] J. Liu, J. Li, Y. Xiang, X. Zhang, and W. Jiang, "Optimal Sizing of Cascade Hydropower and Distributed Photovoltaic Included Virtual Power Plant Considering Investments and Complementary Benefits in Electricity Markets," *Energies*, vol. 12, no. 5, pp. 952, 2019.

[10] C. Ninagawa, "Virtual Power Plant System Integration Technology", *Springer*, 2022.
[11] S. K. Effatpanah, M. H. Ahmadi, et al., "Comparative Analysis of Five Widely-Used Multi-Criteria Decision-Making Methods to Evaluate Clean Energy Technologies: A Case Study, "*Sustainability*, vol. 14, no. 3, 1403, 2022.
[12] M. H. Abbasi, M. Taki, A. Rajabi, L. Li, and J. Zhang, "Coordinated Operation of Electric Vehicle Charging and Wind Power Generation as a Virtual Power Plant: A Multi-Stage Risk Constrained Approach." *Applied Energy,* vol. 239, pp. 1294-1307, 2019.
[13] M. M. Gharavanlou, S. Nojavan, and K. Zareh, "Energy Management of Virtual Power Plant to Participate in the Electricity Market using Robust Optimization," *Journal of Operation and Automation in Power Engineering*, vol. 8, no. 1, pp. 43-56, 2020.
[14] B, Moreno, and G. Díaz. "The Impact of Virtual Power Plant Technology Composition on Wholesale Electricity Prices: A Comparative Study of Some European Union Electricity Markets," *Renewable and Sustainable Energy Reviews*, vol. 99, pp. 100-108, 2019.
[15] Ö. P. Akkaş, and E. Çam, "Optimal Operation of Virtual Power Plant in a Day Ahead Market," *3rd International Symposium on Multidisciplinary Studies and Innovative Technologies (ISMSIT)*, pp. 1-4, 2019.
[16] H. N. Duc, and N. N. Hong, "A Study on the Bidding Strategy of the Virtual Power Plant in Energy and Reserve Market," *Energy Reports*, vol. 6, pp. 622-626, 2020.
[17] Z. Tan, W. Fan, et al., "Dispatching Optimization Model of Gas-Electricity Virtual Power Plant Considering Uncertainty Based on Robust Stochastic Optimization Theory," *Journal of Cleaner Production,* vol. 247, 119106, 2020.
[18] A. Aldegheishem, R. Bukhsh, N. Alrajeh, and N. Javaid, "Faavpp: Fog as a Virtual Power Plant Service for Community Energy Management," *Future Generation Computer Systems,* vol. 105, pp. 675-683, 2020.
[19] A. Alahyari, M. Ehsan, and M. Moghimi, "Managing Distributed Energy Resources (DERs) Through Virtual Power Plant Technology (VPP): A Stochastic Information-Gap Decision Theory (IGDT) Approach." *Iranian Journal of Science and Technology, Transactions of Electrical Engineering*, vol. 44, pp. 279-291, 2020.
[20] M. Natarajan, and A. Kolobov, "Planning with Markov Decision Processes: an AI Perspective, " *Springer Nature*, 2022.
[21] D. Wozabal, and G. Rameseder. "Optimal Bidding of a Virtual Power Plant on the Spanish Day-Ahead and Intraday Market for Electricity," *European Journal of Operational Research,* vol. 280, no. 2, pp. 639-655, 2020.
[22] S. Yin, Q. Ai, Z. Li, Y. Zhang, and T. Lu, "Energy Management for Aggregate Prosumers in a Virtual Power Plant: A Robust Stackelberg Game Approach," *International Journal of Electrical Power & Energy Systems,* vol. 117, 105605, 2020.
[23] K. Borisoot, R. Liemthong, C. Srithapon, and R. Chatthaworn, "Optimal Energy Management for Virtual Power Plant Considering Operation and Degradation Costs of Energy Storage System and Generators, "*Energies*, vol. 16, no. 6, 2862, 2023.
[24] L. Lin, X. Guan, et al., "Deep Reinforcement Learning for Economic Dispatch of Virtual Power Plant in Internet of Energy," *IEEE Internet of Things Journal*, vol. 7, no. 7, pp. 6288-6301, 2020.
[25] C. Xiao, D. Sutanto, K. M. Muttaqi, and M. Zhang, "Multi-Period Data Driven Control Strategy for Real-Time Management of Energy Storages in Virtual Power Plants Integrated with Power Grid," *International Journal of Electrical Power & Energy Systems,* vol. 118, 105747, 2020.
[26] M. Shahidehpour, H. Yamin, and Z. Li, "Market Operations in Electric Power Systems: Forecasting, Scheduling, and Risk Management*, John Wiley & Sons*, 2002.
[27] E. Mashhour, and S. M. Moghadas-Tafreshi, "Bidding Sterategy of Virual Power Plant for Participating in Energy and Spinning Reserve Market—Part II: Numerical Analysis, "*IEEE Transactions on Power Systems*, vol. 26, no. 2, pp. 957-964, 2010.
[28] V. Vahidianasab, and S. Jadid, "Stochastic Multi objective Self-Scheduling of a Power Producer in Joint Energy and Reserves Markets, "*Electric Power Systems Research*, vol. 80, no. 7, pp. 760-769, 2010.

Declaration of Competing Interest

The authors declare that they have no known competing financial interests or personal relationships that could have appeared to influence the work reported in this paper. The ethical issues, including plagiarism, informed consent, misconduct, data fabrication and/or falsification, double publication and/or submission, redundancy, have been completely observed by the authors.

Credit Authorship Contribution Statement

Hamid Reza Hanif: Conceptualization, Data curation, Methodology, Software, Roles/Writing - original draft. **Mohammad Zand:** Conceptualization, Formal analysis, Methodology, Project administration, Roles/Writing - original draft. **Morteza Azimi Nasab:** Conceptualization, Formal analysis, Methodology, Software. **Seyyed Mohammad Sadegh Ghiasi:** Resources, Validation, Roles/Writing - original draft. **Sanjeevikumar Padmanaban:** Conceptualization, Methodology, Supervision.

Bibliography

Hamid Reza Hanif received his B.Sc. and M.Sc. and PHD degrees in Electrical Power Engineering from Iran University of Science and Technology, Iran Tehran in 2014 and 2019 and 2023 respectively. He has authored and co-authored more than 15 papers in international journals and conferences. He has also published a book and co-authored some book chapters. His main research interests include renewable energy, technologies, Microgrids, Power System Planning, Power Systems, Smart grids, Electric vehicles, and fault location.

Mohammad Zand received his B.Sc. and M.Sc. and Ph.D. degrees in Electrical Power Engineering from Islamic Azad University, Tehran Branch, Tehran, Iran, in 2013 and 2016 and 2022 respectively. He has authored and co-authored more than 75 scientific papers in international journals and conferences. His main research interests include renewable energy technologies, Microgrids, Power System Planning Power System, smart grids, electric vehicles, and fault location. Since June 2018, he has been a reviewer and Editorial Board Member of several high-quality journals.

Morteza Azimi Nasab (Member, IEEE) received the B.Sc. and M.Sc. degrees in electrical power engineering from Islamic Azad University, Tehran Branch, Tehran, Iran, in 2014 and 2017, respectively. He is currently a University Lecturer with the University of Applied Sciences and Technology, Tehran, and an External Researcher with the Department of Electrical Engineering, Information Technology and Cybernetic, University of South-Eastern Norway, Norway. He has authored or co-authored more than 25 scientific papers in international journals and conferences. He has also published a book and co-authored ten book chapters. His main research interests include renewable energy technologies, partial shaded PV, MPPT algorithms, smart cities, smart grids, electric vehicles, and fault location. Since June 2020, he has been a reviewer of several high-quality journals.

Seyyed Mohammad Sadegh Ghiasi was born in Iran, in 1984. He received the B.Sc. degree in electrical engineering from Tehran Polytechnic, in 2007, the M.Sc. degree from the Electrical Engineering Department, Iran University of Science and Technology, in 2010, and the Ph.D. degree in power system from Tehran Polytechnic, in 2019. His main researches interests include restructuring and deregulation in power systems, power quality, and transients in power systems.

Sanjeevikumar Padmanaban (Senior Member, IEEE) received the Ph.D. degree in electrical engineering from the University of Bologna, Bologna, Italy, in 2012. He is a Full Professor in Electrical Power Engineering with the Department of Electrical Engineering, Information Technology, and Cybernetics, University of South-Eastern Norway, Norway. He has authored over 750+ scientific papers. He is a Fellow of the Institution of Engineers, India, the Institution of Electronics and Telecommunication Engineers, India, and the Institution of Engineering and Technology, U.K. He received a lifetime achievement award from Marquis Who's Who - USA 2017 for contributing to power electronics and renewable energy research. He is listed among the world's top 2 scientists (from 2019) by Stanford University USA. He received the Best Paper cum Most Excellence Research Paper Award from IET-SEISCON'13, IET-CEAT'16, IEEE-EECSI'19, IEEE-CENCON'19, and five best paper awards from ETAEERE'16 sponsored Lecture Notes in Electrical Engineering, Springer book. He is an Editor/Associate Editor/Editorial Board for refereed journals, in particular the IEEE Systems Journal, IEEE Transaction on Industry Applications, IEEE Access, 83750 VOLUME 11, 2023A. Sagar et al.: Comprehensive Review of the Recent Development of WPT Technologies IET Power Electronics, IET Electronics Letters, and Wiley-International Transactions on Electrical Energy Systems, Subject Editorial Board Member–Energy Sources–Energies Journal, MDPI, and the Subject Editor for the IET Renewable Power Generation, IET Generation, Transmission and Distribution, and FACETS Journal (Canada). Dr. Padmanaban is a fellow of the Institution of Engineers, India, the Institution of Electronics and Telecommunication Engineers, India, and the Institution of Engineering and Technology, U.K. He received the Best Paper cum Most Excellence Research Paper Award from IET-SEISCON 2013, IETCEAT 2016, IEEE-EECSI 2019, and IEEE-CENCON 2019, and five best paper awards from ETAEERE 2016 sponsored Lecture Notes in Electrical Engineering, Springer book. He received the Lifetime Achievement Award from Marquis Who's Who-USA 2017 for contributing to power electronics and renewable energy research. He is listed among the world's top 2% scientists (since 2019) by Stanford University, USA.

Journal of Green Energy Research and Innovation

A Survey of Different Methods for Miner Detection and Challenges of Them in Power Industries

Mohammad Hossein Shakoor

Highlight

- **Some aspects of Mining, blockchain, Hash, Cryptocurrency, Encryption and Decryption**
- **A comprehensive study on different methods of miner detection**
- **Some suggestions to enhance the power electricity consumption**

Graphical Abstract

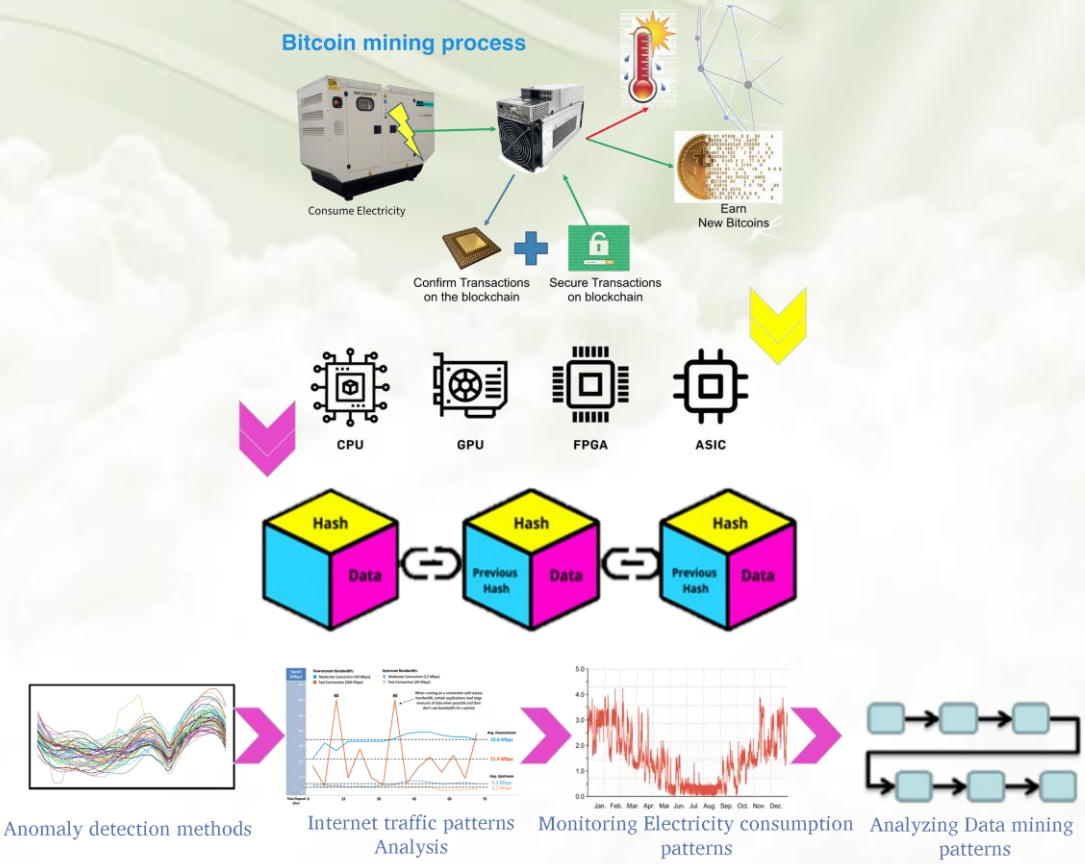

Use your device to scan and read the article online

Citation

M. H. Shakoor, " A Survey of Different Methods for Miner Detection and Challenges of Them in Power Industries," *Journal of Green Energy Research and Innovation*, vol. 1, no. 3, pp. 96-109, 2024.

https://doi.org/10.61186/jgeri.1.3.96

Online ISSN: 3041-9018

Journal of Green Energy Research and Innovation

Journal Homepage: www.jgeri.araku.ac.ir

A Survey of Different Methods for Miner Detection and Challenges of Them in Power Industries

Mohammad Hossein Shakoor *

Department of Computer Engineering, Faculty of Engineering, Arak University, Arak, 38156-8-8349, Iran.

* ***Corresponding Author:*** *mh-shakoor@araku.ac.ir*

ARTICLE INFO

Keywords:
Power consumption,
Cryptocurrency mining,
Miner detection.

Article history:
Received: 20 January 2024;
Revised: 20 February 2024;
Accepted: 2 March 2024;

Article type:
Review Article

ABSTRACT

Cryptocurrency mining requires high consumption power. In recent years, because of the increase in the price of cryptocurrencies and due to the cheap price of electricity in Iran, mining Bitcoin and other cryptocurrencies has been very profitable. Some miners are legally engaged in cryptocurrency mining, but many miners do it illegally and without permission. Since cryptocurrency mining is an operation that consumes a lot of electricity, it is one of the reasons for the lack of electricity, especially in the summer season, and it has caused power outages and financial losses to various industries. In this paper, different methods of detection of illegal mining are reviewed. In this research, by collecting the small number of researches done in the world, a comprehensive study of this issue has been tried. The methods of identifying miners and related consumers are divided into several different categories. Some of them are based-on data mining and mostly to identify consumers who use the output of the converter for the miner device. The second category is related to people who illegally get their electricity from behind the meter or unmetered branches, which are much more difficult to identify than the first type. These methods will be mentioned more in this article. Finally, some suggestions are provided for better identification of these consumers. Furthermore, at the end of the paper, some renewable and new sources of electrical power are discussed for using as an electricity power for miners instead of traditional fossil fuel and gas planes.

1. Introduction

More than a decade has passed since the introduce of digital currencies or cryptocurrencies. Although this innovation has important advantages and capabilities, some of them have also led to some challenges, the most important of which is the increase in electricity consumption, especially in low-price countries, where compared to the rest of the world, the price of electricity for consumers is very low. Because of this reason, cryptocurrency mining is very cost-effective. It requires a lot of power energy and it increases electricity consumption in our country significantly. Therefore, it seems necessary to conduct research in order to detect illegal miners. The first article related to

Bitcoin was published in 2008 by the pseudonym Satoshi Nakamura [1]. In the past decade, although cryptocurrency mining machines have made many improvements in terms of power consumption, they still belong to the high-consumption systems. Cryptocurrency mining imposes a lot of consumption on the power network [2]. According to reports in 2013, every day one billion watt per hours of electricity is spent for Bitcoin mining [3]. That is about the electricity consumption of 30,000 American households. This year, the mining speed was around 60 tera hash per second. With the advancement of technology, not only the hash speed is increased, but also the power consumption of miners decreased drastically. However, by increasing the number of miners, the problem of high-power consumption still remains.

According to research, about 0.55% of the world's electricity is consumed in the digital currency industry [4]. According to statistics, about 5% of the total Bitcoin mining was done in Iran in April 2021. Which more percentage of it is illegal. Miner detection is done for two reasons. The first reason is to identify delinquent consumers in electricity consumption, and the other reason is to identify the location of hidden miners that are robbed. This article is more about the first goal. But the stated methods can also be used for the second purpose. Identification of illegal consumers of cryptocurrency mining is a type of anomaly detection in electricity consumption [5]. The conventional method of identifying consumption anomalies is to compare the consumption of each user with his consumption at similar times in the past [6]. Of course, this method cannot be used for consumers who use unauthorized branches. Some articles [7] have presented methods based on game theory, in which by placing a series of hardware in the distribution network, it is possible to monitor and examine the amount of consumption in different parts and identify significant changes in consumption.

Since this method requires special hardware, it cannot be used everywhere. Rahimi et al. [8] presented a method based on statistics and with artificial intelligence tools, which is based-on a smart network. In this method, sudden changes in consumption are detected first, then users are divided by clustering and high consumption consumers are identified. Some researchers identify mining farms by using the analysis of electricity current characteristics such as current harmonics or identifying specific noises created by cryptocurrency mining power supply devices [6]. This method is also not very effective because there are various devices whose current harmonics or their produced noises are similar to miners and actually make it very difficult to detect a miner. Some methods use clustering to predict the amount of consumption in the next hour and identify any excessive consumption [9]. It is presented in a method based on time series analysis [10], in which the amount of monitor consumption and abnormal consumption is detected using Internet of Things tools. It is presented in a method for detecting abnormality of consumption, which has divided the data into three categories of consumption on working days, holidays and abnormal consumption. After detection of unusual uses, they are again divided into three categories, one of which is miners [11].

Data analysis through different protocols such as NetFlow and IPFIX and data mining and statistical analysis is another way to identify miners [12,13]. An example of these

supervised learning processes in machine learning is the method presented by some papers [14]. In this method, the important discriminative features are extracted from the data flow and the data flow classification operation is performed. In some articles [15], they identify the communication flows between miners and mining pools by analyzing the packets of the Internet network and according to the IP address and MAC address. In this work, packets that have a series of special features and use protocols of miners are detected as suspicious data for extraction. Then, by using the active method and communication with the sender of these packets, it is possible to find out their connection with the miners. Some researches have comprehensively analyzed Bitcoin mining theoretically [3]. Some papers [16,17] have investigated various economic aspects of cryptocurrency mining and analyzed it based-on game analyzing. A lot of research has been done in connection with activities and unauthorized users of cryptocurrencies [18]. Some of these unauthorized activities are private-key theft, spam and malwares. Huang et al. [19] have presented a comprehensive study of cryptocurrency mining malware. Some researchers developed methods that associate the mining bot with its mining pool. In addition, some methods have been able to estimate the number of infected devices produced, identify the income and the duration of infection with mining malware [20].

In this paper, firstly, some important concepts of cryptocurrencies and their extraction are explained. Then the common illegal methods of extracting cryptocurrencies are reviewed. The methods of bypassing the identification of miners are also described briefly, and in the main part, various methods for the detection of miners will be discussed. At the end of the paper, some renewable energy sources are illustrated that are explored for electricity production as a sustainable and eco-friendly alternative to traditional fossil fuels [21].

2. Related Concepts

In this section, some contents related to cryptocurrencies and their mining are explained.

2.1. Encryption and Hash

The main basis of cryptocurrencies is digital encryption. In general, cryptography is divided into several different categories. Key-based encryption includes symmetric and asymmetric encryption [22]. The difference between these two methods is in their key. In symmetric methods, encryption and decryption operations use the same key. The important feature of these methods is their very high speed, and these methods are used for high volume data. An example of this method is MD5. The major disadvantage of these methods is that if the key is leaked during transmission, the entire encrypted data will be revealed. On the other hand, asymmetric methods include methods where the encryption key is different from the decryption key. That is, we encrypt with one key (public key), but the decryption is done with another key (private key). Naturally, in this type of method, revealing the public key does not cause much problem, and the important thing is the private key. Since in these methods, key transfer is not done like in symmetrical methods,

the risk of key leakage is also eliminated. The most famous of these methods can be called RSA and El-Jamal [22]. These methods are mostly used to transfer very important and short data (such as data containing a symmetric encryption key)

There is another type of encryption that is not based on a key. Hashing is one of these methods. In hash operation, the input data of any size (naturally, there are limits to the data length) is entered into the algorithm and the encrypted data is output as a block with a specific length [22]. This operation is not reversible. The output block is the same input data that has been changed with operations such as shift, addition, division and logic. These methods have high speed, but their most important disadvantage is collision. Collision means that the algorithm takes two different data inputs, but a same output block is produced for them. In fact, when the collision occurs, the algorithm will lose its credibility. A famous example of these methods is SHA, which started with SHA-1 and now SHA-256 is used as an encryption method in Bitcoin and many cryptocurrencies. In fact, Bitcoin mining machines are always running SHA-256.

2.2. SHA-256

In encryption, data is converted into a secure format that cannot be read unless you have the key. In encryption, data may be unbounded, but in hashing, data of arbitrary size is converted to fixed-size data. In SHA-256 hash, a 512-bit data string is converted into a 256-bit string. In hash encryption, the hash data is encrypted in such a way that it is not reversible. For this reason, it is almost impossible to convert the mentioned 256-bit hash to its original 512-bit form. The Bitcoin encryption algorithm is SHA-256, which is an extended version of SHA-1,2. What each miner executes billions of times per second is the hashing algorithms and the speed of each miner is determined by the number of hashes per second. SHA-2 is shown in the Figure 1. This algorithm is a combination of logical relations of shift, inflectional combination (and), exclusive arc, exponentiation and contradiction.

2.3. Transaction and Blockchain

A digital coin is a chain of digital signatures of previous owners. Anyone who sells it, with a digital signature on the hash of previous transactions and the public key of the next owner, it transfers it and adds this signature to the end of the chain of previous signatures. In the Figure 2, person #1 hashes the public key of person 2 with the chain of previous transactions and then digitally signs it and transfers it to person 2.

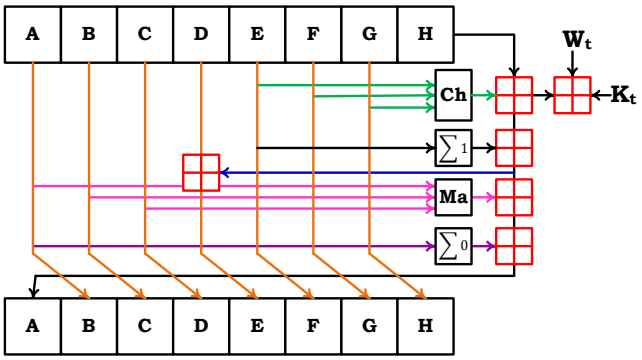

Figure1. Hashing diagram of SHA-2.

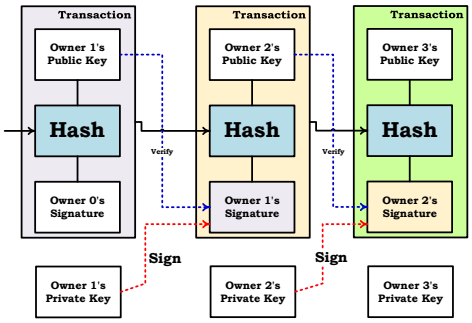

Figure2. Chain of blocks in a blockchain.

For person 2, during the digital signature, the previous chain must be confirmed, while with the private key, he can access his coin and sell it. The problem is that the buyer cannot understand whether the seller is selling for the first time or not. One solution is to have a verification center that works with centralized reason and has all the problems of centralized systems. In fact, by surveying the majority of nodes (miners), the buyer can be informed that the seller will not sell the coin a second time. The solution is to use the time constant as a distributed time server, whose job is to perform the time constant of each block and hashing with the previous blocks. To implement a distributed time server, you must use the work confirmation method. The hash starts with zero bits, the more the number of zeros, the average processing tasks increases exponentially. The difficulty of the work is determined based on the average output of the hash, when the speed increases, the difficulty of the work increases.

2.4. Miners

The operation of confirming the transaction by the miners, which leads to a reward for them, is called the mining operation. As mentioned before, miners perform hash operations many times every second. Four generations of Bitcoin miners have been made, and recently the fifth generation of them, which have more speed and less power consumption, has been presented. Bitcoin mining has been done in five generations by different hardware [3]. In the first generation of this hardware, the main processor i.e., CPU was used. The second generation of miners used graphics processors or GPUs. The third generation of miners used FPGA for mining. ASIC circuits are used in the fourth and fifth generation of cryptocurrency miners. The circuit of this type of miner is designed in such a way that they only implement the hash algorithm and cannot be used in other processing applications. Table 1 compares these different generations.

Table 1. Comparison of different generations of miners in terms of speed and power consumption.

Miner Generation	Hardware	Speed (Hash)	Power Consumption per GH/Sec
1	CPU	1 to 5 MH/Sec	4000 W
2	GPU	0.33 GH/Sec	210 W
3	FPGA	100 to 500 MH/Sec	50 W
4	ASIC	10 to 30 TH/Sec	0.35 W
5	ASIC	70 to 112 TH/Sec	0.0295 W

3. Detection Methods of Mining

The most common illegal methods for mining can be divided into several types. Which are mentioned below.

- Unauthorized branching of the meter
- Using a power distribution system without meter
- Abuse of manufactories with agricultural and industrial electricity
- Using power to extract currency instead of using it for licensed applications
- Branching from remote lines
- Crypto jacking: Using the processor of users when they work with popular sites and software

The main discussion of this paper is to review the methods of miner detection. Here, various methods of miner detection are discussed.

- Statistical processing of meter consumption
- Data mining and processing of meter parameters
- Consumption processing with anomaly detection methods
- Tracking the electricity leakage in a group of consumers
- Analysis of parameters of power distribution lines
- Tracking through the Internet addresses and profiles (Mac, IP, wallet)
- Analysis and tracking of data flows on the Internet
- Sound and heat tracking
- Antiviruses

In the following section, each of these methods is explained.

3.1. Statistical processing of meter consumption

Most of the ordinary consumers and people use the miner for the first time. They use home branches and only one miner device. It is not difficult to identify these consumers according to the changes in their consumption compared to the same period of the previous year, and it is easy to identify the consumers who use meter branches to extract cryptocurrency. The main problem of this method is that many illegal electricity consumers use the branches that bypass the meter. Therefore, it is difficult to identify them by statistical processing of meter [6]. Also, some other illegal consumers use electricity to extract cryptocurrency instead of their authorized applications, such as in industry or agriculture. Therefore, there is no significant statistical change in their consumption. For example, they remove some parts of their production lines that are less economical than mining and use miners on holidays.

3.2. Data mining and processing of meter parameters

In some paper [6] by using data mining and analysis of the parameters measured by the meter, it is possible to trace electricity consumers with miners. This method, like the previous method, is used to identify people who use meter branches to consume the electricity of their miners. One of the limitations of this method is that the meter must be intelligent in order to measure some different parameters of the distribution network. In some of the few researches, the analysis and data mining of parameters of meter is employed for miner detection [5]. For this purpose first, a repeating patterns are

identified, then learning operations are performed with the decision tree to distinguish between miners and non-miners. In this method, firstly, according to the noticeable changes in consumption compared to similar times, the relevant consumer is selected. Then, by processing the parameters measured by the meter, the validity of the miner is confirmed or rejected. Various parameters and characteristics are checked to detect whether the consumer is a miner. For example in the article [5], parameters such as date and time, Power, Cos(Fi), Cos(Fi) L1, L2, L3, Voltage L1, L2, L3 and Reactive Power is used for detection. The main challenge of this method is related to the high false positive error rate. It is because of the similarity of network parameters of miners and some other devices such as water pumps or even electric heaters. Most of these devices are detected instead of miners and the positive detection error increases.

3.3. Anomaly detection methods

Some methods used the abnormalities in consumption for miner detection. Cryptocurrency miners are abnormal and they are distanced among other electricity consumers. These consumers are tracked by data mining and anomaly detection approaches [11]. In this state, consumers are divided into three categories of consumption on working days, holidays and unusual consumption based on consumption time. Then the unusual consumers are again divided into three other categories, one of them is miners. Some other methods [23] have been presented anomaly detection of consumption based-on cloud processing, but they use only for detection of high-consumption customers and not only cryptocurrency miners

3.4. Miner detection based-on reference points

One of the methods of detecting unusual consumers among a set of electricity consumers is based-on batch monitoring [7]. In these methods, consumers are divided into several groups, usually based on geographic location. Then, the main electricity distribution line of that area is monitored with a reference meter, and the total consumption of that area is stored in memory by the meter at certain time. The same work is done by the smart meters of each consumer, at the certain time. For example, every hour, the consumption value of the meter is stored. Then this information is read and analyzed from the consumers' meters and the reference meter. Naturally, the consumption value measured by the reference meter has a difference to summation of the all consumption in the network. It is because of the loss energy in the network. If this difference is greater than a certain limit, it means that there is an unauthorized branching in that area without a meter. The most important challenge for this method is related to all consumers. All of them must have a smart meter. In addition, the hours of the meters must be accurate.

3.5. Analyzing the parameters of power

Some techniques, proposed methods for analyzing the parameters of power lines. These methods are based-on the measurement of power harmonics in the power distribution network [6]. These approaches often have a false positive error. It is because

some high consumption devices have behavior similar to miners in the distribution network. They increase the false positive error of miner detection. In addition, in a distribution power network, most of these parameters are merged together and they do not provide discriminative features. One of the important challenges of this method is the need to have hardware measuring for all consumers to measure these parameters.

3.6. Detection based-on Internet addresses and profiles (Mac, IP, and wallet)

Most of the miners have to use a wallet or mining pool to store or sell their cryptocurrencies. One of the traditional methods for miner detection is based-on the tracking the address of wallets or mining pools in the Internet. Today this method usually is not used. It is because miners use anti-tracking techniques. Some methods use traffic control for detection. They monitor and control the packets that have the same keys. That means, for example, the source and destination IP address, port, and protocol are the same [24]. By monitoring the network, it is possible to identify active miners connected to the pool by analyzing the address. In the flowing discussion of this part, each type of this method is explained. (i.e., identification based on MAC address, IP address and wallet address).

3.6.1. Miner Detection based-on MAC address

Mines, like any other device that connects to the Internet, have two identification addresses, IP address and MAC address. Normally, MAC addresses are fixed and stored in the ROM. Therefore, changing their address is difficult. One of the methods of miner detection is based-on the MAC address. Recently, most ASIC devices have been used for Bitcoin mining. However, GPU rigs are often used for Ethereum. Miners have a specific MAC address range. It is easier to detect some second-hand miners than new ones. Because they have been used before and many of their traces, including their MAC address, have been recorded in some places such as mining pools. This is a traditional method to track mostly mobile phones and their network standards. Because mobile phone can connect to the network without router. It is hard to use this technique for miner devices, because most miner devices are connected to the network with an intermediary, such as a router, and it makes hard to track it by its address [15]. All in all, the use of routers by users makes it difficult to identify a miner by MAC address. Most of the new routers have a section called Mac clone, which it can be covered any desired MAC address for the router, and this MAC address is visible in the WAN network and can filter. Besides, there are other ways to bypass miner identification using a MAC address. One of these methods is to use a VPN with a fixed server address.

3.6.2. Miner Detection based-on IP address

Each device used a temporary address to connect to the Internet. This address is called IP for identification in the network. This address can be changed every time the device is connected to the Internet. Since miner devices are permanently connected to the Internet, this address usually remains constant, unlike most common devices, the IP address of the device is fixed for a long time. Because the IP changes in a mining pool can disrupt the

mining process [15]. There are different ways to prevent the miner detection by IP address. To prevent the miner from being identified by the IP address, users usually use VPNs with a fixed address or VPS. Miner usually cannot register VPN settings on itself. To solve this problem, the purchased VPN must be set on a modem or router. Since the stability of the Internet connection is very important in mining, it is more appropriate to use a router because it allows the user to define two separate Internet connections for it. If one of its accesses is interrupted or disturbed, the network automatically uses an alternative Internet connection. If a large number of miners are used, a switch must be used to connect all of them to the router.

3.6.3. Miner detection based-on wallet address

In the process of mining, the wallet address must be connected to the mining pool to deposit currency to the wallet. The request the cash from the miming pools is done in three ways: automatically based on a time period, reaches the value to a certain level, and by a manual request of user. Therefore, connecting to the mining pool to pay or receive is necessary and must be done through the connection. Internal users usually use an IP address that does not belong to their countries and they usually use the Internet connected to their mining rig by using a VPN with a fixed server address. If this is not possible, they use VPN individually and then enter their panel in the mining pool. Therefore, IP identification with this method, i.e., wallet, is very difficult. Another method of detection that is related to wallet address is used in local digital exchanges. It is intercepted and determined whether the input of digital currency is through mining. This method can be bypassed. Users almost use an interface to transfer their currency of wallet to local exchanges. Usually, users use an intermediary address such as the address of their Trust wallet and first transfer the currency to this address and then deposit it to the local exchange. Therefore, it makes more difficult to detect miner by wallet address [3].

3.7. Analyzing and tracking the data flows on the Internet

One method to miner detection is related to data processing and data streams in the Internet. Different clustering and classification methods are usually used for this purpose. Among the few comprehensive researches, it can be mentioned in the research article [15] in which a very large amount of data streams are used in the Internet. An example of this research was conducted in the Czech Republic. It is the most complete article ever published in this field. In this article, among the 3.6 billion internet data streams, which includes 27.8 billion packets and a volume of nearly 100 terabytes of data, a small number of data have been selected. This selected data includes 16 million streams containing 117 million packets in 54 GB format. Therefore, in most cases, it is impossible to prepare and process such a heavy volume of data. For this reason, we have to go to the information that has been filtered and reduced.

3.8. Sound and heat detection

One of the basic methods of miner detection is the methods based-on sound and heat. Cryptocurrency mining systems generate a lot of heat due to high power consumption and

heavy processing. This heat can be detected with heat detection devices. Furthermore, to cool the miners, ventilation and powerful cooling systems must be used, which produces sound. They can be detected by sound detection. Nowadays most of the modern cryptocurrency mining systems can mine by low noise of sound and with proper ventilation systems. Therefore, this method often fails due to the presence of new mining systems [3].

3.9. Antiviruses to detect malware

In some cases, illegal malwares attempt to extract currency by installing them on computer systems without the permission of the user [25]. It is names as cryptojacking. This challenge is different from the previous challenges and the problem of detection of electricity consumers is not raised in it, but this method is in the form of malware detection. It is the software added to the browser as an extension or intentionally placed inside the website by the designer of that website and uses the processing power of users illegally. This method is known as cryptographic attack or cryptojacking. The corresponding malware code connects the mining bot to the mining pool. Comprehensive research has been done on the malware associated with this type of illegal activity and the number of infected devices has been estimated. The methods for estimating the income and duration of infection with mining malware have also been stated [20].

These unauthorized activities can only be done for some sites that have many users that they are active on the site for a long time. These malwares can be detected by installing updated antiviruses. As it is mentioned before, some of them are not malware, but the site designer put them on the site page to use the user's processor. An example of this code is the CoinHiv Java library in web pages, which is used to mine Monero currency by the processors of site users. Table 2 shows the summarization of all of miner detection methods and their challenges that explained in this section.

Table 2. List of different methods for miner detection and their challenges.

Row	Reference	Miner Detection Method	Challenges
1	[6]	Statistical processing of meter consumption	Require a smart meter, cannot used for illegal branches
2	[5,6]	Data mining and processing of meter parameters	Require smart meter, cannot used for illegal branches
3	[11,21]	Anomaly detection methods	Can be misleading by users
4	[7]	detection based-on reference points	Require smart meter for all users
5	[6]	Analyzing the parameters of power	Require measurement instrument, have false positive problem
6	[15]	Detection based-on MAC address	Can be misleading by users
7	[15]	Detection based-on IP address	Can be misleading by users
8	[3]	detection based-on wallet address	Require processing and analyzing huge data
9	[15]	Analyzing and tracking the data flows on the Internet	Require processing and analyzing huge data
10	[3]	Sound and heat detection	Can be bypassed easily by users
11	[20]	Antiviruses to detect malwares	It is used rarely

4. Proposed and research results to reduce illegal miners

Here some proposed ways are introduced to decrease the unauthorized mining.

- Only low consumption miners and rigs should have a legal license
- Using a meter for all electricity consumers
- Using intelligent meters and reference points to calculate and detect electricity leakage in each area
- Inform people in order to use low power miners
- Processing meter data in order to detect illegal miners
- Monitoring the digital currency exchanges and transfers of cryptocurrency to these exchanges
- Cooperation with the telecommunications system in order to track the illegal miners through the Internet
- Using up-to-date antiviruses to detect mining malware
- Using the new energies for mining
- Amending electricity price and imposing heavy penalties on violators
- Public information in order to detect offenders and use a public information system
- Smart and continuous monitoring of industrial and agricultural electricity consumers
- Setting up smart laboratories to identify miners
- Recognition of mining and servicing and support of authorized cryptocurrency miners
- Establishing specific rules related to the mining, buying and selling of cryptocurrency
- Block some sites that teach illegal mining

5. Conclusion and Suggestions

In this paper, an overview of different methods of detecting unauthorized cryptocurrency mining was done. Also, some methods to bypass the detection and tracking of miners were mentioned. Although most of these tracking methods can be bypassed with different techniques, they work well in many cases and can detect miner devices accurately. Most of the challenges of this part can be solved by coordinating the government departments of countries. For example, with the cooperation of the telecommunication company and the electricity distribution company, it is possible to track unauthorized miners through the Internet. Some other proposed method for this challenge is related to use smart meter especially for agricultural and industrial electricity consumers. Also, all branches in each country must use the meter. Using private source of power may help some of these challenges. In general, using the private company for electricity production and new energies decreases most of the problems of this area. Naturally, if the production and consumption of electricity are done by the non-governmental sector at their expense, the field of better management will be provided, and perhaps it will be profitable for the electricity producers to carry out the extraction as well.

The last suggestion for mining is related to using renewable and new source of electricity power for mining of cryptocurrency. Using renewable sources of electricity power to mine crypto such as Bitcoin and cryptocurrency has been investigated in several studies. It has been found that using sustainable energy, such as hydropower or solar photovoltaic systems, can be financially and economically superior to using conventional fossil fuel systems [26]. Some studies have analyzed the feasibility of using renewable energy sources to power individual miners, shipping containers holding multiple miners, and commercial mining farm containers [27]. The profitability and return on investment of using renewable energy for mining vary depending on factors such as geographic location, solar flux, utility rates, and energy laws. While it may be negative in some locations with low-cost electricity, it can be substantial in other locations, ranging from 34% to 104% in U.S. cities. Overall, some studies suggest that using renewable energy sources for cryptocurrency mining can be financially viable and environmentally friendly [28].

References

[1] S. Nakamoto, "Bitcoin: A Peer-to-Peer Electronic Cash System," 2008.

[2] K. O'Dwyer, and D. Malone, "Bitcoin Mining and its Energy Footprint," *25th IET Irish Signals & Systems Conference 2014 and 2014 China-Ireland International Conference on Information and Communications Technologies*, pp. 280-285, 2014.

[3] N. T. Courtois, M. Grajek, and R. Naik, "The Unreasonable Fundamental in Certitudes Behind Bitcoin Mining," *Arxiv Preprint Arxiv*, 1310,7935, 2013.

[4] K. J. O'Dwyer, and D. Malone, ''Bitcoin Mining and Its Energy Footprint,'' 2*5th IET Irish Signals & Systems Conference 2014 and 2014 China-Ireland International Conference on Information and Communications Technologies (ISSC 2014/CIICT 2014)*, p. 280 – 285, 2014.

[5] M. Amiri, and H. Askari, "Illegal Miner Detection Based on Pattern Mining: a Practical Approach," *Journal of Computing and Security*, vol. 9, no. 2, pp. 1-10, 2022.

[6] B. Dindar, and O. G¨ul, "The Detection of Illicit Cryptocurrency Mining Farms with Innovative Approaches for the Prevention of Electricity Theft," *Energy & Environment*, vol. 33, no. 8, pp. 1663-1678, 2022.

[7] R. Jiang, R. Lu, et al., "Energy-Theft Detection Issues for Advanced Metering Infrastructure in Smart Grid," *Tsinghua Science and Technology*, vol. 19, no. 2, pp. 105-120, 2014.

[8] A. Rahimi, A. Shahrestani, et al., "Filter Based Time-Series Anomaly Detection in AMI using AI Approaches," *2021 5th International Conference on Internet of Things and Applications (Iot)*, pp. 1-6, 2021.

[9] C. Chahla, H. Snoussi, L. Merghem, and M. Esseghir, "A Deep Learning Approach for Anomaly Detection and Prediction in Power Consumption Data," *Energy Efficiency*, vol. 13, no. 8, pp. 1633-1651, 2020.

[10] Z. Ouyang, X. Sun, J. Chen, D. Yue, and T. Zhang, "Multi-View Stacking Ensemble for Power Consumption Anomaly Detection in the Context of Industrial Internet of Things," *IEEE Access*, vol. 6, pp. 9623-9631, 2018.

[11] M. Li, K. Zhang, J. Liu, H. Gong, and Z. Zhang, "Blockchain-Based Anomaly Detection of Electricity Consumption in Smart Grids," *Pattern Recognition Letters*, vol. 138, pp. 476-482, 2020.

[12] B. Claise, B. Trammell, and P. Aitken, Specification of the IP Flow Information Export (IPFIX) Protocol, RFC 7011. IETF. 2013.

[13] A. Almalaq, S. Albadran, and M. A. Mohamed, "An Adoptive Miner-Misuse Based Online Anomaly Detection Approach in the Power System: An Optimum Reinforcement Learning Method," *Mathematics*, vol.11, no.4, pp. 884-884, 2023.

[14] C. Livadas, R. Walsh, D. Lapsley, and W. T. Strayer, "Usilng Machine Learning Technliques to Identify Botnet Traffic," *2006 31st IEEE Conference on Local Computer Networks, Tampa*, pp. 967-974, 2006.

[15] V. Vesely, and M. Zadnik, "How to Detect Crypto Currency Miners? by Traffic Forensics," *Digital Investigation*, vol. 31, 100884, 2019.

[16] J. A. Kroll, I. C. Davey, and E. W. Felten "The Economics of Bitcoin Mining, or Bitcoin in the Presence of Adversaries," *The 12th Workshop on the Economics of Information Security, Washington DC*, 11-12 June 2013.

[17] Y. Lewenberg, Y. Bachrach, Y. Sompolinsky, A. Zohar, and J. S. Rosenschein, "Bitcoin Mining Pools: A Cooperative Game Theoretic Analysis," *AAMAS 15 Proceedings of the 2015 International Conference on Autonomous Agents and Multiagent Systems*, pp. 919–927, 2015.

[18] A. Juels, A. Kosba, and E. Shi, "The Ring of Gyges: Investigating the Future of Criminal Smart Contracts," *Proceedings of the 2016 ACM SIGSAC Conference on Computer and Communications Security*, pp. 283-295, 2016.

[19] D. Y. Huang, and H. Dharmdasani, et al., "Botcoin: Monetizing Stolen Cycles," *Proceedings of the 2014 Network and Distributed System Security Symposium. NDSS*, 2014.

[20] S. T. Ali, D. Clarke, and P. McCorry, "Bitcoin:Perils of an Unregulated Global P2P Currency," *Cambridge International Workshop on Security Protocols*, pp. 294-306, 2015.

[21] S. Solaymani, "A Review on Energy and Renewable Energy Policies in Iran," Sustainability, vol. 13, no. 13, p.7328, 2021.

[22] A. Zakir al-Hosseini, "Data Security," *Nas Publications*, *fifth Edition*, 2012.

[23] L. Feng, S. Xu, et al., "Anomaly Detection for Electricity Consumption in Cloud Computing: Framework, Methods, Applications, and Challenges," *EURASIP Journal on Wireless Communications and Networking*, vol. 2020, no. 1, p.194, 2020.

[24] R. Hofstede, P. Celeda, et al., "Flow Monitoring Explained: from Packet Capture to Data Analysis with Netflow and Ipfix," *IEEE Communications Surveys & Tutorials*, vol. 16, no. 4, pp. 2037-2064, 2014.

[25] S. T. Ali, P. McCorry, P. H. J. Lee, and F. Hao, "Zombiecoin: Powering Next Generation Botnets with Bitcoin," *Financial Cryptography and Data Security Springer*, pp. 34-48, 2015.

[26] Y. Liang, C. B. Saner, et al., "Sustainable Energy-Based Cryptocurrency Mining," *2022 IEEE PES Innovative Smart Grid Technologies - Asia (ISGT Asia),* pp, 789-793, 2022.

[27] M. T. McDoald, K. S. Hayibo, F. Hafting, and J. M. Pearce, "Economics of Open-Source Solar Photovoltaic Powered Cryptocurrency Mining,", *Available at SSRN 4205879*, 2023.

[28] P. Rorich, K. Moloi, T. F. Mazibuko, and I. E. Davidson, "Cryptocurrency Mining Powered by Renewable Energy Using A DC-DC Connection,"*31st Southern African Universities Power Engineering Conference (SAUPEC),* pp. 1-7, 2023.

Declaration of Competing Interest

The authors declare that they have no known competing financial interests or personal relationships that could have appeared to influence the work reported in this paper. The ethical issues, including plagiarism, informed consent, misconduct, data fabrication and/or falsification, double publication and/or submission, redundancy, have been completely observed by the authors.

Credit Authorship Contribution Statement

Mohammad Hossein Shakoor: Conceptualization, Formal analysis, Project administration, Supervision, Validation, Investigation, Methodology, Roles/Writing - original draft.

Bibliography

Mohammad Hossein Shakoor received the B.Sc. degree in Computer Engineering from Shiraz University, Shiraz, Iran, in 1998 and M.S. degree in computer architecture from Isfahan university, Isfahan, Iran, in 2003. He received Ph.D. in Artificial Intelligent of Computer engineering from Shiraz University, Shiraz, Iran in 2016. His research interests include Texture Classification, Pattern Recognition and Computer Vision.